UNIVERSIDADE DE LISBOA

FACULDADE DE MEDICINA VETERINÁRIA

THE POTENTIAL OF ABT-263 AS A THERAPEUTIC AGENT IN SPINAL CORD INJURY-INDUCED PERIPHERAL PATHOLOGY

MARIANA ANTÃO VENTURA MONTEIRO

ORIENTADOR(A):
Doutora Maria Leonor Tavares Saúde

COORIENTADOR(A):
Doutor Jorge Manuel Jesus Correia
Doutora Isaura Vanessa Antunes Martins

2023

UNIVERSIDADE DE LISBOA

FACULDADE DE MEDICINA VETERINÁRIA

THE POTENTIAL OF ABT-263 AS A THERAPEUTIC AGENT IN SPINAL CORD INJURY-INDUCED PERIPHERAL PATHOLOGY

MARIANA ANTÃO VENTURA MONTEIRO

DISSERTAÇÃO DE MESTRADO INTEGRADO EM MEDICINA VETERINÁRIA

JÚRI
PRESIDENTE:
Doutor António José de Almeida Ferreira

VOGAIS:
Doutora Rute Marina Garcia da Noiva
Doutora Maria Leonor Tavares Saúde

ORIENTADOR(A):
Doutora Maria Leonor Tavares Saúde

COORIENTADOR(A):
Doutor Jorge Manuel Jesus Correia
Doutora Isaura Vanessa Antunes Martins

2023

DECLARAÇÃO RELATIVA ÀS CONDIÇÕES DE REPRODUÇÃO DA DISSERTAÇÃO

Nome: Mariana Antão Ventura Monteiro

Título da Tese ou Dissertação: THE POTENTIAL OF ABT-263 AS A THERAPEUTIC AGENT IN SPINAL CORD INJURY-INDUCED PERIPHERAL PATHOLOGY

Ano de conclusão (indicar o da data da realização das provas públicas): 2023

Designação do curso de Mestrado ou de Doutoramento: Mestrado Integrado em Medicina Veterinária

Área científica em que melhor se enquadra (assinale uma):

☐ Clínica ☐ Produção Animal e Segurança Alimentar

☒ Morfologia e Função ☐ Sanidade Animal

Declaro sobre compromisso de honra que a tese ou dissertação agora entregue corresponde à que foi aprovada pelo júri constituído pela Faculdade de Medicina Veterinária da ULISBOA.
Declaro que concedo à Faculdade de Medicina Veterinária e aos seus agentes uma licença não-exclusiva para arquivar e tornar acessível, nomeadamente através do seu repositório institucional, nas condições abaixo indicadas, a minha tese ou dissertação, no todo ou em parte, em suporte digital.
Declaro que autorizo a Faculdade de Medicina Veterinária a arquivar mais de uma cópia da tese ou dissertação e a, sem alterar o seu conteúdo, converter o documento entregue, para qualquer formato de ficheiro, meio ou suporte, para efeitos de preservação e acesso.
Retenho todos os direitos de autor relativos à tese ou dissertação, e o direito de a usar em trabalhos futuros (como artigos ou livros).
Concordo que a minha tese ou dissertação seja colocada no repositório da Faculdade de Medicina Veterinária com o seguinte estatuto (assinale um):

1. ☐ Disponibilização imediata do conjunto do trabalho para acesso mundial;
2. ☐ Disponibilização do conjunto do trabalho para acesso exclusivo na Faculdade de Medicina Veterinária durante o período de ☐ 6 meses, ☒ 12 meses, sendo que após o tempo assinalado autorizo o acesso mundial*;

* Indique o motivo do embargo (OBRIGATÓRIO)

Possível utilização de parte dos dados para publicação.

Nos exemplares das dissertações de mestrado ou teses de doutoramento entregues para a prestação de provas na Universidade e dos quais é obrigatoriamente enviado um exemplar para depósito na Biblioteca da Faculdade de Medicina Veterinária da Universidade de Lisboa deve constar uma das seguintes declarações (incluir apenas uma das três):

1. É AUTORIZADA A REPRODUÇÃO INTEGRAL DESTA TESE/TRABALHO APENAS PARA EFEITOS DE INVESTIGAÇÃO, MEDIANTE DECLARAÇÃO ESCRITA DO INTERESSADO, QUE A TAL SE COMPROMETE.
2. É AUTORIZADA A REPRODUÇÃO PARCIAL DESTA TESE/TRABALHO (indicar, caso tal seja necessário, nº máximo de páginas, ilustrações, gráficos, etc.) APENAS PARA EFEITOS DE INVESTIGAÇÃO, MEDIANTE DECLARAÇÃO ESCRITA DO INTERESSADO, QUE A TAL SE COMPROMETE.
3. DE ACORDO COM A LEGISLAÇÃO EM VIGOR, (indicar, caso tal seja necessário, nº máximo de páginas, ilustrações, gráficos, etc.) NÃO É PERMITIDA A REPRODUÇÃO DE QUALQUER PARTE DESTA TESE/TRABALHO.

Faculdade de Medicina Veterinária da Universidade de Lisboa, 9 de Junho de 2023

Assinaturas: _____ _____

Assinado por: **Maria Leonor Tavares Saúde**
Num. de Identificação: 08455720
Data: 2023.07.19 08:41:56 +0100

Mariana Antão Ventura Monteiro

Acknowledgements

À minha orientadora, Professora Doutora Leonor Saúde, pelo voto de confiança e constante apoio durante estes últimos meses. Obrigada pelos ensinamentos e por ser um exemplo de incessante busca pelo conhecimento, boa liderança e entusiasmo.

À minha coorientadora, Doutora Isaura Martins, por me mostrar os *ins and outs* do laboratório, por todo o conhecimento partilhado, conselhos, paciência, incentivo, ajuda e amizade.

Ao meu coorientador, Professor Doutor Jorge Correia, por toda a ajuda antes e durante o meu estágio. Pela partilha de conhecimentos na área da histopatologia e por toda a disponibilidade ao longo destes meses.

À Doutora Tânia Carvalho pela partilha de conhecimento, disponibilidade e ajuda.

Ao Professor Doutor José Prates pela sua ajuda, disponibilidade e amabilidade na quantificação enzimática do ALT.

À Ana Isidro pela amizade, conselhos e ajuda com os nossos ratinhos. À Raquel Quitéria pela ajuda, organização e por todos os ensinamentos sobre técnicas histológicas. À Dalila por todos os conselhos e por partilhar a sua experiência. Ao restante *lab*, Ana Ribeiro, Aida, Carmen, Daniel, Filipa, Mariana, Lara, Leonor Lameira, Madalena e Patrícia, pela amizade, ajuda e companheirismo.

À *Comparative Pathology Unit,* Ana Biscaia Santos, Ana Margarida Cristovão e Ana Rita Pires pela sua partilha de conhecimento e por toda a ajuda.

Ao *Bioimaging,* José Rino, António Temudo, Ana Nascimento e Aida Lima por toda a disponibilidade e ajuda.

Ao Pedro Ruivo por todos os conselhos.

À Ana Amado, Carlota Molina, Inês Cardoso, Inês Duque e Sandra Carapeto, obrigada pela amizade, por todo o apoio e por estarem lá nos bons e maus momentos, por serem um exemplo de ética de trabalho e disciplina.

À Filipa e Anaísa, amigas de sempre.

À Helena pela sua amizade e por ser uma inspiração.

Ao Diogo e família por todo o extraordinário apoio e carinho durantes estes últimos anos.

Por último, quero agradecer aos meus pais, Fernanda e Augusto, pelo constante apoio e incentivo. *In memoriam*, à minha tia Ana e avó Lilia, que sempre apoiaram os meus sonhos. À restante família pela paciência e compreensão durante estes anos.

This thesis was only possible with the financial support from Prémios Santa Casa Neurociências – Prize Melo e Castro for Spinal Cord Injury Research (MC-36/2020).

Resumo

O potencial do ABT-263 como agente terapêutico na patologia periférica associada a lesões da medula espinhal

Lesões na medula espinhal (LME) são alterações neurológicas severas, caracterizadas por défices motores e sensitivos, que estão frequentemente associados à indução de alterações periféricas secundárias. Duas principais causas responsáveis por esta patologia periférica são: a interrupção mecânica da inervação do Sistema Nervoso Simpático e o seu controlo supra-espinhal; e a resposta inflamatória sistémica associada. A eliminação de células senescentes induzidas por LME, através do uso do senolítico ABT-263, é responsável por uma melhoria significativa da função motora, sensitiva e da bexiga. Estas estão também associadas à redução de citoquinas, quimiocinas e de fatores do fenótipo secretor associado à senescência (SASP). No nosso estudo, colocámos a hipótese de que a acumulação dos fatores SASP na medula espinhal poderia ser responsável pela sua difusão sistémica e, desta forma, a indução de senescência, SASP, e consequentemente patologia nos órgãos periféricos. Como o ABT-263 foi benéfico na medula espinhal, quisemos avaliar se o seu efeito se mantinha na periferia, atenuando as condições secundárias.

Avaliámos o perfil de citoquinas da medula espinhal, fígado e bexiga de murganhos com LME ao nível da T9, tratados com veículo ou ABT-263 em diferentes dias pós-lesão (dpl). Para além disto, a histopatologia e o perfil de senescência foram avaliados usando H&E, e outras colorações, incluindo o SA-β-gal, respetivamente, bem como imunohistoquímica. A análise de imagem e respetivas quantificações foram realizadas usando o QuPath.

Os nossos resultados demonstraram a indução crónica aos 30 dpl na medula espinhal de fatores pro-inflamatórios e uma perda de eficácia do ABT-263 comparado com os 15 dpl. No fígado, aos 15 dpl observou-se a indução de citoquinas inflamatórias e fatores pró-fibróticos. No entanto, o ABT-263 não conseguiu diminuir a expressão destes fatores. Ao mesmo tempo, houve um aumento do número de células senescentes no grupo tratado com ABT-263, sugerindo hepatoxicidade. Isto foi confirmado pela indução de fatores pro-fibróticos e pro-inflamatórios no fígado dos animais tratados com ABT-263 aos 30dpl. Não obstante, aos 15 dpl não havia alterações histopatológicas significativas. O baço não parece ser afetado por lesão a este nível. A bexiga também revelou um microambiente e fenótipo inflamatório e pro-fibrótico. Todavia, os efeitos benéficos do ABT-263 apenas foram observados aos 30 dpl, sugerindo uma possível modulação intermédia entre os 15 e os 30 dpl.

Concluindo, neste momento ainda não foi possível de forma irrefutável demonstrar a existência de um SASP sistémico, responsável pela indução de senescência e pela patologia periférica já descrita. Mais estudos são necessários.

Palavras-chave: Lesão na medula espinhal; Síndrome da Disfunção em Múltiplos Órgãos; Senescência; Fenótipo secretor induzido por senescência; ABT-263.

Abstract

The potential of ABT-263 as a therapeutic agent in spinal cord injury-induced peripheral pathology

Spinal cord injury (SCI) is a serious neurological condition characterized by motor and sensory impairments, often associated with the induction of peripheral secondary conditions. There are two main causes identified for this peripheral pathology: the severance of the sympathetic nervous system and its supraspinal control; and a systemic and chronic inflammatory response. The elimination of SCI-induced senescent cells using the senolytic ABT-263 is responsible for significant motor, sensory and bladder improvements. These are also correlated with the reduction of detrimental cytokines, chemokines and senescent-associated secretory phenotype (SASP) factors. In our study, we hypothesized that the accumulation of SASP factors in the injured spinal cord could be responsible for its systemic spread and induction of senescence, SASP and, consequently, pathology in peripheral organs. As ABT-263 is beneficial for spinal cord repair outcome, we wanted to address if its effect was sustained in the periphery, and, therefore, attenuate secondary conditions.

We evaluated the cytokine profile of the spinal cord, liver and bladder from T9 SCI mice taken from vehicle- and ABT-263-treated animals at different days post-injury (dpi). In addition to this, the histopathology and senescence profile were evaluated using H&E, and other special stainings, including SA-β-gal, respectively, as well as immunohistochemistry to assess inflammation. Image analysis and quantifications were done using QuPath.

Our results showed a chronic induction of pro-inflammatory factors in the spinal cord at 30 dpi and a loss of effectiveness of ABT-263 compared with the 15 dpi. In the liver at 15 dpi, inflammatory cytokines and pro-fibrotic factors were upregulated with SCI, however, ABT-263 was not successful in decreasing their expression. At the same time, an increase in the number of senescent cells was observed in the animals treated with ABT-263 suggesting some degree of hepatotoxicity. This was confirmed by an upregulation of pro-fibrotic and pro-inflammatory factors in the liver of ABT-263-treated animals at 30 dpi. Notwithstanding, at 15 dpi histopathology did not yet show significant pathological alterations. The spleen appeared to not be affected at this injury level. The bladder also revealed a chronic inflammatory and pro-fibrotic microenvironment and phenotype. However, the beneficial effects of ABT-263 were only observed at 30 dpi, suggesting an intermediate modulation by ABT-263 between 15 and 30 dpi.

In conclusion, there is no irrefutable evidence that SASP becomes systemic and is responsible for the induction of senescence and pathology in other organs after SCI, at least at 15 dpi. Further studies are warranted.

Keywords: Spinal Cord Injury; Multiple Organ Dysfunction Syndrome; Cellular Senescence; Senescence-associated Secretory Phenotype; ABT-263.

Resumo alargado

O potencial do ABT-263 como agente terapêutico na patologia periférica associada a lesões da medula espinhal

Lesões na medula espinhal (LME) são alterações neurológicas graves, caracterizadas por défices motores e sensitivos, que estão frequentemente associados à indução de alterações periféricas secundárias.

Etiologicamente, as LME podem dividir-se em traumáticas ou não traumáticas, sendo que nos humanos as lesões mais comuns são as traumáticas. As LME traumáticas são caracterizadas por uma lesão primária, onde ocorre uma disrupção mecânica que danifica vias ascendentes e descendentes da medula espinhal, seguida pelo desenvolvimento de uma lesão secundária causada por uma grande resposta inflamatória local, isquemia e excitotoxicidade. Numa fase crónica, esta resposta diminui de intensidade e há a formação de uma cicatriz glial que constitui uma barreira física entre o tecido saudável e o danificado. Isso impede a propagação da lesão, mas também não permite uma regeneração total da medula espinhal, pois impossibilita ou dificulta a regeneração axonal.

Para além da perda parcial ou completa de função motora e sensorial, os órgãos periféricos também podem ser afetados. As principais causas associadas ao desenvolvimento desta patologia periférica incluem a interrupção mecânica da inervação do Sistema Nervoso Simpático e o seu controlo supra-espinhal; e a resposta inflamatória sistémica associada. Essas alterações serão responsáveis, por exemplo, por aterosclerose, atrofia muscular e osteoporose, depressão e dor crónica, entre outras. No fígado, a bibliografia também descreve o desenvolvimento de esteatose e esteatohepatite, que com o tempo pode evoluir para cirrose e, até mesmo, carcinoma hepatocelular. No baço, o desenvolvimento de disreflexia autonómica pode condicionar o aparecimento da síndrome de imunodepressão associada a LME, que se caracteriza por atrofia esplénica. Já na bexiga, a perda de controlo supra-espinhal leva ao desenvolvimento de hiperreflexia do músculo detrusor, que com a falta de relaxamento do esfíncter uretral externo, provoca uma acumulação de urina e distensão da bexiga. Estes acontecimentos têm também impacto a nível do urotélio com o desenvolvimento de úlceras, não só provocadas pelas elevadas pressões intra-vesicais, mas também pela libertação de norepinefrina e outras hormonas do stress que causam disrupção do mesmo. Estas alterações levam ao desenvolvimento de cistite hemorrágica e crónica.

Até ao momento, há falta de terapêuticas eficazes para o tratamento de LME e as que existem são principalmente sintomáticas. Recentemente, Paramos-de-Carvalho, Martins, et al. (2021) observaram que a eliminação de células senescentes induzidas por LME, através do uso do senolítico ABT-263, é responsável por uma melhoria significativa da função motora, sensitiva e da bexiga. Estas células senescentes são células que se encontram num estado de paragem do seu ciclo celular e podem ser induzidas por vários estímulos, nomeadamente

o envelhecimento, mas também danos tecidulares, como é o caso nas LME. A senescência é responsável por várias alterações fenotípicas nestas células, como o aumento da atividade da enzima β-galactosidase associada à senescência (SA-β-gal) e à produção de fatores do fenótipo secretor associado à senescência (SASP). O SASP, por sua vez, consegue modular o microambiente celular envolvente e induzir senescência parácrina e autócrina. Tanto a SA-β-gal como o SASP foram utilizados como marcadores de células senescentes neste estudo.

Considerando isto, no nosso estudo, colocámos a hipótese de que a acumulação dos fatores SASP na medula espinhal poderia ser responsável pela sua difusão sistémica e, desta forma, a indução de senescência, SASP, e consequentemente patologia nos órgãos periféricos. Como o ABT-263 foi benéfico na medula espinhal, quisemos avaliar se o seu efeito se mantinha na periferia, atenuando possíveis alterações nos órgãos induzidas pela LME. Para dar resposta a estas hipóteses, começámos por avaliar o perfil de citoquinas da medula espinhal aos 30 dias pós-lesão (dpl), seguido do fígado e bexiga aos 15 e 30 dpl de ratinhos com LME ao nível da T9, tratados com veículo ou ABT-263. A fim de avaliar o perfil de citoquinas e quimiocinas, foi utilizado um kit que avalia 111 deste tipo de proteínas de ratinho. Para além disso, a histopatologia e o perfil de senescência foram também caracterizados nos mesmos grupos experimentais, usando H&E e SA-β-gal, respetivamente, e comparados com os perfis de citoquinas. Outras colorações especiais foram utilizadas para realçar e/ou confirmar certos aspetos da histopatologia. A análise de imagem e respetivas quantificações foram realizadas usando o programa QuPath.

Os nossos resultados demonstraram que na espinhal medula aos 30 dpl houve uma diminuição do número de fatores aumentados após LME, com apenas 9 fatores a aparecerem significativamente aumentados nos animais lesionados comparando com os 35 fatores previamente observados aos 15 dpl. Isto sugere o aparecimento de uma tempestade de citoquinas em estadios agudos que esmorece progressivamente com o tempo. Para além disso, a redução na proporção de fatores modulados pelo ABT-263 também sugere uma perda de atividade do senolítico. Dos 9 fatores aumentados aos 30 dpl nos animais lesionados, 3 fatores, que já foram descritos como SASP, já se encontravam aumentados aos 15 dpl. Este achado corrobora a acumulação crónica de células senescentes previamente observada pelo grupo. Ao mesmo tempo, também confirma a perda de eficácia do senolítico, dado que nenhum destes fatores é modulado pelo mesmo.

No fígado, aos 15 dpl observou-se a indução de citoquinas inflamatórias, fatores pró-fibróticos e outros. Apesar de 3 destes fatores estarem descritos como SASP, o facto de nenhum deles ser modulado pelo ABT-263 aos 15 dpl, possivelmente indica que esses fatores não estão a ser produzidos por células senescentes. De facto, a quantificação de células senescentes não acompanha o aumento destes fatores no grupo tratado com veículo. Pelo contrário, há um aumento do número destas células no grupo tratado com ABT-263, o

que sugere algum grau de hepatotoxicidade do composto, já observada em humanos tratados com este fármaco. As células senescentes identificadas são pequenas e localizam-se nos sinusóides do fígado e nos infiltrados inflamatórios, por isso considerámos que podiam ser células de Kupffer, de Ito, linfócitos T ou até células endoteliais. Já 30 dpl, encontramos 30 fatores especificamente aumentados no grupo tratado com ABT-263. Esses fatores têm funções pro-fibróticas, inflamatórias e foram também associados ao desenvolvimento de fígado gordo e esteatohepatite. Desta forma, este aumento pode ser possivelmente justificado pelo aumento concomitante, no mesmo grupo experimental, de células senescentes aos 15 dpl. Essas podem estar a produzir direta ou indiretamente esses fatores. De facto, as funções desses fatores relacionam-se com o tipo de células identificadas como senescentes. Histopatologicamente, as alterações aos 15 dpl são pouco significativas. Observou-se apenas depleção de glicogénio nos animais com LME e alguns infiltrados inflamatórios que se podem correlacionar com os aumentos observados em alguns dos fatores.

O baço não apresentou alterações histopatológicas e da quantificação de células senescentes significativas, possivelmente porque a lesão era muito caudal.

A bexiga apresentou tanto aos 15 como aos 30 dpl a indução de fatores típicos de um microambiente pro-inflamatório, pro-fibrótico e pro-tumoral nos animais com LME tratados com veículo. Aos 15 dpl, observou-se um aumento de 14 fatores no grupo com LME e tratado com veículo. Destes, apenas um dos fatores foi modulado pelo ABT-263. A falta de modulação desses fatores pelo ABT-263 sugere que estes não estão a ser produzidos por células senescentes e, de facto, não há um aumento concomitante no número de células senescentes nos animais com LME, tratados com veículo. A histopatologia observada relaciona-se com o perfil de citoquinas identificado, demonstrando alterações compatíveis com cistite e hiperplasia simples do urotélio. Aos 30 dpl, há um aumento do número de fatores induzidos pela LME. A modulação pelo ABT-263 também é proporcionalmente maior. Contrariamente ao que esperávamos, o número de fatores modulados pelo ABT-263 não diminui com a provável perda de eficácia do ABT-263 aos 30 dpl, sugerindo uma possível modulação intermédia destes fatores entre os 15 e os 30 dpl.

Para além disto, as citoquinas IL-28 A e B foram encontradas aumentadas na medula espinhal, no fígado e na bexiga aos 30 dpl. Estes dois interferões pertencem à terceira família de interferões e, para além das suas funções imunomoduladoras, também induzem uma paragem do ciclo celular em G1, característica de estados de senescência. Apesar de isto não implicar necessariamente o desenvolvimento de um fenótipo de senescência, faz com que o IL-28 seja um potencial candidato a SASP. O facto de se encontrar aumentado nestes órgãos e de ser modulado pelo ABT-263 tanto a nível da medula como da bexiga, reforça esta ideia e que possa estar a ser produzido centralmente e a tornar-se sistémico.

Concluindo, até ao momento ainda não foi possível de forma irrefutável demonstrar a existência de um SASP sistémico, responsável pela indução de senescência e pela patologia periférica já descrita. O ABT-263 demonstrou uma perda de eficácia na modulação do microambiente da espinhal medula aos 30 dpl, enquanto na bexiga o seu efeito aumentou dos 15 para os 30 dpl. No entanto, o fígado revelou sinais de hepatoxicidade aos 30 dpl. Mais estudos são necessários para determinar a evolução da patologia ao longo do tempo e como esta se relaciona com a senescência, bem como determinar o verdadeiro potencial do ABT-263.
Palavras-chave: Lesão na medula espinhal; Síndrome da Disfunção em Múltiplos Órgãos; Senescência; Fenótipo secretor induzido por senescência; ABT-263.

Table of Contents

List of Figures

List of Tables

List of Abbreviations

AD: autonomic dysreflexia

AFOG: Acid Fushin Orange G

AMPA: a-amino-3-hydroxy-5-methyl-4-isoxazole propionic acid

ANS: autonomic nervous system

APPs: Acute Phase Proteins

APR: acute phase response

ATP: Adenosine Triphosphate

AUC: Area under the curve

BMS: Basso Mouse Scale

BSCB: blood-spinal cord barrier

CCL-11: Chemokine (C-C motif) ligand 12

CCL-12: Chemokine (C-C motif) ligand 12

CCL-2/MCP-1: Chemokine (C-C motif) ligand 2/Monocyte Chemoattractant Protein-1

CCL-20: Chemokine (C-C motif) ligand 20

CCL-3/MIP-1α: Chemokine (C-C motif) ligand 3/Macrophage Inflammatory Protein - 1α

CCL-4/MIP-1β: Chemokine (C-C motif) ligand 4/ Macrophage Inflammatory Protein - 1β

CCL-5: Chemokine (C-C motif) ligand 5

CINC-1: Cytokine-Induced Neutrophil Chemoattractant 1

C_{max}: maximum concentration

CNS: central nervous system

CRP: C-Reactive Protein

CSPGs: Chondroitin Sulphate Proteoglycans

CXCL-1, -2, -8, - 9: (C-X-C motif) ligand 1, 2, 8, 9

DAMPs: damage-associated molecular patterns

DPI: days post-injury

DNA: Deoxyribonucleic Acid

ECM: extracellular matrix

EGF: Epidermal Growth Factor

EMH: Extramedullary Haematopoiesis

FGF: Fibroblast Growth Factor

G-CSF: Granulocyte Colony Stimulating Factor

GDF-15: Growth/Differentiation Factor – 15

GM-CSF: Granulocyte-macrophage Colony Stimulating Factor

H&E: Haematoxylin & Eosin

HCC: hepatocellular carcinoma

HGF: Hepatocyte Growth Factor

HSCs: hepatic stellate cells

I-TAC: Interferon-inducible T cell Alpha Chemoattractant

IFN-γ: Interferon γ

IGFBP-X: Insulin Growth Factor Binding Protein – X (X representing any number)

IL - X: Interleukin – X (X representing a number)

IP: intraperitoneal administration

KCs: Kupffer cells

LIF: Leukaemia Inhibitory Factor

LPS: lipopolysaccharides

LSEC: Liver sinusoidal endothelial cells

LX: lumbar vertebrae X (X being any number between 1 and 6)

M1: pro-inflammatory macrophage phenotype

M2: anti-inflammatory macrophage phenotype

MMP-X: Matrix Metalloproteinase – X (X representing any number)

MZ: marginal zone

NAFLD: non-alcoholic fatty liver disease

NASH: non-alcoholic steatohepatitis

NMDA: N-methyl-D-aspartate

OPCs: Oligodendrocyte precursor cells

PAG: periaqueductal grey

PAS: Periodic Acid-Schiff

PD- ECGF: Platelet-derived endothelial cell growth factor

PEDF: Pigment Epithelium-derived Factors

PMC: pontine micturition centre

PMNs: Polymorphonuclear neutrophils

PO: oral gavage

RBP-4: Retinol Binding Protein-4

ROS: reactive oxygen species

SA-β-gal: senescent-associated β-galactosidase

SASP: senescent-associated secretory phenotype

SCI-IDS: spinal cord injury-induced immune depression syndrome

SCI: spinal cord injury

SEM: standard error of the mean

SIRS: systemic inflammatory response syndrome

SNS: sympathetic nervous system

SPNs: sympathetic preganglionic neurons

SX: sacral vertebrae X (X being any number between 1 and 4)

TGF-β: Transforming Growth Factor β

Thpo: Thrombopoietin

TLR4: toll-like receptor 4

TNF-α: Tumour Necrosis Factor-α

TX: thoracic vertebrae X (X being any number between 1 and 13)

VCAM-1: Vascular Cell Adhesion Molecule 1

VEGF: Vascular Endothelial Growth Factor

WISP-1: WNT-1-inducible-signalling pathway protein 1

1. Internship report

The final curricular internship to conclude the degree Integrated Master's in Veterinary Medicine (MIMV) by the Faculty of Veterinary Medicine (FMV), University of Lisbon, took place in LSaúde Lab at Instituto de Medicina Molecular – João Lobo Antunes (IMM-JLA), from 27th Sept 2022 to the 2nd Sept 2023, completing a total of 2064 hours.

At IMM, the student was under the guidance of Professor Leonor Saúde (PhD) and Doctor Isaura Martins (PhD). During this time the student learned and performed a variety of laboratory, histochemical and laboratory animal handling/procedures. In addition to this, executed histopathological evaluations of the liver, spleen and bladder of mice used in the study, with the supervision of Professor Jorge Correia (DVM, PhD).

Having previously acquired the post-graduation degrees of Laboratory Animal Science, both theoretical and practical, from the Faculty of Pharmacy, University of Lisbon, which conferred certification FELASA B, the student was able to perform and consolidate various laboratory animal procedures during the internship.

The internship included the participation and assistance in the performance of contusion spinal cord injuries, performed at the level of the 9th thoracic vertebrae (T9) in mice with 9/10 weeks of age. The student directly executed the handling, fixed anesthetization, through intraperitoneal administration (IP), surgical camp preparation and sutured the animal at the end of the procedure. In addition to this, had the opportunity to observe the surgical procedure, which included the identification of the T9 vertebrae through anatomical landmarks, laminectomy, preparation and positioning of the animal for the contusion injury, performed by an IH impactor with a set force. Following the surgery, the student participated in post-operative care. This included fluid therapy in the first few days after surgery given subcutaneously and manual voiding of the bladders twice daily for the duration of the experiments. During this time, the student learned and participated in different behavioural tests, including open-field locomotor behaviour assessment using the Basso Mouse Scale (BMS) (Basso et al. 2006), horizontal ladder test and thermal nociceptive evaluation (hot and cold) using an IITC's incremental thermal plate. Furthermore, performed drug administrations in the animals through oral gavage and learned to identify signs of pain and discomfort in these animals.

The pathology and histochemical part of the internship included animal sacrifice using the volatile anaesthetic isoflurane and, then, transcardially perfused with 0.9% sodium chloride. The student also had the opportunity to do intracardiac blood collections in these animals. Following these procedures, the student did the necropsies, organ collection (liver, spleen and bladder), sample preservation for different methods, fixation, embedding in OCT and freezing, and learnt how to cryosection the tissues. All stainings and immunohistochemistry protocols were performed by the student with the help and instruction

of the IMM's Comparative pathology unit and the histotechnician Raquel Quitéria. The histopathological evaluation was done by the student and supported by Professor Jorge Correia and Doctor Tânia Carvalho. During this time, the student also learnt how to use different image analysis software, such as QuPath and Image J/Fiji, with the support of IMM's Bioimaging unit.

The laboratory techniques performed by the student were the quantification of ALT enzyme activity and protein using spectrophotometry; and the use of a membrane-based antibody array (Proteome Profiler Mouse XL Cytokine array kit) to quantify the relative expression of mouse cytokines and chemokines of organ homogenates.

All in all, the internship proved an invaluable learning experience, which allowed the student to consolidate and develop self-sufficiency and critical thinking skills in histopathology and in the laboratory environment, along with working on time management and organizational skills. The student also gained a good basis of laboratory animal handling and procedures.

2. Introduction

Spinal cord injury (SCI) is a serious neurological condition characterized by damage to the spinal cord that most of the time permanently alters its function (Ahuja et al. 2017). Beyond the motor and sensory impairments that it can cause, SCI often comes hand in hand with secondary conditions characterized by multiple organ dysfunction that greatly impact the quality of life and longevity of the afflicted (Sun et al. 2016; Goodus and McTigue 2020). Aetiologically, SCIs can be divided into traumatic and non-traumatic. Traumatic SCIs are the most common and occur acutely due to an external mechanic impact such as falls and motor vehicle accidents (World Health Organization et al. 2013; Ahuja et al. 2017). Non-traumatic SCIs tend to appear in older populations. They can have an acute or chronic onset and are associated with tumour development, degenerative disc disease, among others (Ahuja et al. 2017). Due to their importance, frequency and relevance to this thesis's theme, our revision will focus on traumatic SCIs and its peripheral secondary effects, while introducing the concept of senescence and how it can play a role in SCI pathology.

2.1. Traumatic spinal cord injury

2.1.1. Pathophysiology

Traumatic SCIs are pathophysiologically characterized by a primary injury followed by the development of a secondary injury. Chronologically, in humans, this secondary injury is divided into acute (less than 48 hours), subacute (48 hours to 14 days), intermediate (14 days to 6 months) and chronic phases (more than 6 months) (Ahuja et al. 2017).

The primary injury is defined by the initial traumatic event in which there is a mechanical disruption of the spinal cord (Ahuja et al. 2017). This is caused by bone fragments, disc materials and ligaments that became displaced. Usually, these do not completely sever the spinal cord, but compress it (Alizadeh et al. 2019).

The mechanical forces of the primary injury damage ascending and descending pathways in the spinal cord, and disrupt the blood-spinal cord barrier (BSCB) and blood vessels, causing ischemia, injury to the neuronal and glial cell membranes, ionic dysregulation and proapoptotic signalling (Ahuja et al. 2017; Alizadeh et al. 2019; Badhiwala et al. 2019). Eventually, this prompts a secondary injury cascade, defined as a "series of cellular, molecular and biochemical phenomena that can continue to self-destruct spinal cord tissue and impede neurological recovery following SCI" (Alizadeh et al. 2019).

In the acute phase of this secondary injury, haemorrhage and disruption of the BSCB exposes the spinal cord to the influx of inflammatory cells (neutrophils, monocytes (later macrophages) and lymphocytes), cytokines (Tumour Necrosis Factor-α (TNF-α), Interleukin-1β (IL-1β)) and vasoactive peptides (Ahuja et al. 2017; Y. Zhang et al. 2021). There is also the activation of astrocytes, part of the BSCB, which play an important immunomodulatory role (Alizadeh et al. 2019) (Fig.1). This great inflammatory response combined with the disruption of the BSCB progressively contributes to the swelling of the spinal cord. Eventually, it can lead to further mechanical compression and extension of the injury to multiple spinal cord segments (Ahuja et al. 2017).

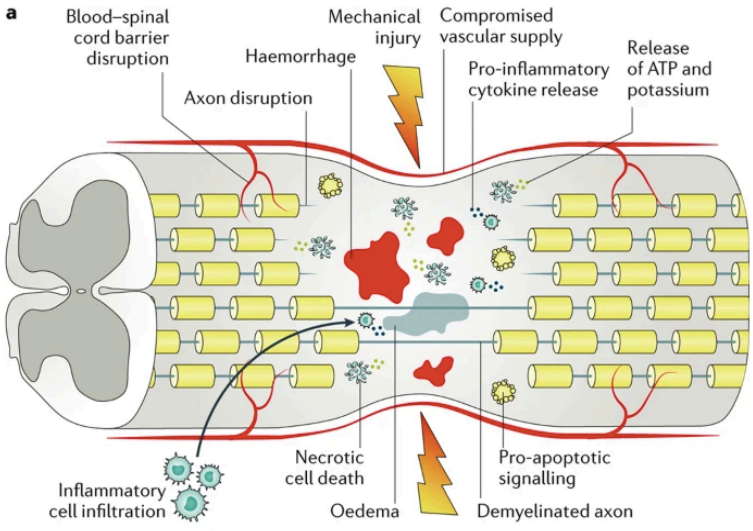

Figure 1 - Acute phase of the secondary injury cascade after a spinal cord injury. Characterized by oedema, haemorrhage, ischaemia, inflammatory cell infiltration, the release of cytotoxic products and cell death. Adapted from Ahuja et al. (2017).

In the transition between the acute and subacute phases, there is a loss of intracellular and extracellular ionic homeostasis provoked by ischemia and excitotoxicity

(Ahuja et al. 2017). Excitotoxicity, in turn, results from cyclic overactivation of NMDA (N-methyl-D-aspartate), AMPA (α-amino-3-hydroxy-5-methyl-4-isoxazole propionic acid) and kainite receptors by excitatory neurotransmitters, such as glutamate and aspartate, released from dying neurons and astrocytes (Ahuja et al. 2017; Y. Zhang et al. 2021). The resultant calcium influx, in neurons and glia, activates Calpains, which lead to mitochondrial dysfunction, ionic imbalance (increase in intracellular sodium, calcium, hydrogen, chlorine ions and water) and finally cell death (Ahuja et al. 2017). Ongoing necrosis of these cells releases Adenosine Triphosphate (ATP), Deoxyribonucleic Acid (DNA) and potassium, activating microglial cells. Following the neutrophil invasion, microglia and monocyte-derived macrophages infiltrate the injury site, further propagating the inflammatory response and contributing to the apoptosis of neurons and oligodendrocytes (Ahuja et al. 2017). These phagocytic cells are a double-edged sword, as they promote the clearance of damaged cells and myelin debris yet can also cause further damage through the release of free radicals, responsible for lipid peroxidation, DNA oxidative damage and protein oxidation (Ahuja et al. 2017). The spinal cord's microenvironment influences the polarization of phagocytic cells, which can either acquire a pro-inflammatory (M1) or pro-repair (M2) phenotype. However, similarly to the detrimental effects of prolonged M1 macrophage activity, M2 macrophages, when in excess, also contribute to fibrotic scar formation (David and Kroner 2011; Alizadeh et al. 2019). Lymphocytes also infiltrate the injured spinal cord in the first-week post injury and persist chronically (Fig. 2) (Sroga et al. 2003; Alizadeh et al. 2019). These immune cells, similarly to macrophages, can play both detrimental and pro-repair roles in the injured spinal cord (Jones 2014).

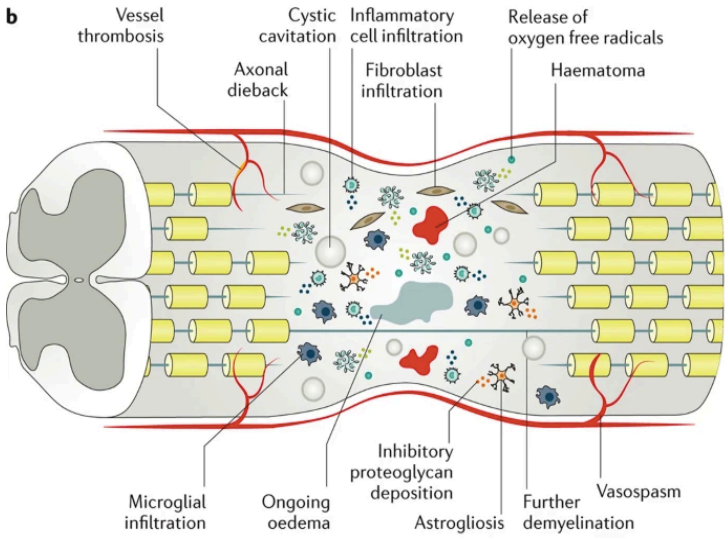

Figure 2 - Subacute phase of the secondary injury cascade after a spinal cord injury. Ischaemia continues due to ongoing oedema, thrombosis and vasospasm. There is also persistent inflammatory cell infiltration with cell death. Astrocytes proliferate and deposit extracellular matrix components in the perilesional area. Adapted from Ahuja et al. (2017).

In the intermediate-chronic phase of injury, the acute inflammatory response wanes and there is an attempt at remyelination, vascular reorganization and neuronal plasticity with changes in the extracellular matrix (ECM) (Ahuja et al. 2017). In humans and rats, but not in mice, the elevated cell volume loss promotes the formation of cystic cavities, that coalesce with time (Ahuja et al. 2017). Surrounding these cavities, reactive hypertrophic astrocytes proliferate and interweave (astrogliosis), condensing with secreted ECM (such as Chondroitin Sulphate Proteoglycans (CSPGs) and Tenascin) to form a glial scar (Fig. 3) (Ahuja et al. 2017; Alizadeh et al. 2019).

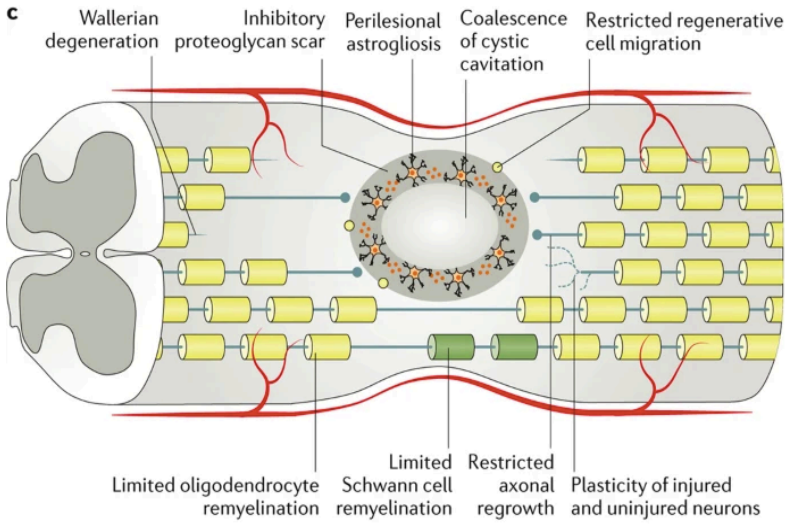

Figure 3 - Intermediate and chronic phases of the secondary injury cascade after a spinal cord injury. Wallerian degeneration, maturation of the astrocytic scar, becoming a potent inhibitor of axonal regeneration, and cystic cavity coalescence characterizes these phases. Adapted from Ahuja et al. (2017).

Resident and infiltrating inflammatory cells contribute to the formation of this glial scar by producing cytokines (such as IL-1β and IL-6), chemokines and enzymes which activate glial cells, namely astrocytes, oligodendrocyte precursor cells (OPCs) and microglia (Alizadeh et al. 2019). Astrocytes are activated by damage-associated molecular patterns (DAMPs), cytokines and chemokines. They function as a spatial barrier between damaged/ fibrotic and healthy tissue. Later, a second overlapping population of astrocytes help maintain this structure (scar-forming astrocytes) (Bradbury and Burnside 2019). OPCs can both contribute to remyelination or increase the expression of NG2, a proteoglycan connected to neuronal entrapment (Bradbury and Burnside 2019). Fibroblasts are also present and contribute to the production of Fibronectin, Collagen and Laminin in the ECM of the spinal cord (Alizadeh et al. 2019; Bradbury and Burnside 2019). In addition to this, they are a source of axon-repulsing molecules like Semaphorins (Alizadeh et al. 2019). Pericytes, in conjunction with fibroblasts, are able to detach from blood vessels and migrate to the injury site and form a fibrotic core, which matures within 2 weeks post-injury (Alizadeh et al. 2019;

Bradbury and Burnside 2019). In addition to this, the reactive cellular responses also continue in the spared tissue, mainly due to Wallerian degeneration of susceptible demyelinated axons (Ahuja et al. 2017; Bradbury and Burnside 2019). In the mature glial scar, activated microglia/macrophages occupy the innermost part and are surrounded by OPCs, while reactive astrocytes are in the outer layer and form a cellular barrier (Alizadeh et al. 2019).

The inhibitory effect of ECM on axonal growth and the resultant glial scar is a potent physical and biochemical hindrance to axonal regeneration and anatomical plasticity through neurite outgrowth. Nonetheless, this glial scar has also an important beneficial role in limiting the spread of cytotoxic molecules and inflammatory cells to the surrounding uninjured tissue, isolating the injury site (Bradbury and Burnside 2019).

2.1.2. Clinical manifestations and peripheral pathology

SCIs often result in partial or complete loss of sensorimotor function (Ahuja et al. 2017). The degree of loss will depend on the location and type of injury and, consequently, which tracts and nuclei are affected, with motor dysfunction, for example, resulting both from the severance of supraspinal tracts, demyelination and death of motor neurons (Grumbles and Thomas 2017). In addition to the disruption of sensorimotor function, peripheric organs can also be affected, because of the induced disruption of the sympathetic nervous system (SNS), and its supraspinal control (Henke et al. 2022), and by a systemic inflammatory response that often persists as chronic low-grade inflammation (Anthony and Couch 2014; Sun et al. 2016; Bloom et al. 2020; Goodus and McTigue 2020; Jeffries and Tom 2021). In the context of this revision only hepatic, splenic and bladder pathology will be covered.

2.1.2.1 Systemic inflammatory response

The inflammatory microenvironment in a SCI has been proven to be responsible for an immediate inflammatory systemic response driven by the liver (Anthony and Couch 2014; Goodus and McTigue 2020).

Inflammatory cytokines produced locally at the injury site of the spinal cord, such as TNF-α, IL-1α, IL-1β and IL-6, pass through the disrupted or intact BSCB, enter the bloodstream and reach the liver (Banks et al. 1995; Pan and Kastin 2008; Kwon et al. 2009; Siegel and Zalcman 2009; Mukhamedshina et al. 2017; Goodus and McTigue 2020). Rapidly, the liver initiates an acute phase response (APR), producing Acute Phase Proteins (APPs), which amplify the inflammatory and immune responses (Fleming et al. 2012; Goodus and McTigue 2020). Primarily, these APPs, which include chemokines such as Cytokine-Induced Neutrophil Chemoattractant 1 (CINC-1), Monocyte Chemoattractant Protein-1 (MCP-1/CCL2) and C-X-C motif chemokine ligand 1 (CXCL-1), have the purpose of promoting a

return to homeostasis through the recognition and elimination of pathogens, the clearance of necrotic and apoptotic cells, the increase in adhesion and chemotaxis of phagocytic cells and lymphocytes, and protection against reactive oxygen species (ROS) within the damaged spinal cord (Goodus and McTigue 2020). Other APPs are also elevated in the blood post-SCI, such as C-Reactive Protein (CRP), Serum Amyloid A, Serum Amyloid P, Haptoglobin, α1- Antichymotrypsin, and Fibrogen (Goodus and McTigue 2020). However, this response often becomes disproportionate, leading to a systemic inflammatory response syndrome (SIRS), in which multiple organs are reversibly or irreversibly affected (Chakraborty and Burns 2022).

Chronically, this inflammation is also maintained by other mechanisms. The reduction in lean mass with the proportional increase of fat mass and obesity play a role in this maintenance, as adipose tissue produces pro-inflammatory cytokines such as IL-6 and TNF-α (Da Silva Alves et al. 2013). In addition to this, immunosuppression caused by splenic dysfunction and hypothalamic-pituitary-adrenal axis overactivation leads to recurrent infections that further contribute to the systemic inflammatory state (Allison and Ditor 2015; Jeffries and Tom 2021). Gut dysbiosis and increased permeability of the intestinal wall also contribute to the overall systemic inflammation and hepatic inflammation, through the translocation of bacteria (Kigerl et al. 2016; Goodus and McTigue 2020).

This systemic inflammation will be responsible for the pathology seen in many organs, including the cardiovascular system (associated with the development of atherosclerosis), the musculoskeletal system (muscle atrophy and osteoporosis), the nervous system (depression and chronic pain), the hepatobiliary system (non-alcoholic fatty liver disease (NAFLD), non-alcoholic steatohepatitis (NASH) and metabolic syndrome), among others (Sun et al. 2016; Bloom et al. 2020; Bigford and Garshick 2022).

2.1.2.2 Liver

2.1.2.2.1. Liver pathology after spinal cord injury

After SCI, and subsequent APR, the liver starts to show signs of inflammation, with an increase in Kupffer cells (KCs) (Sauerbeck et al. 2015; Goodus and McTigue 2020). Cytokines and chemokines also increase significantly in the liver, namely IL-1α, IL-1β, CXCL-1 and CCL2 (Campbell et al. 2005; Goodus and McTigue 2020). This liver inflammation and KC activity will contribute to leukocyte recruitment, namely neutrophils and monocytes, to the injured spinal cord (Campbell et al. 2008). In addition to the circulating cytokines from the injury site that initiate the APR of the liver and promote its initial inflammation, other factors also contribute to and sustain this inflammation, namely the increase in permeability of the intestinal wall, allowing the translocation of gut bacteria that enter the bloodstream activating KCs (Liu et al. 2004; Kigerl et al. 2018; Goodus and McTigue 2020). These cells will produce

a range of factors such as TNF-α, IL-1, IL-6, IL-10, IL-18, CXCL-1, CXCL-2, CXCL-8, CCL2, CCL5, Macrophage Inflammatory Protein (MIP)-1α (CCL3), MIP-1β (CCL4), ROS and Prostaglandins, which will stimulate bone-marrow-derived monocytes and neutrophils to infiltrate the inflamed liver (Kazankov et al. 2019; Goodus and McTigue 2020; Hwang et al. 2021; Huby and Gautier 2022). KCs can also recruit T lymphocytes, through IL-1 and IL-18 (Wang and Zhang 2019).

In the first week after injury, there is also an accumulation of lipids in the liver of cervical and midthoracic spinal cord injured rats (Sauerbeck et al. 2015). One of the reasons behind this accumulation might be explained by the elevated circulation of fatty acids that exceed the liver's oxidative capacities and thus are stored in the form of triglycerides in the hepatocytes (Goodus and McTigue 2020). This excess circulation of fatty acids might be explained by bouts of sympathetic overactivity, that have been described after SCI, which lead to spikes of adipose tissue lipolysis (Goodus and McTigue 2020). Another possible reason for lipid accumulation is *de novo* lipogenesis in the liver through the significant increase of precursors and mature Ceramides, which are potent lipid signalling molecules and regulators of inflammation and apoptosis (Chang et al. 2011; Sauerbeck et al. 2015). Their production may be stimulated by endotoxins coming from the intestine (Chang et al. 2011). In the liver, these Ceramides can induce Insulin resistance, oxidative stress and inflammation (Pagadala et al. 2012). Systemically, they can be responsible for central nervous system (CNS) toxicity (Goodus and McTigue 2020). Hepatic Ceramide production can have a second spike, rising again at chronic time points (Sauerbeck et al. 2015). In addition to this, TNF-α, which is acutely elevated in the liver, can also stimulate lipogenesis genes and the production of ceramides, and when released into circulation will induce adipocyte lipolysis and a subsequent increase in fatty acids (Sauerbeck et al. 2015; Goodus and McTigue 2020).

Inflammation and hepatic steatosis has been shown to persist chronically after SCI in humans and rats (Sauerbeck et al. 2015; Goodus et al. 2018; Goodus and McTigue 2020; Goodus et al. 2021). In mice, long-term changes in the permeabilization of the intestinal epithelia and gut dysbiosis have been described, derived from immunosuppression and impaired intestinal motility following SCI (Balzan et al. 2007; Kigerl et al. 2016; Kigerl et al. 2018). This might be one of the explanations for the chronic maintenance of liver inflammation after SCI. Hepatocyte and KC sensitization to gut-derived Lipopolysaccharides (LPS) can also play a part in the non-resolving inflammation (Goodus and McTigue 2020). Other two factors contributing to the liver's chronic inflammation are local iron sequestration and anti-inflammatory medication part of the SCI patient therapeutic (Sauerbeck et al. 2013; Goodus and McTigue 2020). Iron sequestration often comes hand-in-hand with iron deficiency anaemia, common in patients with SCI (Sauerbeck et al. 2013). This happens due

to toll-like receptor 4 (TLR4) signalling Hepcidin secretion by the liver, which binds to hepatic cells and degrades hepatic Ferroportin, impairing iron exportation (Sauerbeck et al. 2013). The same happens in the basolateral membrane of enterocytes, leading, overall, to systemic iron depletion.

Chronic hepatic steatosis is characteristic of NAFLD. When this steatosis is associated with inflammation we enter in a more advanced stage of liver disease called NASH (Ikura 2014). If left untreated, the continuous inflammation in NASH precipitates the development of cirrhosis or hepatocellular carcinoma (HCC); both situations are common in SCI patients (Goodus and McTigue 2020; Peiseler and Tacke 2021).

In addition to the factors discussed above, lesions at the level of T7 or above disrupt the supraspinal control of the sympathetic innervation to the liver and lead to an aberrant intraspinal plasticity, which leads to reflex sympathetic overactivation (Zhang et al. 2013; Ueno et al. 2016; Gaudet et al. 2018). This overactivation reduces hepatic blood flow and increases TNF-α production and other inflammatory cytokines through the activation of α-adrenergic receptors in the KCs (Goodus and McTigue 2020). The pro-steatosis function of TNF-α and the activation of β-adrenergic receptors in the hepatocytes increase the liver's lipid content, contributing to steatosis (Goodus and McTigue 2020).

The SCI-induced liver inflammation and steatosis described above are likely associated with the disruption of systemic insulin function, glucose and lipid homeostasis (Goodus & McTigue, 2020). Possible mediators of this situation are TNF-α and ceramides, which impair insulin signaling (De Alvaro et al. 2004; Jelenik et al. 2017).

It is still poorly understood if SCI-induced liver pathology is responsible for metabolic dysfunction or vice-versa (Goodus and McTigue 2020). However, studies point that steatosis and inflammation precede the development of metabolic dysfunction (Sauerbeck et al. 2015; Goodus et al. 2018).

2.1.2.3. Spleen

2.1.2.3.1. Spinal cord injury and spleen pathology

The spleen is directly innervated by the sympathetic nervous system. The nerve fibres in the spleen regulate intrasplenic blood pressure (Andrew and Kaufman 2001) and communicate with leukocytes, which possess neurotransmitter receptors (Noble et al. 2018).

In rodents, the greatest density of sympathetic preganglionic neurons (SPNs) that innervate the spleen are located between thoracic spinal levels T4 and T9 (Ueno et al. 2016; Noble et al. 2018). Therefore, the level at which SCI occurs will have a different impact on spleen pathology (Zhang et al. 2013).

After an upper thoracic or cervical SCI, a normal innocuous stimulus below the level of injury, such as colon distension or full bladder, initiates an exaggerated reflex reaction that activates SPNs (Zhang et al. 2013). This leads to vasoconstriction and, overall, an increase in systemic blood pressure. The baroreceptors located in the aortic arch relay this information to the brain and brainstem, which in turn activate the parasympathetic system to slow down heart rate, and inhibit SPNs to stop vasoconstriction, therefore trying to resolve high blood pressure (Zhang et al. 2013; Eldahan and Rabchevsky 2018). However, injuries above T6 disrupt supraspinal control over the sympathetic system, leading to an overactivation of the sympathetic nervous system below the level of injury (Noble et al. 2018). In this case, we have the foundations of autonomic dysreflexia (AD), characterized by hypertension and a low heart rate (Zhang et al. 2013; Eldahan and Rabchevsky 2018). During each round of AD activated by normal splanchnic stimuli, the uncontrolled depolarization of SPNs causes high levels of norepinephrine to accumulate in the spleen (Zhang et al. 2013). With time, this uncontrolled reflex activation aggravates, due to the development of complex neuronal networks which will integrate the splenic-sympathetic circuitry throughout the thoracic, lumbar and sacral spinal cord (Ueno et al. 2016). This is not only responsible for splenic pathology, but also for systemic pathology, including the gastrointestinal tract, liver pathology and immune suppression (Sauerbeck et al. 2015; Brommer et al. 2016; Kigerl et al. 2016; Kigerl et al. 2018).

The overactive sympathetic reflexes and the increase in stress hormone concentrations cause leukopenia, splenic atrophy and leukocyte dysfunction, characteristics common to SCI-induced immune depression syndrome (SCI-IDS) (Lucin et al. 2007; Zhang et al. 2013). The norepinephrine released in the spleen interacts with β_2-adrenergic receptors of splenic macrophages and lymphocytes and inhibits the transcription of pro-inflammatory cytokines TNF-α and IL-1β (Noble et al. 2018). The signalling pathway behind this is further amplified by serum glucocorticoids, which upregulate the target receptors, increasing lymphocyte sensitivity to norepinephrine (Lucin et al. 2009). The overactivation of these β_2-adrenergic receptors will ultimately cause apoptosis of multiple splenic leukocyte populations and, therefore, splenic atrophy (Lucin et al. 2009). There is a reduction in the numbers of $CD11b^+$ macrophages, MHCII-positive antigen-presenting cells, circulating monocytes, splenic and circulating cytotoxic ($CD8^+$) and helper ($CD4^+$) T cells and mature follicular and marginal zone (MZ) B cells, with immature B cells not being able to repopulate the spleen (Popovich et al. 2001; Noble et al. 2018). SCI and high levels of cytokines are further related to reduced leukocyte expression of cell adhesion molecules and macrophage phagocytic ability (Noble et al. 2018). All in all, splenic leukopenia is going to limit the capacity for antigen recognition, phagocytosis, antibody production and lysis (via complement) of pathogens (Lucin et al. 2007; Noble et al. 2018).

The resultant SCI-IDS is going to increase the incidence of infections, namely pneumonia and inferior urinary tract infections (Brommer et al. 2016).

In mid-thoracic lesions, such as in T9, although the supraspinal control of the spleen is mostly preserved and, thus, the leukocyte splenic populations will react normally to stimuli, the sympathetic pre-ganglionic innervation to the bone marrow is not, as it lies between T8 and lumbar vertebra 1 (L1) (Lucin et al. 2007; Blomster et al. 2013; Noble et al. 2018). Therefore, T9 lesions will mostly or completely ablate sympathetic control of the bone marrow (Lucin et al. 2007), making the spleen the main source of monocyte-derived macrophages that infiltrate the spinal cord after an injury (Blomster et al., 2013).

2.1.2.4. Bladder

2.1.2.4.1. Spinal cord injury and bladder pathology

In a normal bladder, precise sensory information must be conveyed to the CNS to control micturition (Holstege and Collewijn 2009). This is done through afferent fibres from the bladder wall to the sacral spinal cord (Holstege and Collewijn 2009). Mechanoreceptors in the muscle wall relay information through myelinated (A-δ) fibres and unmyelinated C-fibres (Holstege and Collewijn 2009). The latter are only activated by high filling pressures. The information from C-fibres is then sent to higher centres, both in the brainstem, hypothalamus and thalamus and, eventually, from the thalamus to the cortex (Holstege and Collewijn 2009) (Fig. 4). Not all information becomes conscious, only C-fibres contribute to alert the individual of high bladder pressure and the need to urinate (Holstege and Collewijn 2009).

Motor innervation of the bladder and sphincters is both done by the autonomic nervous system (ANS) and the somatic nervous system. The sympathetic nervous system, located between T10 and L2 is responsible for decreasing bladder pressure during the filling phase. The parasympathetic nervous system, located between sacral vertebrae 2 (S2) and S4, on the other hand, is responsible for detrusor muscle contraction and bladder emptying (Holstege and Collewijn 2009; Perez et al. 2022). The external urethral sphincter is innervated by the somatic system as the sphincter is composed of striated muscle (Holstege and Collewijn 2009). The motoneurons behind its control continuously contract this sphincter. Therefore, inhibition of these neurons has to occur for micturition to happen (Holstege and Collewijn 2009).

The periaqueductal grey (PAG), the central grey matter of the midbrain, receives information relayed from both A-δ fibres and C-fibers (Holstege and Collewijn 2009). This structure decides when micturition is going to take place, on the basis of information from more rostral structures (Holstege and Collewijn 2009; Perez et al. 2022). The PAG is going

to project to the pontine micturition centre (PMC) and with the information relayed from the forebrain and the ascending sensory information from the bladder decide whether to activate the cells in the PMC (Fig. 4 – blue and red (Pelvic nerve)) (Holstege and Collewijn 2009). The PMC in turn can simultaneously excite the detrusor muscle and inhibit the internal urethral sphincter, through the activation of parasympathetic preganglionic neurons (Fig.4 – green), and inhibit the external striated urethral sphincter muscle, indirectly leading to its relaxation by supressing the Onuf's nucleus (Fig. 4 – red (Pudendal nerve)), so that a synergic micturition can occur (Holstege and Collewijn 2009; Perez et al. 2022). The sympathetic outflow to the bladder will also be inhibited (Fig. 4 – red (Hypogastric nerve)) (Fowler et al. 2008). The contraction of the detrusor muscle and voiding will be maintained by sacral reflex arc activation (Perez et al. 2022).

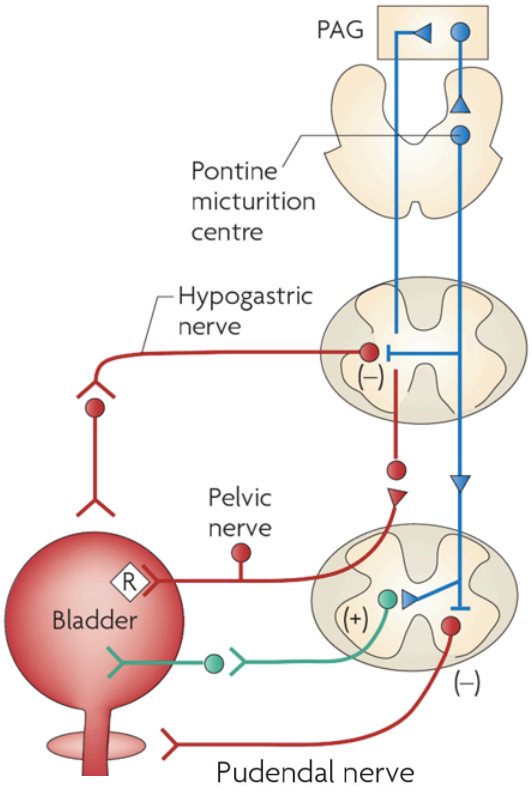

Figure 4 - Control of micturition. The PMC, activated by the PAG (blue), is going to excite the detrusor muscle and inhibit the internal urethral sphincter through the activation of parasympathetic preganglionic nuclei (green). At the same time, the PMC is going to inhibit the sympathetic (Hypogastric nerve) and pudendal (somatic) outflow to the external urethral sphincter (red). This diagram does not show the generation of conscious bladder sensations, nor the mechanisms behind the switch from storage to voiding, both of which may involve cerebral circuits above the PAG. Source from Fowler et al. (2008)

Considering the information above, it is now possible to understand that a traumatic SCI is going to cause a range of pathological events in the bladder. Most of the deficits are caused by the disruption of supraspinal control of the bladder (Herrera et al. 2010). By preventing communication between the PMC and the sacral reflex arc, there will be no inhibition of the reflex arc activation, leading to detrusor muscle hyperreflexia and, as the external urethral sphincter cannot be inhibited, no sphincter relaxation. Overall, this causes the so-called detrusor-sphincter dyssynergia (Perez et al. 2022). Accumulation of urine leads to overdistension of the bladder and the constant high intravesical pressures have repercussions in the upper urinary tract and can lead to hypertrophy of the smooth muscle mass (Herrera et al. 2010; Perez et al. 2022).

Common to the SCI population is a sustained ulceration of the uroepithelium, leaving the bladder vulnerable to chronic and haemorrhagic cystitis and an increased risk of bladder cancer (Perez et al. 2022). Bladder afferents to the detrusor muscle are also known to be found in the uroepithelium. After injury, these afferents release norepinephrine that, together

with other systemic stress hormones, will disrupt tight junctions, leading to uroepithelium disruption and haematuria (Perez et al. 2022). Consequently, allowing urine to cross the uroepithelial barrier, leads to inflammatory cell infiltration that in turn can further contribute to tight junction disruption (Apodaca et al. 2003; Perez et al. 2022).

2.1.3. Medical management and treatment

In the acute phase of a SCI, the first medical procedure is haemodynamic control (Ahuja et al. 2017). This is important to avoid systemic hypotension and spinal cord hypoperfusion. Furthermore, early decompression of the spinal cord is important to avoid further ischaemia and, therefore, the worst secondary injury responses (Ahuja et al. 2017). The acute use of steroids is also a gold standard procedure after SCI. Methylprednisolone, a potent synthetic glucocorticoid, upregulates anti-inflammatory cytokine release and reduces oxidative stress, enhancing neural cell survival (Ahuja et al. 2017). Chronic management entails symptomatic management and rehabilitation. This involves an interdisciplinary approach to ameliorate the quality of life and combat the associated secondary conditions (Ahuja et al. 2017).

It is evident that new approaches are needed, with new drugs and treatments being studied and tested to improve neuroprotection and avoid neurodegeneration.

A new breakthrough was achieved recently by Paramos-de-Carvalho, Martins, et al. (2021), where a persistent accumulation of senescent cells was described in injured spinal cords in a non-regenerative mammalian model, the mouse. When senescent cells were eliminated, through the use of senolytic drugs (ABT-263), there was a significant improvement in the motor, sensory and bladder functions of the injured animals. This improvement was associated with a significant reduction in detrimental cytokines, chemokines and senescent-associated secretory phenotype (SASP) factors. This makes senolytics promising new drugs for the treatment of SCIs, in particular in the control of inflammation (Paramos-de-Carvalho, Martins, et al. 2021).

ABT-263, in particular, is an oral bioavailable drug with senolytic and anti-neoplasic functions (Tse et al. 2008; Zhu et al. 2016). It acts by inhibiting anti-apoptotic Bcl-2 family proteins, thus, promoting apoptosis of senescent cells, where these proteins are often upregulated (Zhu et al. 2016). The pharmacokinetic profile of ABT-263 is characterized by a low volume of distribution, a bioavailability of 50%, when administered in a lipid-based formulation, and in the dog a half-life of 8.9 hours. In mice treated with a 50 mg/kg dose the maximum plasma concentration (C_{max}) was 5.4μmol/L and the area under the curve (AUC) 54μmol/L (Tse et al. 2008). Nevertheless, there is still lack of information about this drug, namely, exactly how its metabolized and the extent of its adverse effects, with studies highlighting gastrointestinal problems, thrombocytopenia and neutropenia as common

toxicities (Wilson et al. 2010). At the moment the drug is being tested and studied in phase I and phase II trials.

2.2. Senescence

In order to better understand the objectives of this work, it is important to introduce senescence and how it could underlie the pathology seen in different organs after SCI.

Cellular senescence is a form of stable cell cycle arrest of diploid cells, which limits their proliferative lifespan (Calcinotto et al. 2019). Senescent cells accumulate with age as telomeres get shorter, but can also be induced by a variety of stimuli, e.g., oncogene activation, DNA damage, oxidative stress and tissue damage. Even though often associated with ageing and deleterious effects, these cells also play important and beneficial roles, such as wound healing, tissue repair, cellular reprogramming and embryonic development (Muñoz-Espín and Serrano 2014; Rhinn et al. 2019).

When trying to identify senescent cells it is important to use at least three hallmarks of senescence (Fig. 5). These include: activity of senescent-associated β-galactosidase (SA-β-gal); cell cycle inhibitors such as $p16^{INK4a}$, $p21^{CIP1}$, and p53; altered cell size; senescence-associated heterochromatin foci; accumulation of lipofuscin; DNA damage foci; loss of Lamin B1; upregulation of some microRNAs; among others. In addition, these metabolic active cells will secrete a SASP rich in chemokines, cytokines, growth factors, proteases, and matrix components, which will influence the surrounding microenvironment (Calcinotto et al. 2019; Paramos-de-Carvalho, Jacinto, et al. 2021).

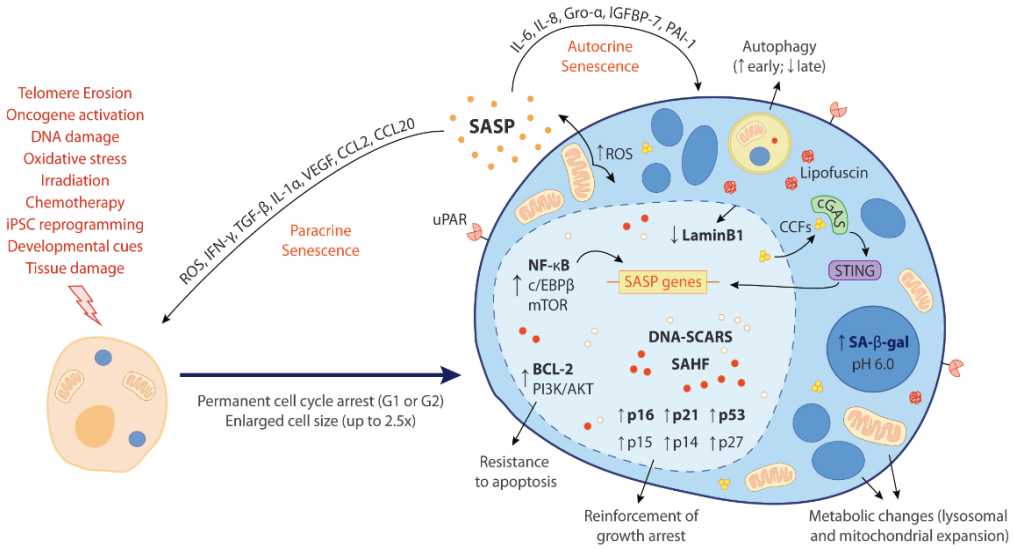

Figure 5 - Hallmarks of senescence. Different stimuli can induce cellular senescence (red). These lead to permanent cell cycle arrest and the cell gains certain features. Namely, the upregulation of key cell cycle inhibitors (p16, p21, p53, p15, p14, p27), anti-apoptotic pathways BCL-2 and P13K/AKT, SA-β-gal activity, SASP, among others depicted in the image. There are also phenotypic alterations such as cellular enlargement, lipofuscin accumulation and mitochondrial and lysosomal expansion. The SASP secreted can induce paracrine senescence and reinforce the senescent program in an autocrine manner. The factors in bold are the most common associated with senescence. Source from Paramos-de-Carvalho, Jacinto, et al. (2021).

SASP is also responsible for paracrine senescence, in which senescence induces senescence, through a variety of factors such as ROS, Interferon Gamma (IFN-γ), Transforming Growth Factor β (TGF-β), IL-1α, VEGF, CCL2 and CCL20 (Calcinotto et al. 2019). This paracrine senescence has been related to the promotion of tumorigenesis, ageing and lack of regeneration. Autocrine senescence also occurs, with some factors reinforcing the senescence program (Calcinotto et al. 2019).

SASP effects on the microenvironment can be beneficial or detrimental depending on the time from the beginning of senescence and the associated SASP (Fig. 6). A transient SASP is often correlated with beneficial effects, anti-fibrotic and anti-inflammatory effects and immune clearance of the senescent cell to avoid their accumulation and persistence (Fig. 6). Contrastingly, a persistent SASP, maintained and promoted by paracrine senescence is detrimental by promoting pro-fibrotic and pro-inflammatory effects on the microenvironment (Fig. 6) (Paramos-de-Carvalho, Jacinto, et al. 2021).

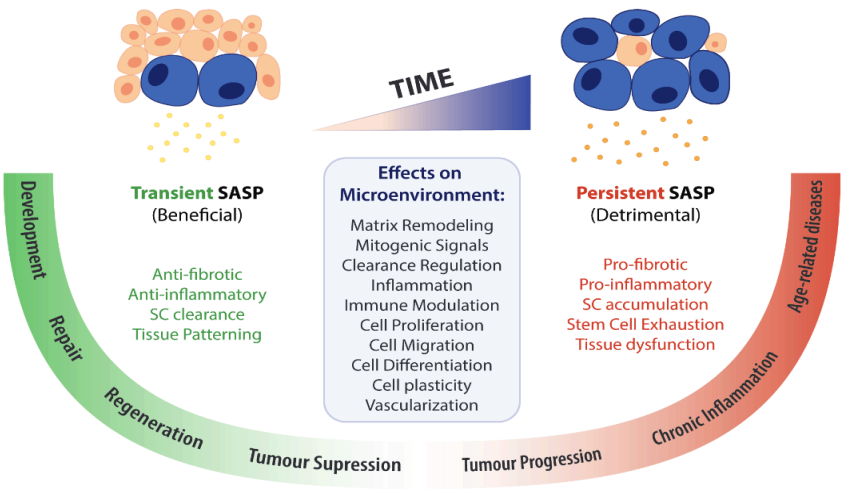

Figure 6 - Transient versus persistent effects of the SASP. Schematic representation of the beneficial and detrimental effects of the SASP in function of their time persistence. Source from Paramos-de-Carvalho, Jacinto, et al. (2021).

In the liver, senescence has been associated with a variety of chronic liver diseases. Senescent hepatocytes have been linked to NAFLD (Aravinthan and Alexander 2016; Ogrodnik et al. 2017) and their accumulation with the progression of the disease (Aravinthan et al. 2013; Aravinthan and Alexander 2016; Papatheodoridi et al. 2020). Insulin resistance has also been associated with hepatocyte senescence (Aravinthan et al. 2013; Aravinthan et al. 2015). Cholangiocyte senescence has been demonstrated in advanced stages of chronic parenchymal liver disease, such as NAFLD (Aravinthan and Alexander 2016). These senescent cholangiocytes impair biliary function, promoting paracrine senescence in hepatocytes and blunt liver regeneration (Ferreira-Gonzalez et al. 2018). Other liver cells,

such as hepatic stellate cells (HSCs), are often activated by hepatocyte and biliary damage and senescence, therefore, promoting fibrosis by the deposition of ECM components (Huda et al. 2019). After an acute insult, these cells eventually become senescent and are cleared as a homeostatic mechanism to impede further fibrosis (Krizhanovsky et al. 2008). However, when the insult persists, as is the case in NAFLD, these cells accumulate and promote further inflammation, advancing fibrosis and even tumorigenesis (Krizhanovsky et al. 2008; Fujita and Narumiya 2016).

In the spleen, a senescent microenvironment, which develops with age, has been described (El-naseery et al. 2020; Budamagunta et al. 2021). This, associated with changes in splenic microarchitecture, is related to changes in immune cell localization and function, being responsible for an altered immune function and higher susceptibility to infections and cancer (El-naseery et al. 2020; Budamagunta et al. 2021).

Finally, in the bladder, senescence has been associated in the urothelium with the loss of barrier function, altered signalling and sensation of bladder fullness, leading to symptoms of frequency and urgency (Klee et al. 2018). Senescence in the bladder has also been associated with the progression of bladder cancer, although in some instances was shown to limit further tumour development (Santin et al. 2020).

2.3. Aims and objectives

Paramos-de-Carvalho, Martins, et al. (2021) showed that the sub-acute pro-inflammatory and pro-fibrotic microenvironment detected in the spinal cord after an injury is successfully modulated by the administration of the senolytic drug ABT-263. This molecular modulation also translated into histopathological, motor, sensory and bladder function improvements. Thus, the non-regenerative microenvironment observed in the spinal cord after an injury might be explained by the accumulation of senescent cells and their SASP.

Knowing that SASP contains factors that can induce paracrine senescence in neighbouring cells, we hypothesized that a chronic accumulation of senescent cells in the spinal cord will produce enough SASP factors, which by becoming systemic, will induce senescence and SASP in peripheral organs. These peripheral induced senescent cells would then be responsible for the multiple organ dysfunction observed, mainly in the liver, spleen and bladder. As ABT-263 was shown to be effective in improving spinal cord pathology we wanted to know if it could also have a beneficial effect in these peripheral organs by eliminating senescent cells.

To answer these hypothesis, firstly, we wanted to characterize the proteomic profile of the spinal cord at 30 dpi to verify if the 15 dpi pro-inflammatory and pro-fibrotic profile continued chronically, and if the effect of ABT-263 treatment would persist at chronic stages. After verifying the chronic persistence of the SASP and other cytokines and chemokines, we

characterized the proteomic profile of peripheral organs, with and without ABT-263 treatment.

This study also sought to compare the proteomic profile with the histopathology, with and without senolytic treatment, for detection of potential correlations. Finally, we wanted to see how the proteomic profile and the histopathology correlated with fluctuations in the number of senescent cells. In other words, could a deleterious microenvironment and related pathology be associated with increased numbers of senescent cells in these organs.

3. Material and methods

3.1. Ethical statement

All handling, surgical and post-operative care were approved by the Instituto de Medicina Molecular - João Lobo Antunes (IMM-JLA) internal animal welfare responsible committee (Organização Responsável pelo Bem-Estar Animal - ORBEA) and the Portuguese competent authority (Direção Geral de Alimentação e Veterinária - DGAV), complying with the European Directive 2010/63/EC and with the Portuguese Law on animal care that transposes the Directive (DL 113/2013). All efforts were made to minimize the number of animals used as well as any suffering.

3.2. Sample characterization and experimental groups

The samples used in this study were collected during the study of Paramos-de-Carvalho, Martins, *et al.* (2021). All the details from the animals used, husbandry, SCI operatory and post-operatory care, drug treatment, behavioural tests and sample collection can be found in this paper.

In brief, the samples used were collected from SCI animals with a moderate-to-severe (force: 75 Kdyne; displacement: 550-750 mm) contusion at the level of T9, done using the Infinite Horizon Impactor (Precision Systems and Instrumentation, LLC.) (Scheff et al. 2003). The mean applied force and tissue displacement were equal between the experimental groups.

Only animals with certain biomechanical and behavioural injury criteria (displacement between 550-750 mm and BMS average score of $\leq$0.5 across both hindlimbs at 1 dpi, respectively) were included in the study. Considering these parameters, a total of 27 mice were used in the study. 9 of these animals were used to perform a histopathological/immunohistochemical analysis and the remaining 18 for a molecular analysis through cytokine array.

After performing SCI, animals were randomly assigned to each experimental group and end-point. Considering the above SCI animals, two experimental groups were created: the ABT-263-treated group and the vehicle-treated group.

ABT-263-treated animals were given a senolytic drug ABT–263 (Selleckchem, S1001, 50mg/kg/day), which eliminates senescent cells, once daily by oral gavage (PO) between 5 to 15 dpi, while the BSCB was still disrupted.

At the same time, vehicle-treated animals were given corn oil PO (Corn oil, Sigma, C8267) during the same period.

In SCI animals, bladders were manually voided twice daily for the duration of the study.

Sham-injured animals were subjected to laminectomy at the same level of the SCI serving as controls.

The researchers were blinded for the duration of the study and data analysis.

In the selection of endpoints, it was taken into consideration the phases of injury evolution, 15 dpi (subacute), where 18 animals were used, and 30 dpi (chronic), using 9 animals, in the mouse contusion model (Ahuja et al. 2017).

3.3. Histopathological and imunohistochemical analysis

3.3.1. End-points

Three animals from each experimental group (ABT-263, Vehicle, and Sham) were randomly selected at 15 dpi for histological analysis.

3.3.2. Tissue processing

Mice were anaesthetized with a ketamine/xylazine mix (120mg/kg +16mg/kg, IP) and transcardially perfused with 0.9% sodium chloride followed by 4% PFA perfusion for 10 minutes. *A post-mortem* anatomical assessment of the spinal cord was carried out to confirm the place of contusion.

The liver, spleen and bladder were collected and put in 10% neutral buffered formalin.

3.3.2.1. Liver

The right lobe of the liver was separated from the rest of the lobes, divided in 3 equal parts (internal, medial and external) and embedded in OCT for cryosectioning. This was done by snap freezing the blocks in isopentane cooled to -70ºC to -80ºC in liquid nitrogen. The blocks were stored at -80ºC until sectioning.

The right lobe was sectioned transversally at 10µm using a cryostat (Leica CM 3050S) at -18ºC. Five sets of 10 slides each were sectioned from each block.

Slides were stored at -20ºC until needed. Every block, as well as every slide, was coded until the end of each analysis.

The left lobe of the liver was also separated from the remaining lobes, embedded in paraffin and sectioned at 5µm using a microtome (Leica RM 2245).

3.3.2.2. Spleen and Bladder

The entire organ was divided into 2 segments across its longest axis, embedded in OCT and snap frozen as described above. The sections were obtained transversally from the midline of the organ to either side.

The blocks were cryosectioned at 5µm.

Slides were stored and identified as described in 3.3.2.1.

3.3.3. Stainings and immunohistochemistry

3.3.3.1. Stainings

All organs collected were routinely stained with Haematoxylin & Eosin (H&E). Other special stainings were used in the case of the liver to highlight and quantify specific characteristics. Therefore, it was used Oil Red O (to quantify lipid accumulation) (Sigma O0625), Acid Fushin Orange G (AFOG) (to quantify collagen deposition, fibrosis and protein accumulation) (Aniline Blue (Riedel-de Haen ref.32703), Orange G (Sigma O7252-25G), Acid Fuchsin (Chroma-Gesellschaft ref.10765, 11505)), Periodic Acid-Schiff (PAS) (to quantify glycogen deposition) (Sigma 395B-1KT) and Perls Prussian Blue (to quantify iron sequestration/accumulation) (Sigma HT20-1KT)).

To evaluate and quantify the number of senescent cells a SA-β-gal staining kit (Cell Signalling, #9860, optimal pH 5.9-6.1) was used. This assay determines SA-β-gal activity in cells, one of the many hallmarks of senescence (Paramos-de-Carvalho, Jacinto, et al. 2021).

The stainings used in each case are described in more detail in Table 1.

Table 1 - Stainings specificities by organ

Organ	Embedding	Staining
Liver	Paraffin (Left lobe)	HE; PAS; Perls Prussian Blue
	OCT – Frozen (Right lobe)	Oil Red O; AFOG; SA-β-gal
Spleen	OCT - Frozen	HE; SA-β-gal
Bladder	OCT - Frozen	HE; SA-β-gal

3.3.3.2. Immunohistochemistry

T Cells and liver resident macrophages (Kupffer cells) were identified using anti-CD3 (1:500, Abcam, ab5690) and anti-Clec4f (1:200, Thermo Fisher, PA5 – 47396), respectively.

Clec4f is a specific marker of murine KCs and helps distinguish, in association with other markers, these resident macrophages from monocyte-derived macrophages (Scott et al. 2016).

For this particular immunohistochemistry, antigen retrieval was performed at pH 6 and 95ºC using PT Link (Pre-treatment module for tissue specimens, Leica Biosystems) for 1 hour. Sections were then incubated for 30 minutes with 3% hydrogen peroxide in methanol, washed (EnVision Flex Wash Buffer, Dako, K8007), and blocked for 40 minutes at room temperature (RT) (Protein Block Serum-free, Dako, X0909). Following this, the sections were incubated for 1 hour at RT with the primary antibody, washed and further incubated with the secondary antibody. The sections incubated with anti-CD3 were then incubated with a ready-to-use α-rabbit conjugated with HRP secondary antibody (EnVision Flex conjugated with HRP (α-rabbit), Dako, K4010) for 30 minutes at RT. The sections incubated with anti-Clec4f were incubated with a donkey anti-goat conjugated with HRP secondary antibody (1:2000, Thermo Fisher, PA1-28664) for 30 minutes at RT. The sections were once more washed, revealed with DAB (Dako, K3468) for 2 to 5 minutes and counterstained with Harris Haematoxylin (Bio-optica, 05-06004E).

3.3.4. Histopathological analysis

All the organs collected were blindly analysed using a brightfield optical microscope (DM2500, Leica Biosystems). A histopathological exam was performed. Some of the histopathological characteristics observed with H&E were corroborated by special stainings, as described above.

3.3.5. Imaging

All the images used and presented in this work were either acquired using a NanoZoomer-SQ digital slide scanner (Hamamatsu) or a brightfield microscope (Leica DM2500) using 10x, 20x (both HC PL FLUOTAR) and 40x and 100x (both HCX PL FLUOTAR) with a colour camera (Leica DFC450).

3.3.5.1. Quantification of inflammatory cells

The number of inflammatory infiltrates was manually counted in the H&E slides and normalized for the area of tissue using QuPath (Bankhead et al. 2017).

KCs were quantified using positive pixel detection for DAB colouration by threshold definition with QuPath (Bankhead et al. 2017). The measurements of KCs were expressed as a percentage of the total cross-sectional area of tissue.

T lymphocytes were manually quantified using the QuPath cell counter and normalized for the area of tissue (Bankhead et al. 2017).

The averages of each group were calculated.

3.3.5.2. Quantification of lipid accumulation

Oil Red O stained slides were quantified for lipid accumulation using positive pixel quantification by the definition of a colour threshold with QuPath and normalized for the area of tissue (Bankhead et al. 2017). The measurements of Oil Red O positive cells were expressed as a percentage of the tissue cross-sectional area.

3.3.5.3. Quantification of SA-β-gal positive cells

A complete set of 10 slides of each organ for each animal was stained for SA-β-gal and scanned using NanoZoomer-SQ digital slide scanner. TIFF images of each section of the slide were taken using NDP-viewer (Hamamatsu) and given a code. All the images acquired were quantified for blue-marked SA-β-gal^{+} cells using image analysis software (QuPath) (Bankhead et al. 2017). The number of SA-β-gal^{+} cells was automatically counted after the definition of a colour threshold and normalized for the area of tissue.

3.4. Cytokine arrays

The molecular analysis of cytokine and chemokine expression in the spinal cord, liver and bladder homogenates at 15 dpi and 30 dpi was performed using a Proteome Profiler Mouse XL Cytokine Array (ARY028; R&D Systems, Minneapolis, MN, USA), which detects simultaneously 111 mouse cytokines.

The homogenates were prepared by homogenizing the organs in lysis buffer (PBS/1% Triton X-100/protease) and phosphatase inhibitors - cOmplete™, EDTA-free Protease Inhibitor Cocktail (Roche, 11873580001). Protein concentration was determined by DC Protein Assay (BioRad, 5000111) and read using a microplate reader (Tecan Infinite M200). For the spinal cord 200 mg of protein was used for the cytokine array, while for the remaining organs 300 mg of protein was used. In summary, nitrocellulose membranes were blocked for 1 hour; then, the specific amount of protein content was added and incubated overnight in a rocking platform at 4ºC. The following day, the membranes were washed and incubated with streptavidin-HRP for 30 minutes and after being washed again, spot detection was enhanced by the addition of a chemiluminescence reagent. The membranes were read

on Amersham 680 (GE Healthcare) and dots density was quantified using Image Studio Lite software.

The factors of interest were then grouped according to their known roles, although some of them can have other functions and their action can be different according to the organ where they were identified. See Table 2 for factors and their functions.

Table 2 – Cytokine array factors and respective functions.

Factor	Function	Reference
Angiopoietin-1	Angiogenic factor (SC; Bladder). Liver fibrosis and HSCs activation (Liver).	Taura et al. 2008; Ritz et al. 2012; Karlsson et al. 2021; The Human Protein Atlas 2022d
C Reactive Protein	Inflammatory factor (Bladder). Associated with bladder cancer.	Chuang et al. 2010; Karlsson et al. 2021; O'Brian et al. 2021; The Human Protein Atlas 2022d
CCL-2	Liver fibrosis and HSCs activation; Inflammatory factor (Liver).	Degré et al. 2012; Ehling et al. 2014; Chen et al. 2018; Xi et al. 2021
CCL-3/4	Inflammatory factors (Bladder).	Coppé et al. 2010; Karlsson et al. 2021; The Human Protein Atlas 2022d
CCL-6	Inflammatory factor (Liver).	Chen et al. 2018; Poulsen et al. 2022
CCL-11	Inflammatory factor (SC).	Paramos-de-Carvalho, Jacinto, et al. 2021; Paramos-de-Carvalho, Martins, et al. 2021
CCL-12	Pro-inflammatory factor (SC; Liver).	Sarafi et al. 1997; Chen et al. 2018; Poulsen et al. 2022
CCL-17	Inflammatory factor (Bladder).	Karlsson et al. 2021; The Human Protein Atlas 2022d
Complement components C5/C5a	Inflammatory factors (Bladder).	Karlsson et al. 2021; The Human Protein Atlas 2022d
Complement Factor D	Inflammatory factor (Liver; Bladder).	Karlsson et al. 2021; The Human Protein Atlas 2022d
CXCL-9	Liver fibrosis and HSCs activation (Liver). Inflammatory factor (Bladder). Associated with bladder cancer.	Wasmuth et al. 2009; Sahin et al. 2012; Gonzalez et al. 2014; Chen et al. 2018; Guo et al. 2018; Nazari et al. 2020; Li et al. 2021; Poulsen et al. 2022
Cystatin C	Tumoral marker (Bladder).	Tokarzewicz et al. 2018
Endoglin	Angiogenesis promotor and regulator (Bladder).	Karlsson et al. 2021; The Human Protein Atlas 2022d
Epidermal Growth Factor (EGF)	Growth Factor; Mitogen and tumour promotor (Bladder).	Cheng et al. 2002; Coppé et al. 2010; Kuo 2014; Lin et al. 2022
Fibroblast Growth Factor (FGF) acidic	Anti-steatotic and anti-fibrotic factor (Liver).	Karlsson et al. 2021; The Human Protein Atlas 2022d
FGF-21	Growth factor (Bladder).	Karlsson et al. 2021; Salgado et al. 2021; The Human Protein Atlas 2022d
Gas6	Liver fibrosis and HSCs activation; NAFLD and NASH progression (Liver).	Bárcena et al. 2015; Smirne et al. 2019; Tutusaus et al. 2020
Granulocyte Colony - Stimulating Factor (G-CSF)	Growth and inflammatory factor (Bladder). Associated with bladder cancer.	Karlsson et al. 2021; The Human Protein Atlas 2022d
Granulocyte macrophage Colony -	Growth factor (Bladder).	Karlsson et al. 2021; The Human Protein Atlas 2022d

Stimulating Factor (GM-CSF)		
Growth/Differentiation Factor – 15 (GDF-15)	Anti-inflammatory factor (Bladder).	Coppé et al. 2010; Wischhusen et al. 2020
Hepatocyte Growth Factor (HGF)	Growth factor (Bladder).	Coppé et al. 2010; Karlsson et al. 2021; The Human Protein Atlas 2022d
I-TAC	Inflammatory factor (SC; Liver). Liver fibrosis and HSCs activation (Liver).	Helbig et al. 2004; Paramos-de-Carvalho, Jacinto, et al. 2021; Paramos-de-Carvalho, Martins, et al. 2021
IFN-γ	Liver fibrosis and HSCs activation (Liver). Inflammatory factor (Liver; Bladder).	Knight et al. 2007; Coppé et al. 2010; Luo et al. 2013; Karlsson et al. 2021; The Human Protein Atlas 2022d
Insulin Growth Factor Binding Protein 1(IGFBP-1)	Growth factor (Bladder).	Karlsson et al. 2021; The Human Protein Atlas 2022d
IGFBP-2	Tumour suppression factor (Bladder).	Coppé et al. 2010; Tang et al. 2019
IGFBP-3	Growth factor (Bladder).	Coppé et al. 2010; Karlsson et al. 2021; The Human Protein Atlas 2022d
IL-1α	Inflammatory factor (Bladder).	Coppé et al. 2010; Karlsson et al. 2021; The Human Protein Atlas 2022d
IL-5	Fibrosis and HSCs activation (Liver). Inflammatory factor (Bladder). Associated with bladder cancer.	Reiman et al. 2006; Lee et al. 2013; Karlsson et al. 2021; The Human Protein Atlas 2022d
IL-6	Pro-inflammatory factor (Liver).	Calcinotto et al. 2019; Karlsson et al. 2021; The Human Protein Atlas 2022b
IL-7	Pro-inflammatory factor (SC; Liver)	Bao et al. 2018
IL-10	Anti-inflammatory factor (Bladder).	Karlsson et al. 2021; The Human Protein Atlas 2022d
IL-11	Fibrosis and HSCs activation; NAFLD and NASH progression (Liver). Inflammatory factor (Liver; Bladder). Associated with bladder cancer.	Wu et al. 2013; Widjaja et al. 2019; Karlsson et al. 2021; Dong et al. 2021; The Human Protein Atlas 2022d; Fung et al. 2022
IL-12p40	Inflammatory factor (Bladder).	Kalin'ski et al. 2001; Walter et al. 2001; Cooper and Khader 2007; Tyagi et al. 2010; Karlsson et al. 2021; The Human Protein Atlas 2022d
IL-13	Anti-inflammatory factor (Bladder).	Coppé et al. 2010; Karlsson et al. 2021; The Human Protein Atlas 2022d
IL-27p28	Fibrosis and HSCs activation (Liver). Inflammatory factor (Liver; Bladder).	Mitra et al. 2014; Kourko et al. 2019; Min et al. 2021
IL-28 A/B	Pro-inflammarory factor (SC; Bladder).	Manivasagam et al. 2022
IL-33	Inflammatory factor (SC; Liver; Bladder). Fibrosis and HSCs activation (Liver).	Kochiashvili and Kochiashvili 2014; Weiskirchen and Tacke 2017; Saito et al. 2020; Yamagishi et al. 2022; Jensen et al. 2018; Tan et al. 2018; Yazdani et al. 2018; Paramos-de-Carvalho, Jacinto, et al. 2021; Paramos-de-Carvalho, Martins, et al. 2021

Leptin	Inflammatory and fibrogenic factor (Liver).	Martínez-Uña et al. 2020; Petrescu et al. 2022
Leukaemia Inhibitory Factor (LIF)	Induction of APP production, fibrogenesis, cell adhesion, attenuation of hepatic steatosis and insulin resistance (Liver).	Moran et al. 1997; Hisaka et al. 2004; Karlsson et al. 2021; The Human Protein Atlas 2022c; Yuan et al. 2022
Lipocalin-2	Fibrosis and HSCs activation (Liver). Inflammatory factor (Bladder).	Moschen et al. 2017; Chen et al. 2020; Ahn et al. 2021
Matrix Metalloproteinases-2 (MMP-2)	Fibrosis and HSCs activation (Liver). Angiogenesis promoter and regulator (Bladder).	Naim et al. 2017; Karlsson et al. 2021; The Human Protein Atlas 2022d
MMP-3	Extracellular matrix and wound healing factors (Bladder).	Coppé et al. 2010; Karlsson et al. 2021; The Human Protein Atlas 2022d
Osteopontin	Fibrosis and HSCs activation; Inflammatory factor (Liver).	Wen et al. 2016
Pentraxin 3	Pro-inflammatory factor (Liver).	Feder et al. 2020
Periostin	Pro-fibrotic factor (Liver). Extracellular matrix and wound healing factor; cell adhesion factor (Bladder).	Sugiyama et al. 2016; Kumar et al. 2018; Karlsson et al. 2021; The Human Protein Atlas 2022d
Pigment Epithelium-derived factor (PEDF)	Neuroinflammatory and neurotrophic factor (SC).	Takanohashi et al. 2005; Stevens et al. 2019; He et al. 2022
Platelet-derived endotelial cell growth factor (PD-ECGF)	Growth factor. Tumoral marker (Bladder).	Sawase et al. 1998; Shimabukuro et al. 2005; Karlsson et al. 2021; The Human Protein Atlas 2022d
Pref-1	Fibrosis and HSCs activation (Liver). Growth factor (Bladder).	Karlsson et al. 2021; The Human Protein Atlas 2022d
Proliferin	Growth factor; vascular modulation factor (Bladder).	Karlsson et al. 2021; The Human Protein Atlas 2022d
RAGE	Inflammatory factor; NAFLD and NASH progression (Liver).	Pusterla et al. 2013; Asadipooya et al. 2019; Weinhage et al. 2020
Reg3G	Inflammatory factor (Liver).	Chen et al. 2019; Karlsson et al. 2021; The Human Protein Atlas 2022d
Retinol Binding Protein 4 (RBP4)	NAFLD and NASH progression (Liver).	Huang and Xu 2022
Thrombopoietin (Thpo)	Haemostatic and Neurotrophic functions (SC).	Yang et al. 2016
TNF-α	Inflammatory factor; NAFLD and NASH progression (Liver).	Tiegs and Horst 2022
Vascular Cell Adhesion Molecule 1 (VCAM-1)	NAFLD and NASH progression (Liver).	Furuta et al. 2021
Vascular Endothelial Growth Factor (VEGF)	Growth Factor; Fibrosis and HSCs activation (Liver). Associated with endothelial cell proliferation and migration, apoptosis inhibition and permeabilization of blood vessels.	Calcinotto et al. 2019; Martínez-Uña et al. 2020; Karlsson et al. 2021; The Human Protein Atlas 2022a; Darmadi et al. 2022; Lin et al. 2022
WNT-1-inducible-signalling pathway protein 1 (WISP-1)	NAFLD and NASH progression (Liver). Extracellular matrix and wound healing factor; cell adhesion factor (Bladder).	Karlsson et al. 2021; Pivovarova-Ramich et al. 2021; The Human Protein Atlas 2022d

3.5. Statistical analysis

GraphPad Prism 9 was used for data visualization and statistical analysis. All statistical analysis was done using one-way ANOVA with multiple comparisons, followed by

Bonferroni's post hoc test. All data was expressed as mean ± standard error of the mean (SEM), with statistical significance determined at p-values < 0.05.

4. Results

4.1. Cytokine and chemokine profile characterisation in different organs

4.1.1. Spinal Cord

4.1.1.1. Chronic induction of pro-inflammatory cytokines in the spinal cord is observed in injured animals and is partially reverted by the senolytic treatment

Considering that Paramos-de-Carvalho et al. (2021) observed a chronic accumulation of senescent cells until 60 dpi, it was paramount to start by evaluating if the accumulation of these senescent cells at the injury site correlated with the perpetuation of a detrimental local microenvironment at 30 dpi, as it was described at 15 dpi. To shed some light on the matter, tissue homogenates of the experimental groups (laminectomized (sham), vehicle- and ABT-263-treated injured animals) were evaluated using a proteome XL mouse cytokine array. Measurements were performed on the spinal cord at a later time-point (30 dpi). For the complete list of factors see Annex 1 Supplementary Table 1.

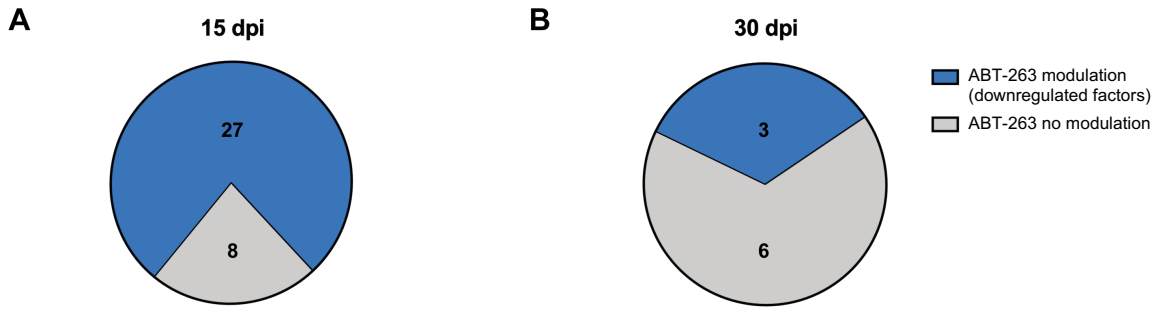

Figure 7 - Evolution of downregulated factors by ABT-263 treatment between 15 and 30 days post-injury. In blue, factors downregulated by ABT-263. In grey, factors where no effect by ABT-263 was observed. (A) At 15 dpi, 35 factors were upregulated after SCI and from those, 27 were downregulated by ABT-263. (B) At 30 dpi, 9 factors were upregulated after SCI and only 3 were downregulated by ABT-263.

At 30 dpi, we found only 9 factors upregulated after injury, in contrast with the 35 factors found at 15 dpi (Fig. 7). Of these 9 factors only 33% were decreased by ABT-263 treatment. A considerable reduction of ABT-263 modulation, when compared with the 77% of factors that were downregulated with the treatment at 15 dpi in the spinal cord (Fig. 7).

Our data showed a significant increase in the levels of the pro-inflammatory interferons IL-28A/B in the spinal cord of vehicle-treated SCI animals compared to the controls (sham) at 30 dpi. These returned to control levels in animals treated with ABT-263 (Fig. 8). The same behaviour happened to Pigment Epithelium-derived Factor (PEDF) and to Thrombopoietin (Thpo) (Fig. 8). PEDF has known neuroinflammatory and neurotrophic

functions and Thpo has haemostatic and neurotrophic functions (Takanohashi et al. 2005; Yang et al. 2016; Stevens et al. 2019; He et al. 2022; Manivasagam et al. 2022). Interestingly, these factors are specific for the 30 dpi, as these were not increased at 15 dpi (Paramos-de-Carvalho, Martins, et al. 2021).

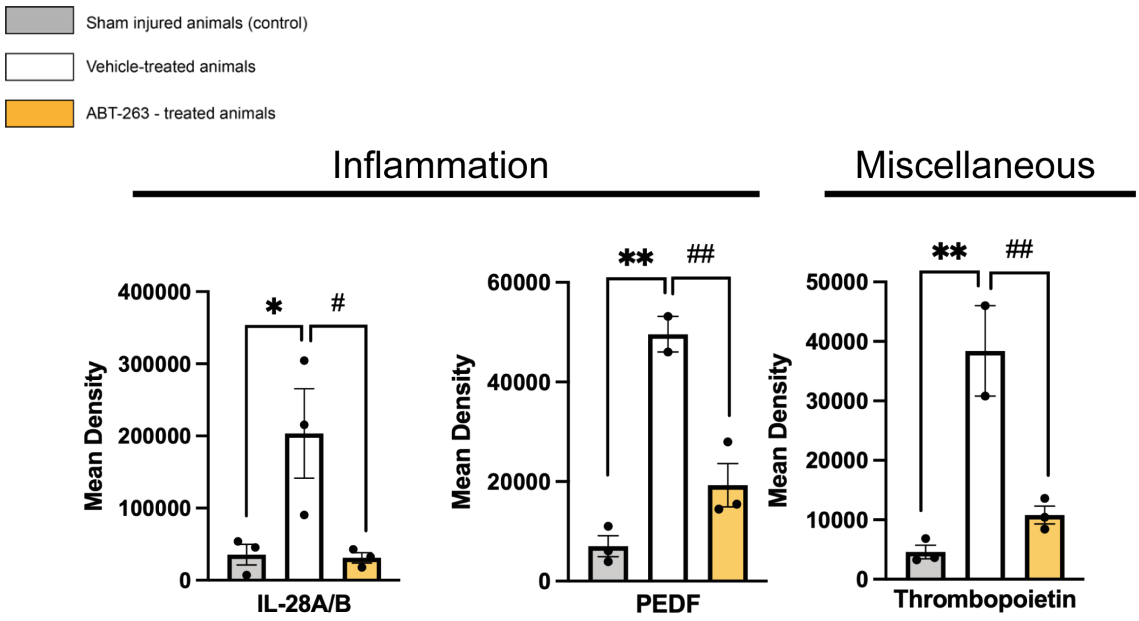

Figure 8 - ABT-263 treatment reduces inflammatory factors induced after spinal cord injury in the spinal cord at 30 days post-injury. Cytokine and chemokine expression was measured in spinal cord homogenates from sham (grey), vehicle (white), and ABT-263 treated (yellow) spinal cord injured animals at 30 days post-injury (dpi). These factors were significantly increased after SCI in the vehicle-treated animals compared to controls and the treatment with ABT-263 was effective in decreasing these factors to basal sham injured levels. Factors were divided into different groups regarding their role: Inflammation and Miscellaneous. (n=2/3) Data is presented as mean density and expressed as mean ± SEM. *p<0.05, **p<0.01, sham versus vehicle; #p<0.05, ##p<0.01, vehicle versus ABT-263.

Similarly, the following factors were only upregulated at 30 dpi in the spinal cord. The angiogenic factor, Angiopoietin-1, and another two pro-inflammatory factors (CCL-12 and IL-7) were also upregulated in the vehicle-treated injured animals compared to controls at 30 dpi, but were not modulated by ABT-263 (data not shown). These factors seem to be specifically induced at later time-points, as these were not upregulated in vehicle-treated injured animals at 15 dpi (Paramos-de-Carvalho, Martins, et al. 2021). IL-7 is also considered a SASP factor (Coppé et al. 2010).

There were three inflammatory cytokines (IL-33, CCL-11 and Interferon-inducible T cell Alpha Chemoattractant (I-TAC)) (Table 2), known SASP factors, whose expression increased with the injury (vehicle-treated injured animals) both at 15 dpi (Paramos-de-Carvalho, Martins, et al. 2021) and 30 dpi (Fig. 9). However, these were not significantly modulated by treatment with ABT-263 at 30 dpi, contrary to what happened at 15 dpi (Paramos-de-Carvalho, Martins, et al. 2021).

Overall, a pro-inflammatory profile is clearly present at 30 dpi in the spinal cord with factors that were already activated at 15 dpi and new ones that seem to be activated only at later time-points.

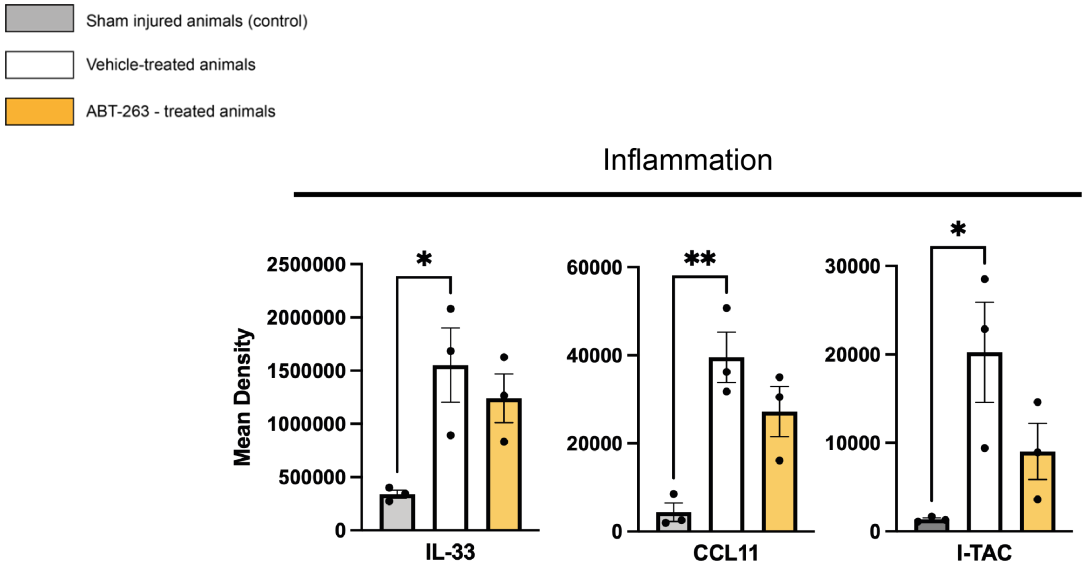

Figure 9 - Inflammatory cytokines IL-33, CCL11 and I-TAC increase after a spinal cord lesion at 30 days post-injury. Cytokine and chemokine expression was measured in spinal cord homogenates from sham injured control (grey), vehicle (white), and ABT-263 treated (yellow) spinal cord injured animals at 30 dpi. IL-33, CCL11 and I-TAC are also known SASP factors. ABT-263 did not decrease the levels of these cytokines. Data is presented as mean density and expressed as mean ± SEM. (n=3) *p<0.05, **p<0.01, sham versus vehicle.

4.1.2. Liver

4.1.2.1. Pro-inflammatory cytokines and growth factors are induced in the liver 15 days after a spinal cord injury

Considering our hypothesis that the spinal cord pro-inflammatory and pro-fibrotic profile can become systemic, we measured the cytokine and chemokine expression in liver homogenates from sham, vehicle- and ABT-263-treated injured animals at 15 dpi.

At 15 dpi the cytokine arrays revealed a statistically significant increase in the levels of inflammatory factors (Leptin, IL-6, Reg3G, Complement Factor D), fibrosis factor (Periostin), growth factor (VEGF), Leukaemia Inhibitory Factor (LIF) and anti-steatotic and anti-fibrotic factor (FGF acidic) in the liver. The 8 factors found upregulated in the liver after SCI were not successfully decreased by ABT-263 treatment (Fig. 10) (Supplementary Table 2 – Annex 1). For the complete list of factors see Annex 1 Supplementary Table 2.

Even though it is possible to observe a decrease in Leptin levels in the ABT-263-treated injured animals compared to the vehicle-treated animals, this is not statistically significant (Fig. 10). This adipokine can act as an inflammatory and fibrogenic factor in the liver (Petrescu et al. 2022).

VEGF, a known SASP factor, only showed a small tendency for reduction in ABT-263-treated spinal cord injured animals (Fig. 10). Leptin is known to induce VEGF, which is associated with endothelial cell proliferation, cell migration, apoptosis inhibition and permeabilization of blood vessels, contributing to liver pathology (Martínez-Uña et al. 2020; Karlsson et al. 2021; The Human Protein Atlas 2022a).

IL-6 showed similar behaviour to Leptin and VEGF (Fig. 10). This cytokine is another known SASP factor and pro-inflammatory cytokine. (Calcinotto et al. 2019; The Human Protein Atlas 2022b).

Leukaemia Inhibitory Factor (LIF), also a SASP factor, belongs to the IL- 6 family and showed similar behaviour in this study to the factors described above (Fig.10). It is known to be upregulated during tissue injury and in the liver has been associated with a variety of functions, ranging from APP production induction in hepatocytes, fibrogenesis and cell adhesion, to attenuation of hepatic steatosis and insulin resistance (Moran et al. 1997; Hisaka et al. 2004; Karlsson et al. 2021; The Human Protein Atlas 2022c; Yuan et al. 2022).

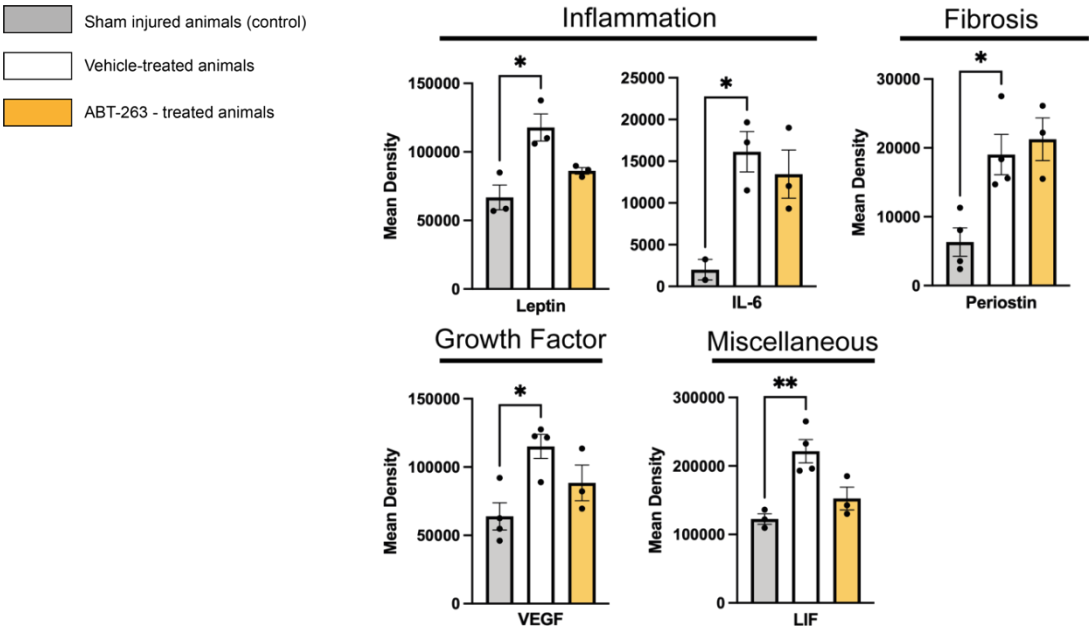

Figure 10 - Leptin, Periostin, and senescence-associated secretory phenotype (SASP) pro-inflammatory cytokine IL-6, VEGF and LIF increase in the liver after a spinal cord lesion at 15 days post-injury. Cytokine and chemokine expression was measured in liver homogenates from sham (grey), vehicle (white), and ABT-263 treated (yellow) spinal cord injured animals at 15 dpi. Factors were divided into different groups regarding their role: Inflammation, Fibrosis, Growth Factors and Miscellaneous. IL-6, VEGF and LIF are known SASP factors. (n=3) Data is presented as mean density and expressed as mean ± SEM. *p<0.05, **p<0.01, sham versus vehicle.

4.1.2.2. At 30 days post-injury, ABT-263 treatment causes the upregulation of several factors in the liver

Cytokine and chemokine expression was also measured in liver homogenates from sham injured controls, vehicle- and ABT-263-treated spinal cord injured animals at 30 dpi.

At 30 dpi the only two factors upregulated in the vehicle-treated injured animals were the pro-inflammatory factor Pentraxin 3, and the pro-fibrotic factor Periostin (Fig. 11) (Table 2). The treatment with ABT-263 was successful in reducing the levels of these factors (Fig. 11). Periostin levels remained elevated from 15 dpi through to 30 dpi in vehicle-treated injured animals (Fig.10 & 11).

In addition to this, 30 factors were found to be specifically induced by ABT-263 (Fig. 12). These factors have been implicated in liver fibrosis and HSCs activation, as well as, liver inflammation and the progression of NASH. Indeed, **Angiopoietin-1; CCL2; CXCL9; I-TAC; Gas 6; IFN-γ; IL-5; IL-11; IL-27p28; IL-33; Lipocalin-2; MMP-2; Osteopontin; Pref-1; VEGF** have been associated with liver fibrosis and HSCs activation; **CCL2; CCL6; CCL-12; I-TAC; IFN-γ; IL-7; IL-11; IL-28A/B; IL-33; Osteopontin; Leptin; RAGE; TNF-α** with liver inflammation; and **RAGE; Retinol Binding Protein 4 (RBP4); Gas6; IL-11; Vascular Cell Adhesion Molecule 1 (VCAM-1); WISP-1**) with NAFLD and the progression of NASH (Table 2). For the complete list of factors see Annex 1 Supplementary Table 2.

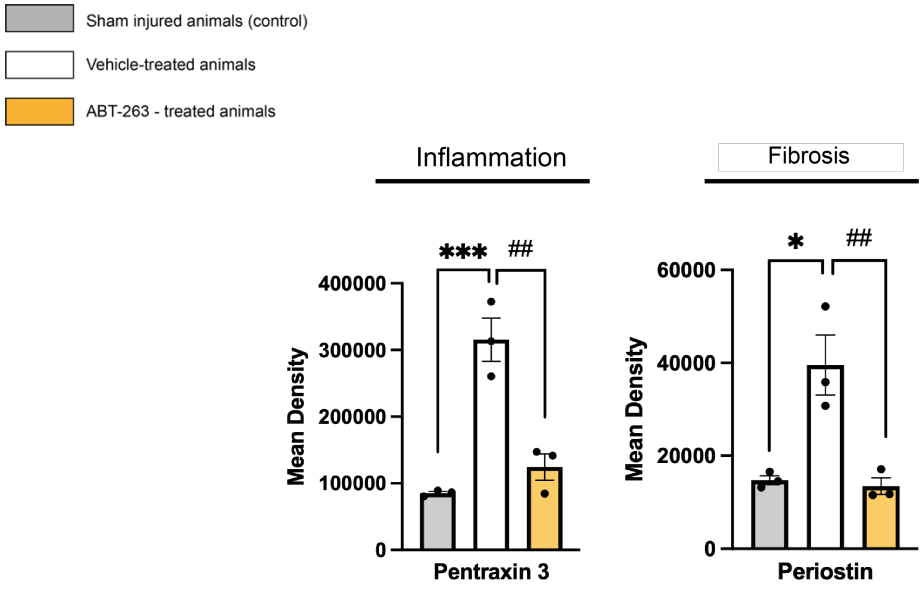

Figure 11 - ABT-263 treatment reduces Pentraxin 3 and Periostin induced after spinal cord injury in the liver at 30 days post-injury. Cytokine and chemokine expression was measured in liver homogenates from sham (grey), vehicle (white), and ABT-263 treated (yellow) spinal cord injured animals at 30 dpi. Both factors were significantly increased after SCI (vehicle-treated animals) compared to controls and the treatment with ABT-263 was effective in decreasing these factors to basal sham injured levels. Factors were divided into different groups regarding their role: Inflammation and Fibrosis. (n=3) Data is presented as mean density and expressed as mean ± SEM. *p<0.05, ***p<0.001, sham versus vehicle; ##p<0.01, vehicle versus ABT-263.

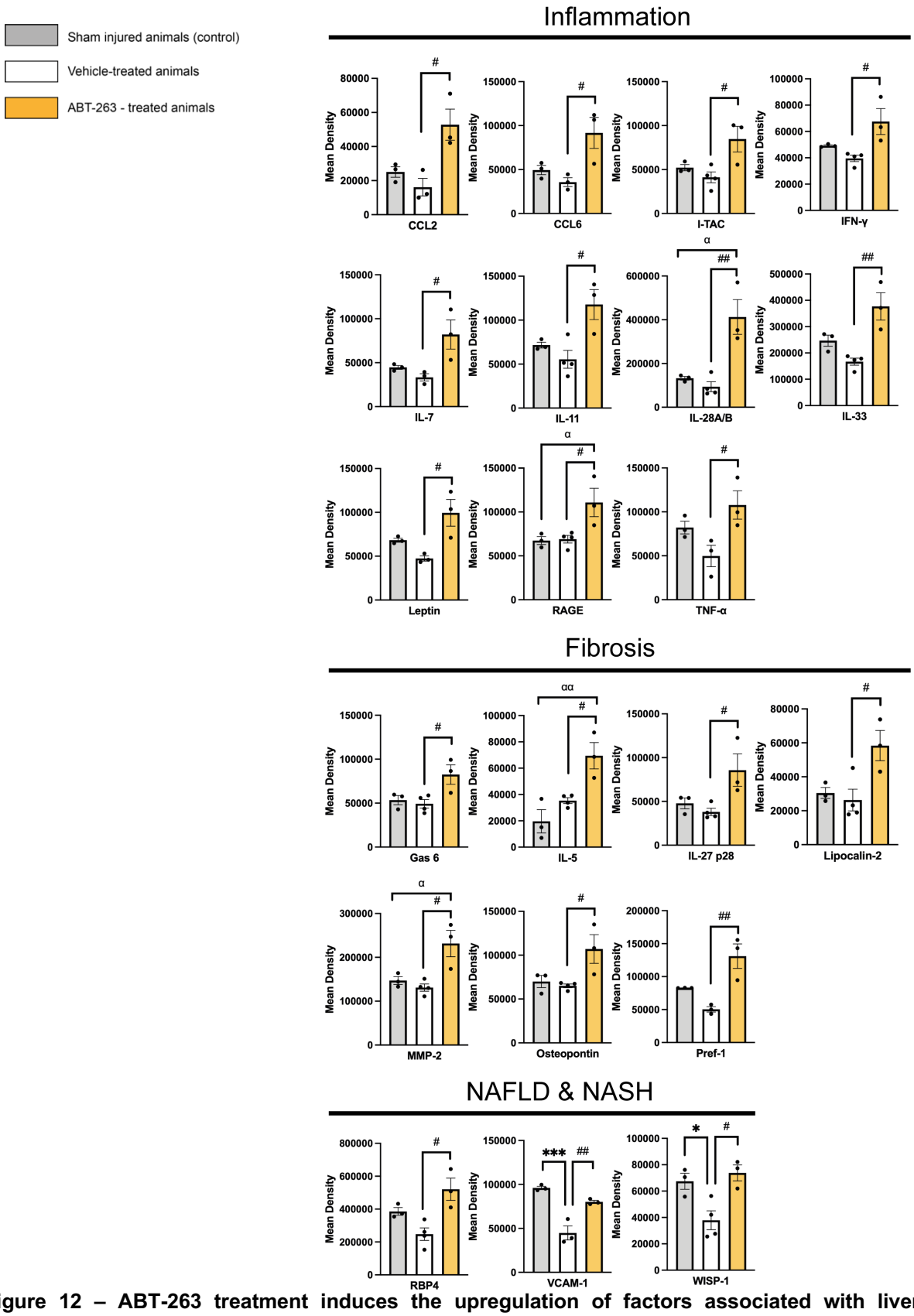

Figure 12 – ABT-263 treatment induces the upregulation of factors associated with liver inflammation, fibrosis and NAFLD and the progression of NASH. Cytokine and chemokine expression was measured in liver homogenates from sham (grey), vehicle (white), and ABT-263 treated (yellow) spinal cord injured animals at 30 dpi. Factors were divided into different groups regarding their role: Inflammation, Fibrosis and NAFLD & NASH. (n=3/4) Data is presented as mean density and expressed as mean ± SEM. ***p<0.001, sham versus vehicle; #p<0.05, ##p<0.01, vehicle versus ABT-263; αp<0.05.

4.1.3. Bladder

4.1.3.1. Senolytic treatment reduces the expression of pro-tumorigenic Epidermal Growth Factor in the bladder of spinal cord injured animals at 15 days post-injury

Cytokine and chemokine expression was also measured in bladder homogenates from sham injured controls, vehicle- and ABT-263-treated spinal cord injured animals at 15 dpi.

Epidermal Growth Factor (EGF) was increased in vehicle-treated injured animals compared to sham (non-injured) at 15 dpi in the bladder (Fig. 13). At the same time, there was a reduction of EGF in the ABT-263-treated injured animals, returning to non-injured (sham) levels (Fig. 13). This factor is a potent mitogen and tumour promoter, and it is also a known SASP factor (Cheng et al. 2002; Coppé et al. 2010) (Table 2).

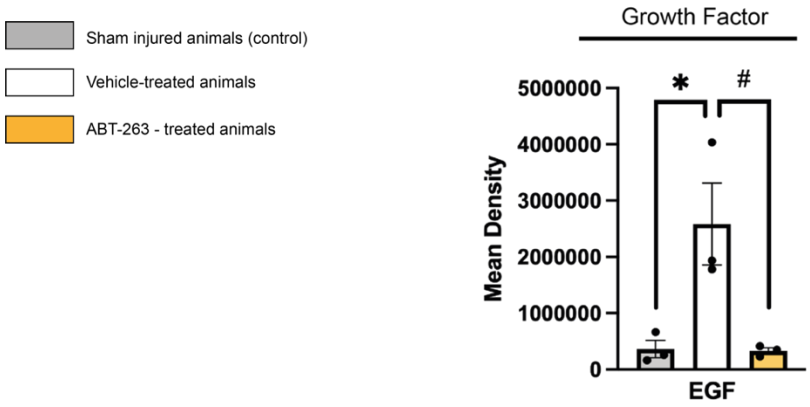

Figure 13 - ABT-263 treatment reduces bladder Epidermal Growth Factor (EGF) levels after spinal cord injury at 15 days post-injury. Cytokine and chemokine expression was measured in bladder homogenates from sham (grey), vehicle- (white), and ABT-263-treated (yellow) spinal cord injured animals at 15 dpi. EGF is a growth factor associated with bladder tumorigenesis and cancer progression. This factor is also part of the senescence-associated secretory phenotype (SASP). (n=3) Data is presented as mean density and expressed as mean ± SEM. *p<0.05, sham versus vehicle; #p<0.05, vehicle versus ABT-263.

4.1.3.2. Pro-inflammatory factors are induced in the bladder after a spinal cord injury

We observed that SCI (vehicle-treated animals) induced a significant increase in several pro-inflammatory cytokines and chemokines, and tumor factors when compared with non-injured animals (sham) (Fig. 14). However, ABT-263 was not successful in modulating this response (Fig. 14). In fact, some factors (CCL-3/4; CXCL9; IL-11; IL-12p40; IL-33; C5/C5a; Cystatin C; Insulin-Growth Factor Binding Protein – 2 (IGFBP-2) and Granulocyte Colony Stimulating Factor (G-CSF)) remained elevated in the ABT-263-treated group (Fig. 14). These factors can be divided into groups based on their function: Inflammation (CCL-3, CCL-4, CXCL9, IL-5, IL-11, IL12p40, IL-33, complement component C5/C5a, CRP, Complement Factor D) (Fig. 14A); tumoral markers (Cystatin C and Platelet-derived

endothelial cell growth factor (PD-ECGF)) (Fig. 14B); tumour suppression factor (IGFBP-2) (Fig. 14B); and growth factor (G-CSF) (Fig. 14C) (Table 2). Of these, CCL-3 and IGFBP-2 are known SASP factors (Coppé et al. 2010). For the complete list of factors see Annex 1 Supplementary Table 3.

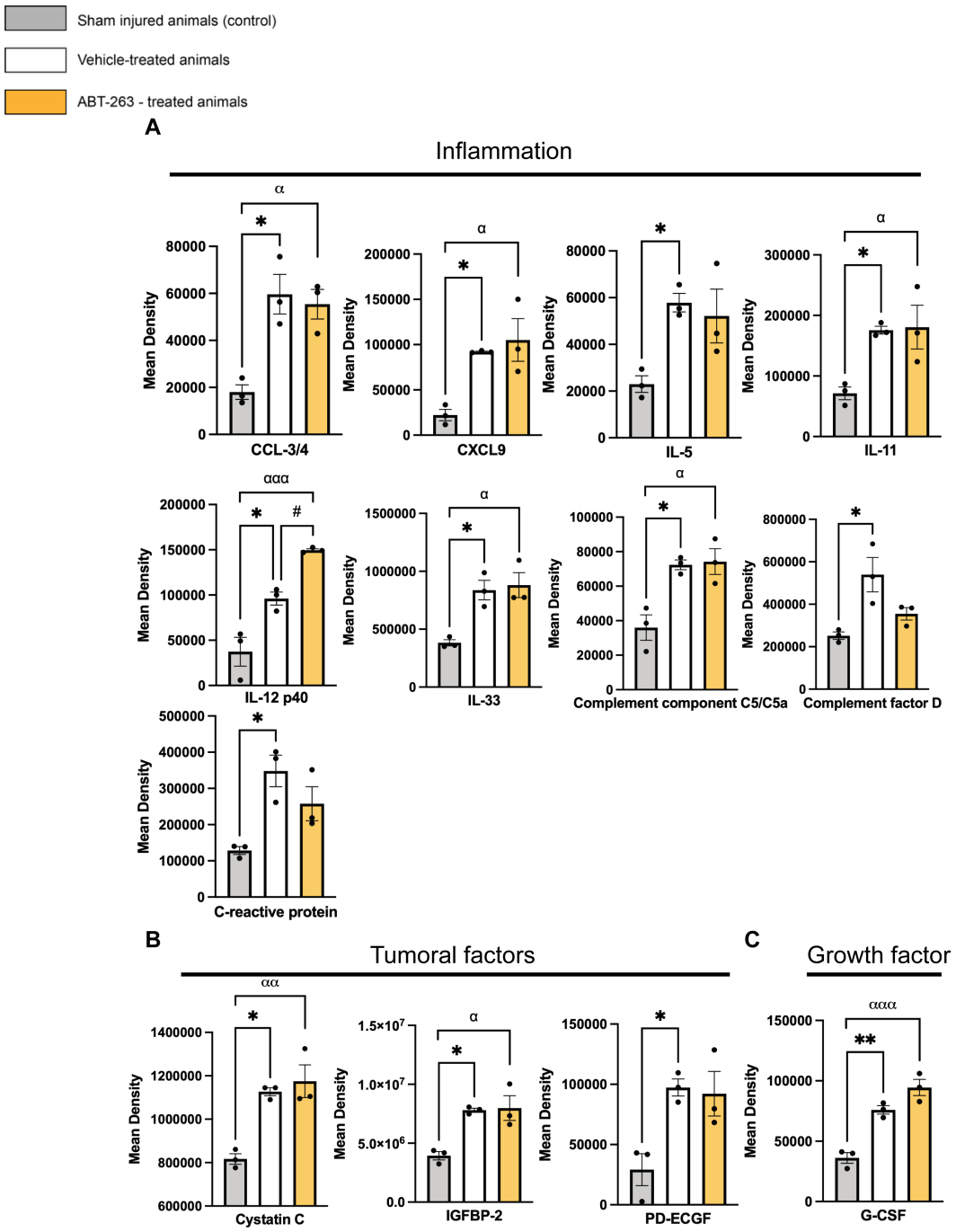

Figure 14 - Many pro-inflammatory and tumour-related factors are increased in the bladder of injured animals, independently of treatment at 15 days post-injury. Cytokine and chemokine expression was measured in bladder homogenates from sham (grey), vehicle- (white), and ABT-263-treated (yellow) spinal cord injured animals at 15 dpi. The factors were divided into several groups regarding their role: (A) inflammation, (B) tumoral factors and (C) growth factors. Some factors, such as CCL-3 and IGFBP-2, have been previously described as senescence-associated secretory phenotype (SASP) factors. (n=3) Data is presented as mean density and expressed as mean ± SEM. *p<0.05, **p<0.01, sham versus vehicle; #p<0.05, vehicle versus ABT-263; αp<0.05, ααp<0.01, αααp<0.001, control versus ABT-263.

4.1.3.3. Senolytic treatment decreases bladder levels of pro-inflammatory factors and growth factors induced after a spinal cord injury at 30 days post-injury

Cytokine and chemokine expression was also measured in bladder homogenates from sham (non-injured), vehicle- and ABT-263-treated spinal cord injured animals at 30 dpi. For the complete list of factors see Annex 1 Supplementary Table 3.

Several inflammatory factors, Growth/Differentiation Factor – 15 (GDF-15), IL-5, IL-11, Lipocalin-2, IL-12p40, IL-27p28, IL-28 A/B, IL-13 (Fig. 15A), as well as the growth factors IGFBP-1, PD-ECGF, Pref-1 and Proliferin (Fig. 15B) were increased in the bladder after a SCI (vehicle) at 30 dpi when compared to controls (Fig. 15). ABT-263 was successful in modulating these factors by reducing their levels (Fig. 15). GDF-15 and IL-13 are also known SASP factors (Coppé et al. 2010). The pro-inflammatory factors IL-5, IL-11, IL-12p40 and the growth factor PD-ECGF were also elevated after a SCI in the bladder of 15 dpi-vehicle-treated animals (Fig.14A). Complement components C5/C5a, CRP, IL-33 and IGFBP-2 (SASP factors) were also, similarly to what was observed at 15 dpi (Fig. 14A), induced at 30 dpi in the bladder of vehicle-treated animals after the lesion (not shown) with no effect of ABT-263.

In addition to these, other proteins such as inflammatory factors (CCL17, IFN-γ, IL-1α), angiogenesis promoters/regulators (Angiopoietin-1, Endoglin, Matrix Metalloproteinases -2 (MMP-2)), growth factors (Fibroblast Growth Factor 21 (FGF-21), Granulocyte macrophage - Colony Stimulating Factor (GM-CSF), Hepatocyte Growth Factor (HGF), IGFBP-3), and extracellular matrix and wound healing factors (MMP-3, Periostin, WNT-1-inducible-signalling pathway protein 1 (WISP-1)) were also significantly elevated in the bladders of vehicle-treated animals at 30 dpi when compared to non-injured animals (sham) (not shown). Nevertheless, ABT-263 treatment did not have an effect in reducing their levels. HGF, IFN-γ, IGFBP-3, IL-1α and MMP-3 are also SASP factors (Coppé et al. 2010).

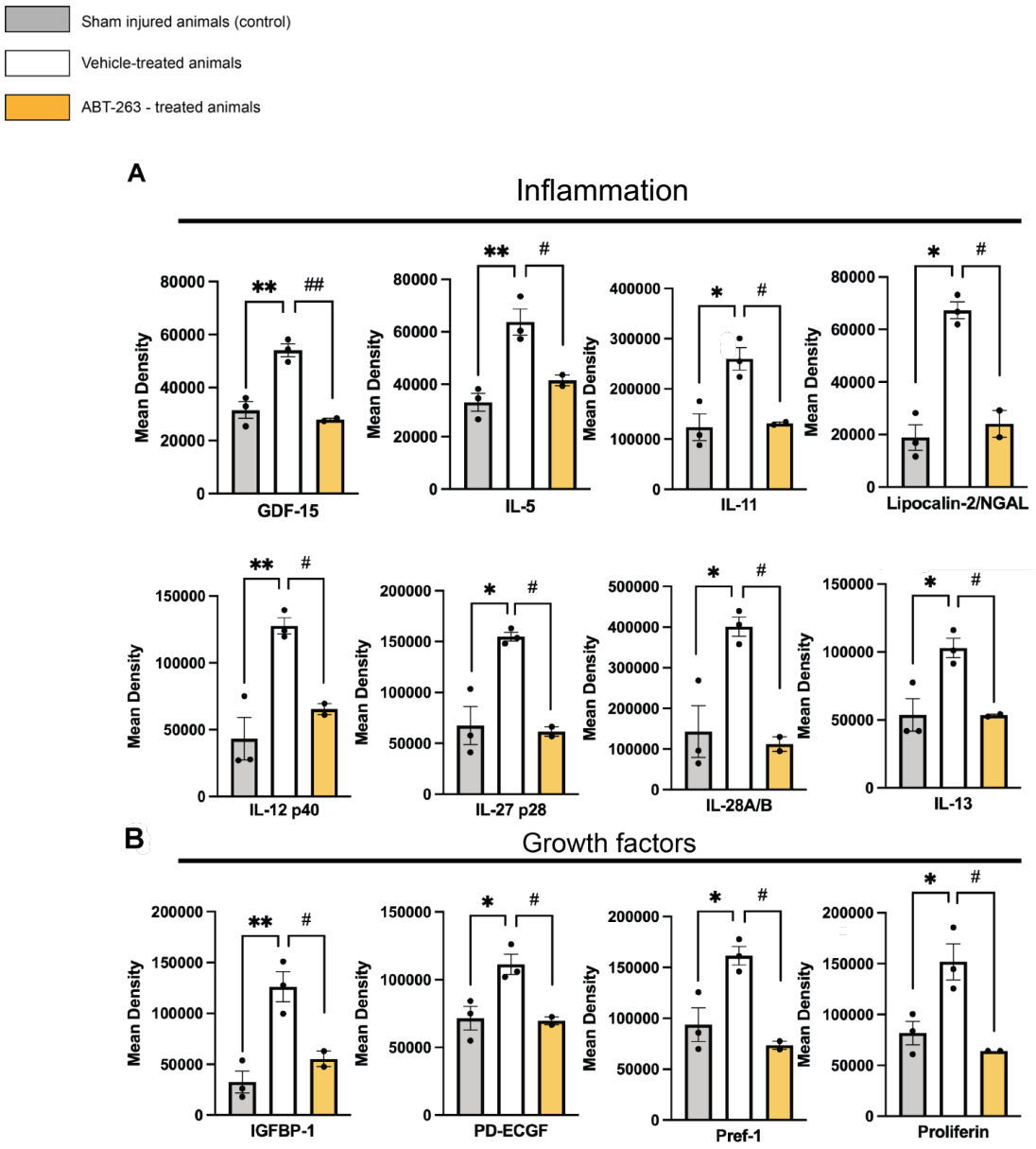

Figure 15 - ABT-263 treatment reduced several pro-inflammatory factors and growth factors induced after spinal cord injury in the bladder at 30 days post-injury. Cytokine and chemokine expression was measured in bladder homogenates from sham (grey), vehicle- (white), and ABT-263-treated (yellow) spinal cord injured animals at 30 dpi. The factors were divided into two groups regarding their role: (A) inflammation and (B) growth factors. Some factors, such as GDF-15 and IL-13, have been previously described as known senescence-associated secretory phenotype (SASP) factors. (n=2/3) Data is presented as mean density and expressed as mean ± SEM. *p<0.05, **p<0.01, sham versus vehicle; #p<0.05, ##p<0.01, vehicle versus ABT-263.

All in all, considering our data we observed a total of 14 factors that were upregulated in vehicle-treated injured animals at 15 dpi, with only EGF being successfully decreased by ABT-263-treatment (Supplementary Table 3 – Annex 1). Indeed, 9 of these factors kept significantly elevated even with ABT-263 administration. Interestingly, ABT-263 treatment elevated the expression of IL-10 an anti-inflammatory factor (not shown) and of IL-12p40 (Fig. 14A). These values contrast with those observed at 30 dpi, where the number of

upregulated factors in vehicle-treated injured animals increased to 31 and where 15 of which were decreased by ABT-263 (Fig.16) (Supplementary Table 3 – Annex 1).

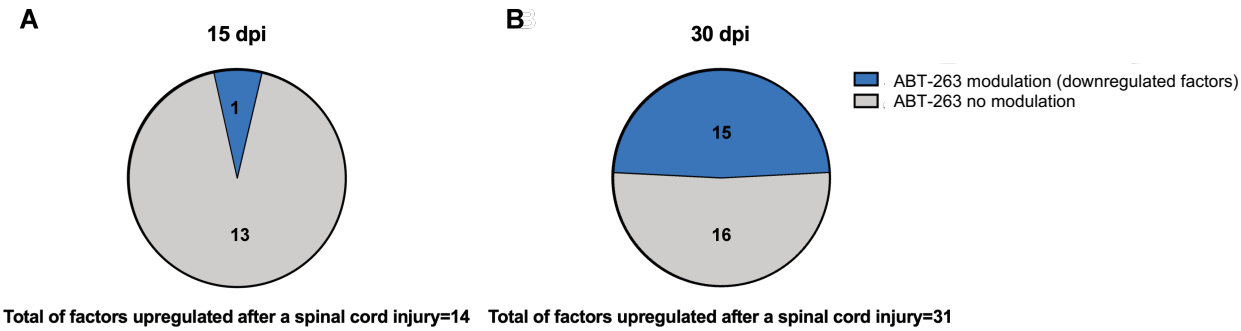

Figure 16 – Modulation by ABT-263 of bladder cytokine and chemokine expression between 15 and 30 days post-injury. (A) At 15 dpi 14 factors were upregulated after spinal cord injury (SCI), and only 1 was downregulated by ABT-263 treatment. (B) At 30 dpi 31 factors were upregulated after injury and, from those, 15 were downregulated by ABT-263. In blue, factors downregulated by ABT-263. In grey, factors where no effect by ABT-263 was observed.

4.2. Histopathological and immunohistochemistry analysis of peripheral organs of spinal cord injured animals treated and non-treated with ABT-263

After analysing the proteomic microenvironment, we evaluated the organ histopathology in the different experimental groups.

4.2.1. Liver

4.2.1.1. A spinal cord injury induces a slight increase in inflammatory infiltrates at 15 days post-injury, which is not reverted by ABT-263 treatment

Overall, both experimental groups presented a normal liver parenchymal architecture. The vehicle- and ABT-263-treated injured animals revealed a depletion of glycogen from the hepatocytes (Fig. 17B'-C'). These cells presented minimal occasional vacuolation and a dense cytoplasm (Fig. 17B-C), compared to the controls (sham). The controls presented hepatocytes with irregular and poorly defined clear spaces in the cytoplasm ("feathery cytoplasm") and a central nucleus, characteristic of glycogen accumulation (Fig. 17A). This background finding is commonly found in the liver of animals not fasted previously to sacrifice (Thoolen et al. 2010). The content of the vacuoles was confirmed using PAS staining, with positive glycogen accumulation marked in bright magenta (Fig. 17A', B' and C').

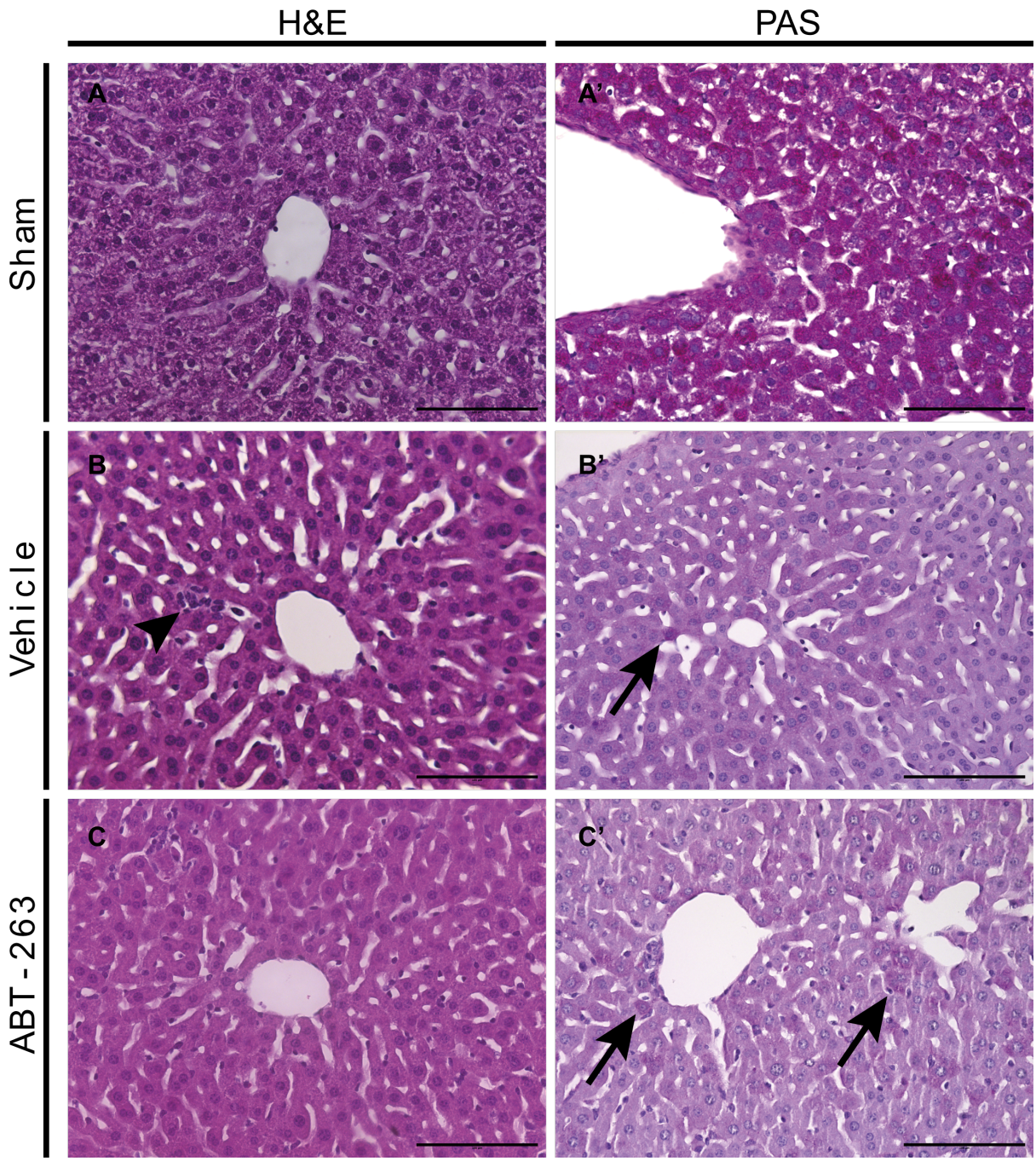

Figure 17 - Glycogen depletion of spinal cord-injured animals (vehicle-treated and ABT-263 treated) in comparison with the controls (sham injured animals). (A) Sham injured animal presenting hepatocytes with vacuolated cytoplasm. (A') Periodic-acid Schiff (PAS) staining shows a great accumulation of glycogen in bright magenta. (n=3) (B) & (C) Vehicle and ABT-263 treated spinal cord injured animals presenting hepatocytes with a none to minimally vacuolated cytoplasm. (n=6) (B) Extramedullary haematopoiesis (arrowhead). (B') & (C') Some cells display deposition of glycogen in bright magenta (arrows). (A), (B) & (C) Haematoxylin and Eosin (H&E) staining. (A'), (B') & (C') PAS staining. 400x. Scale bars = 100µm.

In addition to the cytoplasmatic differences described above, most lesions consisted of minimal multifocal spots of extramedullary haematopoiesis (EMH), mainly located in the portal tracts (zone 1), and few in the sinusoids in the midzonal area (zone 2) and around the central vein (zone 3) (Fig. 18E and E'). Furthermore, minimal multifocal inflammatory cell infiltrates were also present in the three zones of the liver (Fig. 18). These foci varied

between mixed cell infiltrates (neutrophils and mononuclear cells) and mononuclear cell infiltrates (macrophages, monocytes, lymphocytes and few plasma cells). The former were most often associated with small foci of necrosis (Fig. 18A and B). The latter were commonly located in zone 1 of the liver in the portal tracts surrounding the biliary duct (Fig.18D). When in small numbers and if not increased compared to controls, these findings are common in the liver of mice and are considered background lesions (Thoolen et al. 2010).

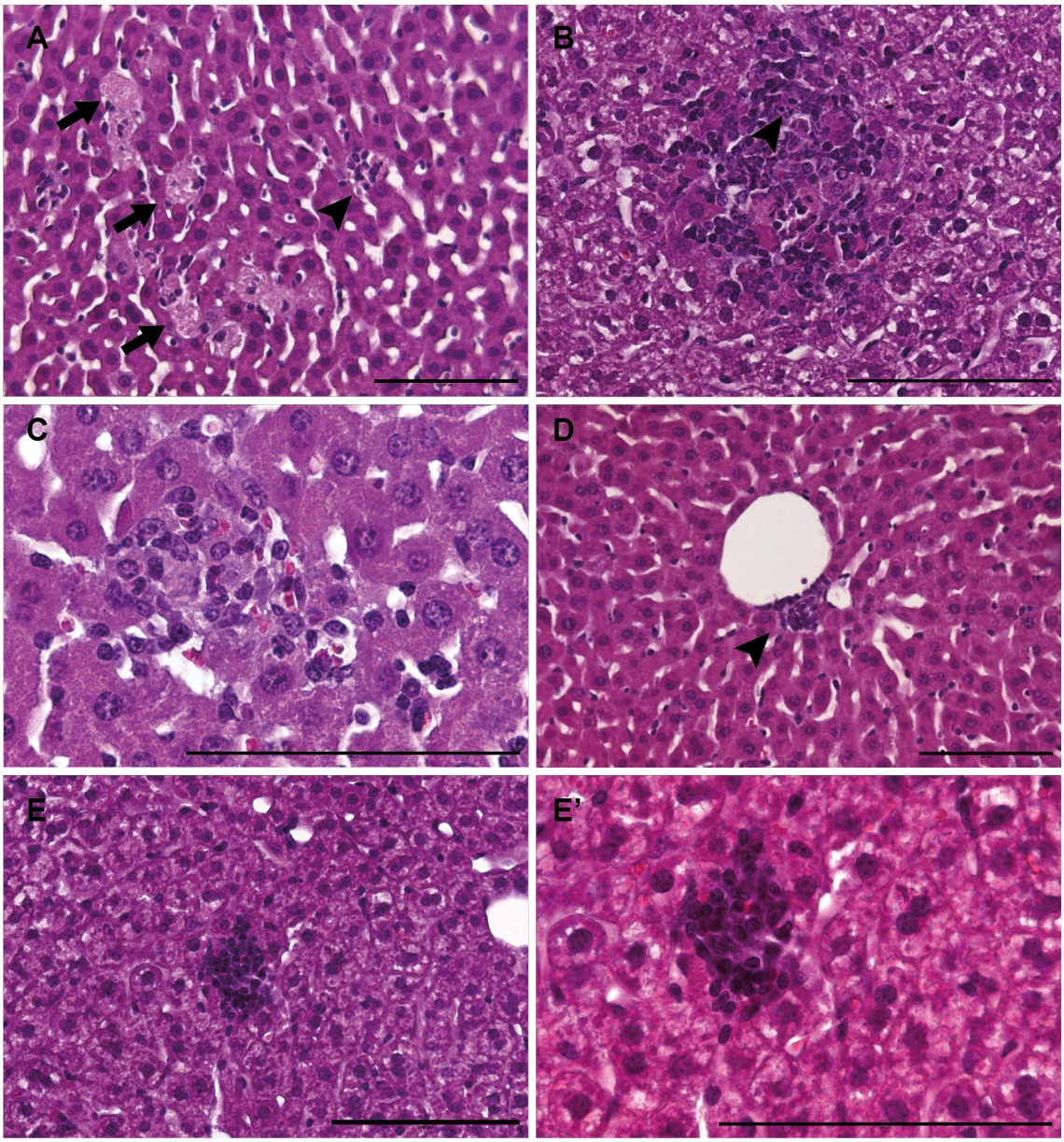

Figure 18 – Representative images of background lesions present in the liver across all experimental groups. (A) Necrosis, hepatocytes, multifocal, minimal (arrows). Inflammatory infiltrate, mixed, multifocal, minimal (arrowhead). The former shows some inflammatory cell infiltrates. The latter is also associated with necrosis. It is possible to identify polymorphonuclear neutrophils and mononuclear cells. The necrotic hepatocytes show a pale cytoplasm, karyorrhexis and karyolysis with nuclear dissolution. (B) Inflammatory infiltrate, mixed, multifocal, minimal. It is possible to identify neutrophils and other mononuclear cells, such as macrophages, plasma cells and lymphocytes. There is necrosis associated with this inflammatory infiltrate, with the presence of karyorrhexis (arrowhead). (C) Inflammatory infiltrate, mononuclear, multifocal, minimal. There are also some neutrophils present in this infiltrate. However, the main cells present are mononuclear cells. (D) Cell infiltrate, mononuclear, centrilobular, multifocal, minimal (arrowhead). (E) Extramedullary haematopoiesis,

midzonal, focal, minimal. (E') Close-up of E. H&E staining. (n=3) (A), (B), (D) and (E) 400x. (C) and (E') 1000x. Scale bars = 100µm.

Nonetheless, to objectively evaluate if there was an increase in inflammation, represented by more inflammatory infiltrates, these foci of inflammation were manually counted and plotted to identify if there were statistically significant differences between the groups (Fig. 19).

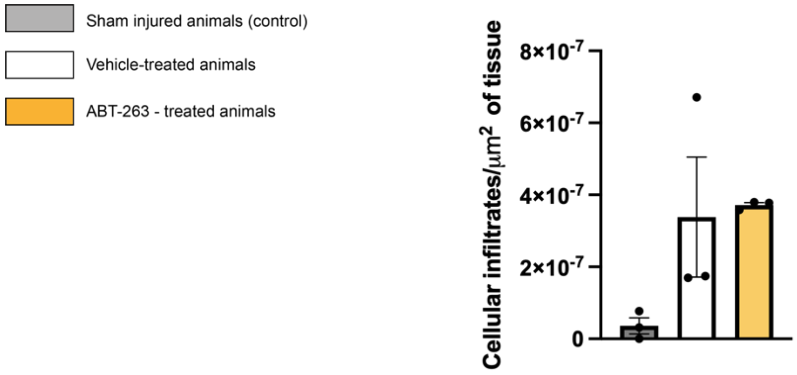

Figure 19 - Spinal cord injury suggests an increase in the number of inflammatory infiltrates. Inflammatory infiltrates were manually counted in sham (grey), vehicle- (white) and ABT-263-treated (yellow) spinal cord injured animals. (n=3). Data is expressed by the number of cellular infiltrates per μm^2 of tissue area and expressed as mean ± SEM

As the graph above shows, there seems to exist an increase in the number of inflammatory infiltrates in both spinal cord injured animals (vehicle and ABT-263) compared to the sham controls (non-injured). However, this difference is not statistically significant.

All in all, at this time point (subacute-to-chronic stage of SCI) the H&E staining revealed a depletion of glycogen and apparently increased inflammatory infiltrates after injury. ABT-263 did not have any apparent effect on these findings.

4.2.1.2. Spinal cord injury did not alter the number of T lymphocytes and Kupffer Cells in the liver

In order to further evaluate the inflammatory state of the liver at 15 dpi, in particular, the number of KCs and T lymphocytes, Clec4f and CD3 immunohistochemistry was performed, respectively.

The gross evaluation of the immunohistochemistry images did not reveal any apparent difference in the number of cells between experimental groups. KCs were evenly dispersed in the sinusoids of the liver (Fig. 20A', B', and C'). Similarly, tissue-resident T lymphocytes were also present in the sinusoids and the parenchyma of the liver (Fig. 20A, B, and C). In addition to this, these cells were also present in the portal tracts (typical location of resident memory T lymphocytes) (Fig. 20E) and in the inflammatory infiltrates, already

described above (Fig. 20D). Some of the mononuclear inflammatory infiltrates observed with H&E can also be described as granulomas.

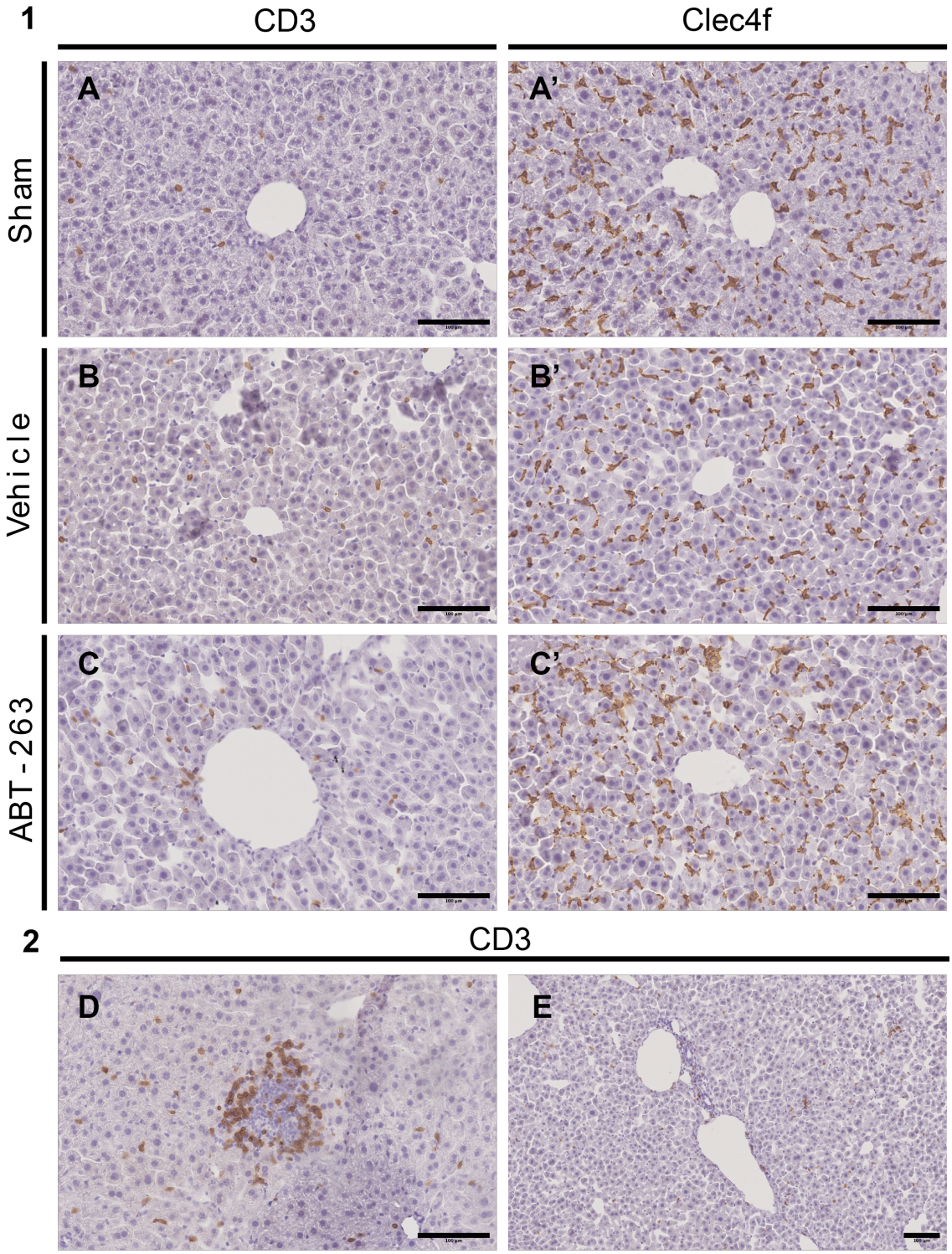

Figure 20 - CD3 and Clec4f immunohistochemistry did not reveal any apparent difference in the number of T lymphocytes and Kupffer cells, respectively, between experimental groups. 1. (A), (B) and (C) representative transversal sections showing hepatic CD3 immunoreactivity in brown in sham, vehicle- and ABT-263-treated injured animals. 200x. (A'), (B') and (C') representative transversal sections showing hepatic Clec4f immunoreactivity in brown in sham, vehicle-and ABT-263-treated injured animals. 200X. 2. (D) Detail showing T lymphocytes, in brown in the outer layer of a microgranuloma. 200x. (E) Detail showing the presence of T lymphocytes in a portal tract. (n=3) 100X. Scale bar = 100µm

The number of KCs was quantified as the area of tissue positive for Clec4f. There was no difference observed between the injured (vehicle- and ABT-263-treated) and non-injured animals (sham) (Fig. 21). The values were all very similar and close to 15%.

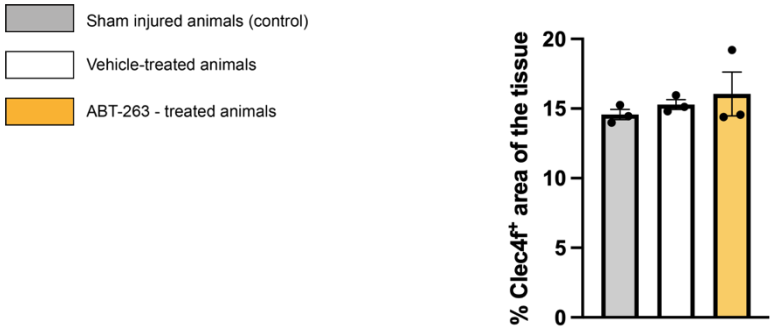

Figure 21 - Spinal cord injury does not affect the number of Kupffer cells in the liver at 15 days post-injury. The percentage of positive Clec4f area of liver tissue of each animal was automatically calculated using positive pixel detection in QuPath. This calculation was performed in sham (controls) in grey, vehicle-treated animals in white and ABT-263- treated animals in yellow. (n=3) Data is presented in percentage of Clec4f positive area of the tissue and expressed as mean ± SEM.

The quantification of $CD3^+$ cells was made by manually counting the number of cells and normalizing for the area of liver tissue. Similarly to Clec4f, there was no difference between the experimental groups (Fig. 22).

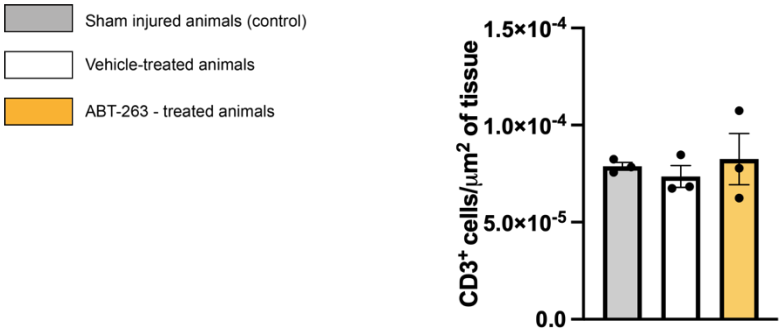

Figure 22 - Spinal cord injury does not affect the number of liver T lymphocytes. CD3 positive cells were manually counted and their number was divided by the area of liver tissue calculated using QuPath. This calculation was performed in sham animals in grey, vehicle-treated animals in white and ABT-263-treated animals in yellow. (n=3). Data is presented as CD3 positive cells per μm^2 of tissue and expressed as mean ± SEM.

SCI does not alter the number of KCs and T lymphocytes in the liver when compared to controls at 15 days after injury. The location and morphology of the cells were also normal.

4.2.1.3. Spinal cord injury induces a small increase in the liver's lipidic content at 15 days post-injury

After a SCI there is lipid accumulation, which in turn can lead to steatosis, the main characteristic of NAFLD (Goodus et al. 2021). Thus, to better evaluate the degree of lipid

accumulation in our samples we performed the special staining Oil Red O, which stains lipids in red.

Staining revealed small, but few, droplets of lipids in the cytoplasm of the hepatocytes without nucleus displacement, predominantly located in zone 2 of the lobule (Fig. 23). Histologically, vehicle- and ABT-263-treated spinal cord injured animals appeared to have a greater lipidic content than controls (sham) (Fig. 23B and C). Analysis of the positive percentage of Oil Red O was quantified using QuPath image analysis software (Fig. 24). This quantification did not reveal statistically significant differences between experimental groups (Fig. 24).

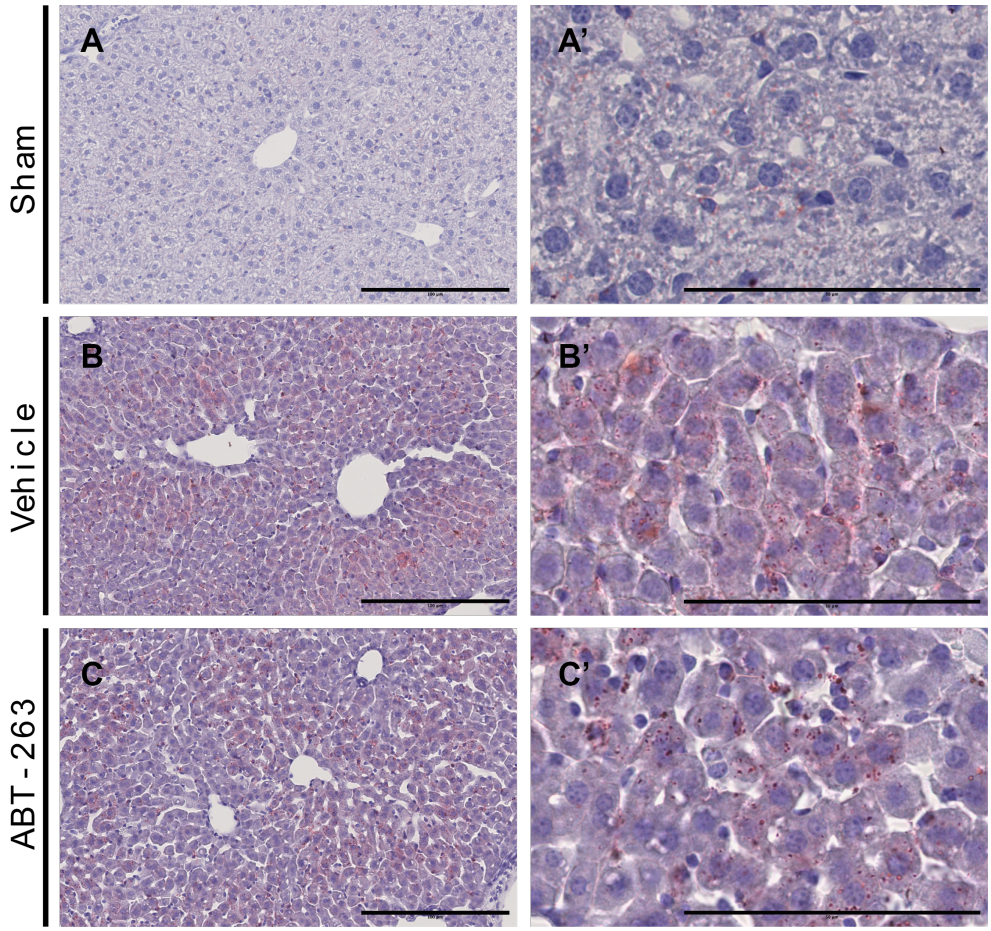

Figure 23 - Spinal cord injury appears to induce a slight histopathological increase in lipid content of the hepatocytes at 15 days post-injury, however, it is not significant. Representative liver transversal sections showing diffuse lipid accumulation in red of sham animals (A), vehicle (B) and ABT-263-treated (C) spinal cord injured animals. 200x. Scale bars = 100µm. (A'), (B') and (C') respective images showing small lipid droplets in the cytoplasm of the hepatocytes without nuclear displacement. 800x. Scale bars = 50µm. (n=3) Oil Red O staining.

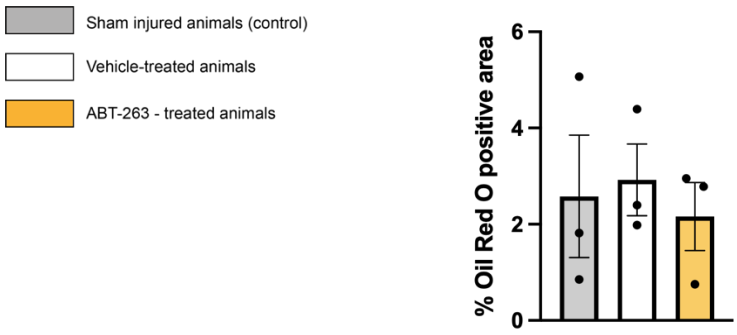

Figure 24 – Spinal cord injury does not alter the liver's lipidic content at 15 days post-injury. The percentage of Oil Red O positive area was automatically quantified using QuPath. This calculation was performed in sham controls (grey), vehicle-treated animals (white) and ABT-263- treated animals (yellow). (n=3). Data is presented as a percentage of Oil Red O positive area and expressed as mean ± SEM.

4.2.1.4. Spinal cord injury does not induce liver fibrosis at 15 days post-injury

Even though, there were no signs of fibrosis in the H&E slides, a set of slides was stained with AFOG to confirm the lack of fibrosis in the analysed groups.

Both controls (sham injured) and SCI animals, irrespective of treatment, revealed no signs of fibrosis (Fig. 25). The blue collagen-rich areas were normally located, mainly in the portal tracts and in less quantity surrounding the central veins and in the capsule of the liver (Fig. 25).

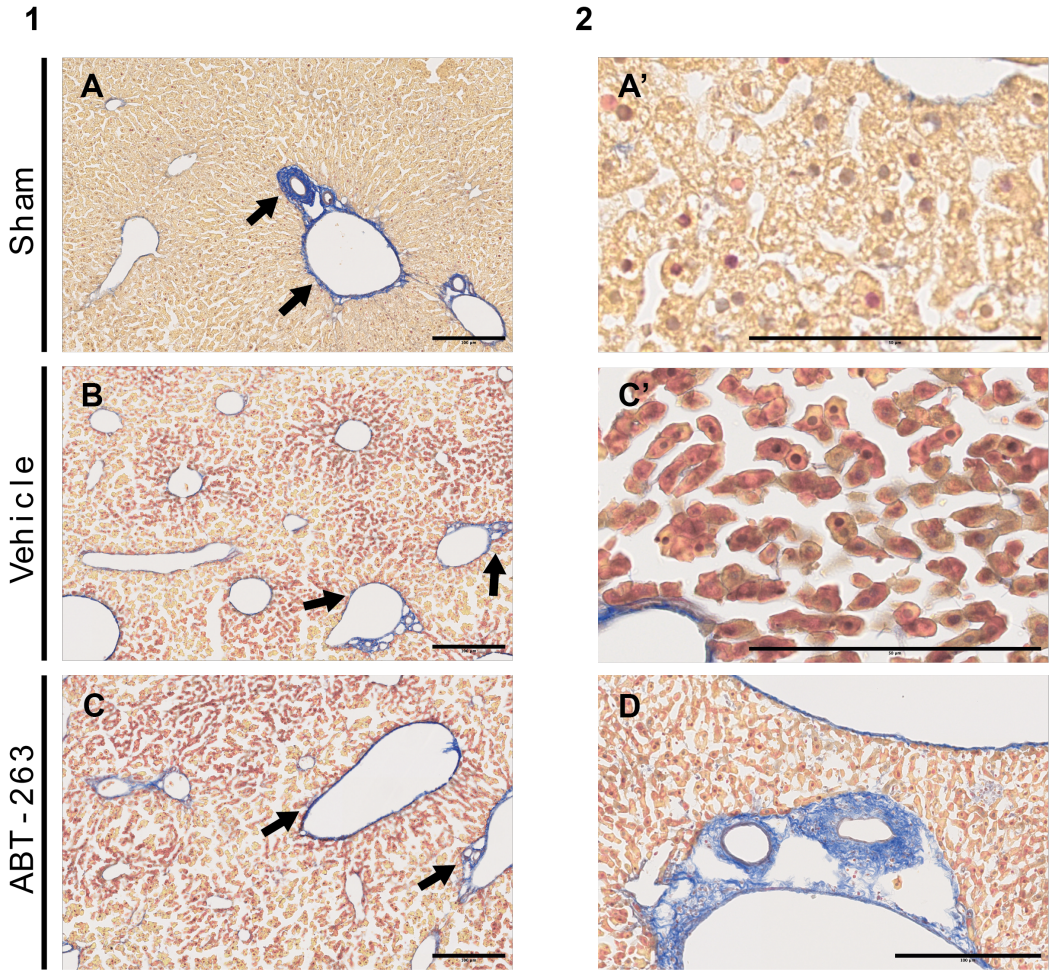

Figure 25 - Spinal cord injury did not cause liver fibrosis at 15 days post-injury. Sham (A), vehicle (B) and ABT-263 (C) representative transversal sections showing in blue collagen fibres (arrows) and in red hepatocytes rich in protein (highlighted in C'). (A') and (C') hepatocytes, details. (D) Detail of portal tract showing abundant normal collagen deposition in blue. AFOG staining. (n=3). (A), (B) and (C) 100x. Scale bars = 100μm (A') and (C') 800x. Scale bars=50μm (D) 200x.

4.2.1.5. Spinal cord injury does not induce iron sequestration in the liver at 15 days post-injury

Iron sequestration has also been described post-SCI in rats (Goodus et al. 2018) and in NAFLD/NASH (Hamada and Hirano 2022). Therefore, to evaluate iron sequestration in the liver, Perls Prussian Blue staining was performed, staining iron deposition in blue.

At 15 dpi, we observed little to no iron accumulation in the liver (Fig. 26). The few Perls Prussian Blue positive cells seemed to be located in the sinusoids of the liver and most probably corresponded to KCs (Fig. 26).

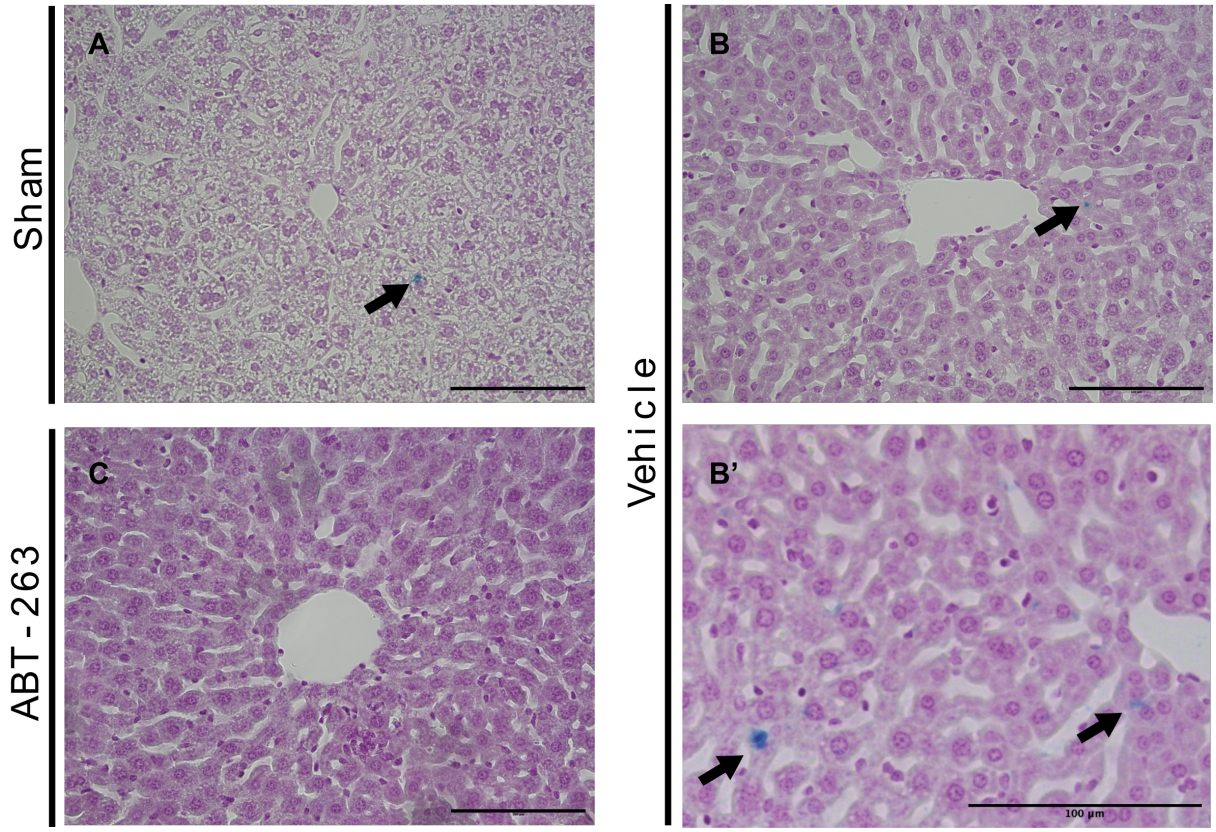

Figure 26 - Spinal cord injury does not induce iron sequestration in the liver at 15 days post-injury. (A), (B) and (C) representative transversal sections of hepatic Perls Prussian Blue stained sections from sham (A), vehicle- (B & B') and ABT-263-treated (C) injured animals, respectively. There is little to no accumulation of iron in the liver. Non-heme iron stains blue (arrows). Perls Prussian Blue staining. (A), (B) and (C) 400x. (B') 700x. (n=3). Scale bars=100µm.

4.2.2. Spleen

4.2.2.1 T9 spinal cord injury does not cause apparent spleen pathology/alterations at 15 days post-injury

Histologically, vehicle- and ABT-263-treated spinal cord injured animals were very similar to controls (sham). Nevertheless, it appeared to exist a minimal decrease in white pulp cellularity in the injured groups compared to controls (Fig. 27). Extramedullary haematopoiesis of all cellular lines (myeloid, erythroid, and megakaryocytic) was present, however, there were no apparent differences between groups.

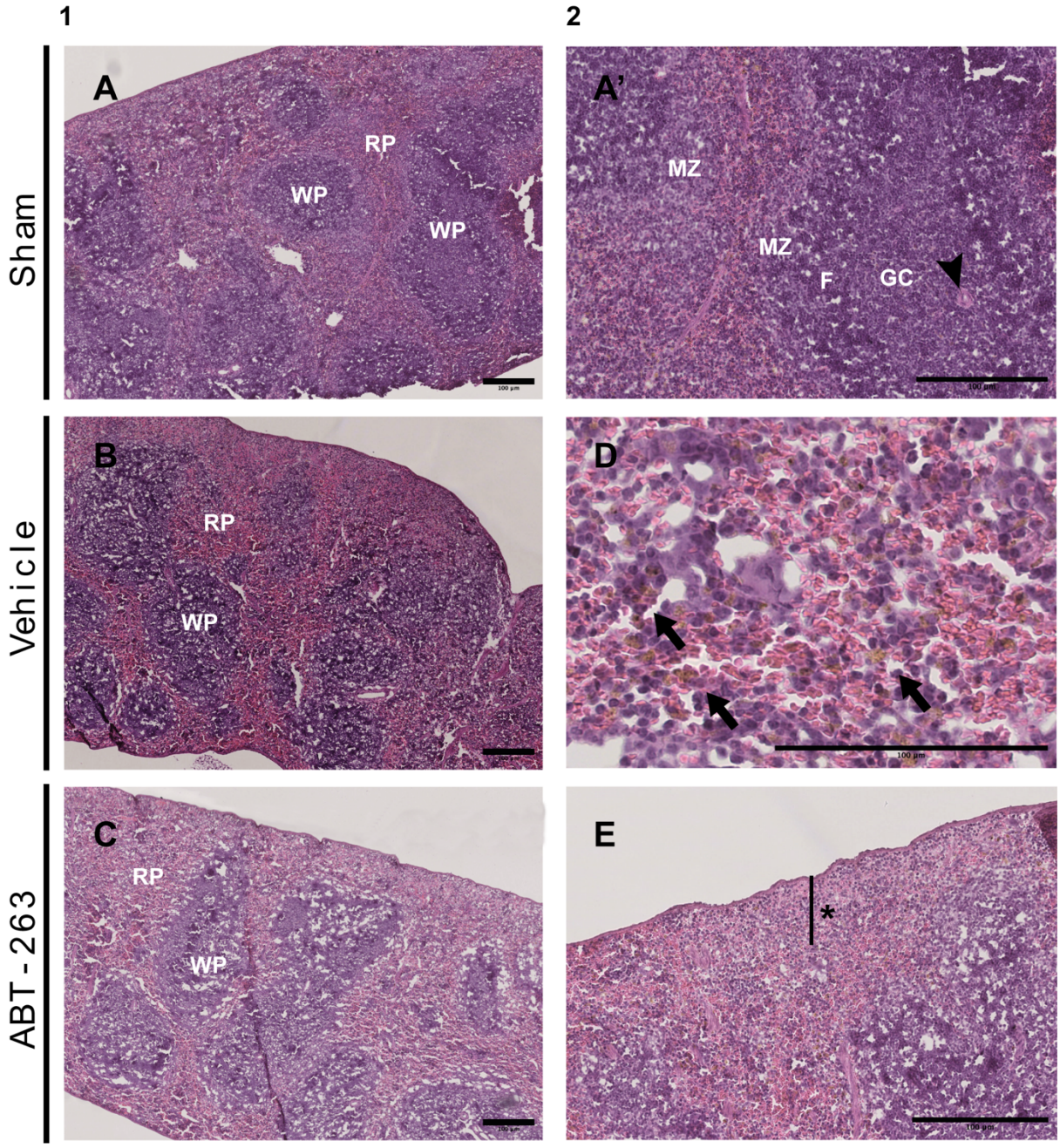

Figure 27 - Spinal cord injury does not cause apparent spleen pathology at 15 days post-injury. Representative longitudinal sections of the spleen of sham (A), vehicle- (B), and ABT-263-treated (C) spinal cord injured animals. RP - Red pulp; WP - White pulp; MZ - Marginal zone; F - follicle; GC - Germinal center; Arrowhead - central arteriole; Arrows - haemossiderin; Asterisk - Subcapsular monocyte pool. Haematoxylin & Eosin. (n=3). (A), (B), (C) 50x. (A') 100x. (D) 400x. (E) 100x. Scale bars = 100μm

In an attempt to better evaluate differences in white pulp between experimental groups, QuPath was used to quantify both white pulp and red pulp. This revealed no statistically significant difference between groups in both red pulp and white pulp areas (Fig. 28).

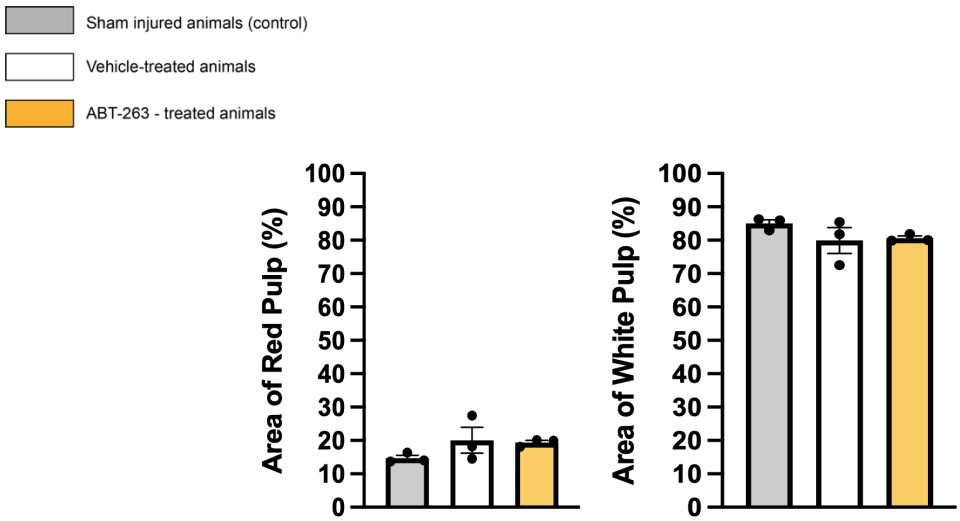

Figure 28 - Spinal cord injury does not affect spleen´s red or white pulp area. The percentage of area of red and white pulp was automatically measured using QuPath and normalized for the area of tissue analysed. This calculation was performed in sham (control) (grey), vehicle- (white), and ABT-263-treated animals (yellow). (n=3). Data is presented as the percentage of area and expressed as mean ± SEM.

4.2.3. Bladder

4.2.3.1 ABT-263 decreases the bladder's inflammatory state observed after a spinal cord injury at 15 days post-injury

Overall, the bladders of the spinal cord injured animals (vehicle- and ABT-263-treated) presented a visible abnormal distension (Fig. 29B and 29C), compared to controls (sham) which presented the normal folds of an empty bladder (Fig. 29A).

Considering the urothelium, the vehicle-treated animals presented a simple focal minimal-to-mild urothelium hyperplasia and minimal urothelium erosion (Fig. 30A), compared to controls (Fig. 29A and 29A'1). In one of the vehicle-treated animals it was also possible to identify apoptotic bodies (Fig. 30A). In comparison to the vehicle-treated injured animals, the ABT-263 treated animals had almost non-existent hyperplasia and epithelial erosion (Fig. 29C and 29C'1). All experimental groups presented normal eosinophilic inclusions in the cytoplasm of umbrella cells (Fig. 29 and detail shown by arrowhead in figure 30A).

Now considering the submucosa, compared to controls (Fig. 29A'2), the vehicle-treated animals had multiple inflammation hallmarks (Fig. 29B'2). The submucosa presented diffuse-to-multifocal, mild-to-moderate mixed inflammatory infiltrates, mainly composed of mononuclear cells, such as lymphocytes, plasma cells, monocytes and macrophages and few polymorphonuclear neutrophils (PMNs) (Fig. 30C). In addition to this, these animals also presented multifocal mild oedema, mild-to-moderate haemorrhage with the presence of macrophages with haemosiderin granules and mild fibrosis that extended to the muscle layers of the bladder (detrusor muscle) (Fig. 29B'2 and 30D). The ABT-263 treated animals, on the other hand, had a reduction of these inflammatory parameters (Fig. 29C'2). The

number and size of the mixed inflammatory infiltrates decreased, as well as, the oedema, with only one animal presenting mild haemorrhage and fibrosis.

The muscularis propria or detrusor muscle in the vehicle-treated animals compared to the controls presented minimal mixed inflammatory infiltrates (PMNs and mononuclear infiltrates) along with minimal multifocal fibrosis (infiltrating from the submucosa) and necrosis (Fig. 29B'3 and 30E). Contrarily, the ABT-263-treated had an almost normal muscular layer, very similar to controls (Fig. 29C and 29C'3).

The adventitia, the most outer layer of the bladder, composed by loose connective tissue and adipose tissue presented some alterations in the vehicle- and ABT-263-treated animals compared to the controls (Fig. 29B'4). The adipose tissue of the vehicle-treated animals presented a moderate mixed inflammatory infiltrate (PMNs and mononuclear cells) and necrosis (Fig. 30F and G). In addition to this, the connective tissue presented the same type of inflammatory infiltrate, although mild, and minimal haemorrhage (Fig. 30F and G). Conversely, the ABT-263 treated injured animals also had the same type of inflammatory infiltrates, however, these were mild.

All in all, the histopathological analysis shows that SCI appears to induce a subacute to chronic-active inflammation of the bladder wall with foci of simple hyperplasia and erosion of the urothelium, compatible with interstitial cystitis. The bladder also appears to have lost its ability to contract due to the abnormal distension and lack of folds compared to controls. The ABT-263-treated group appears to be able to modulate the bladder's inflammation as animals also show the same inflammatory signs, although to a lesser extent. Nonetheless, at 15 dpi these bladders continue abnormally distended compared to controls.

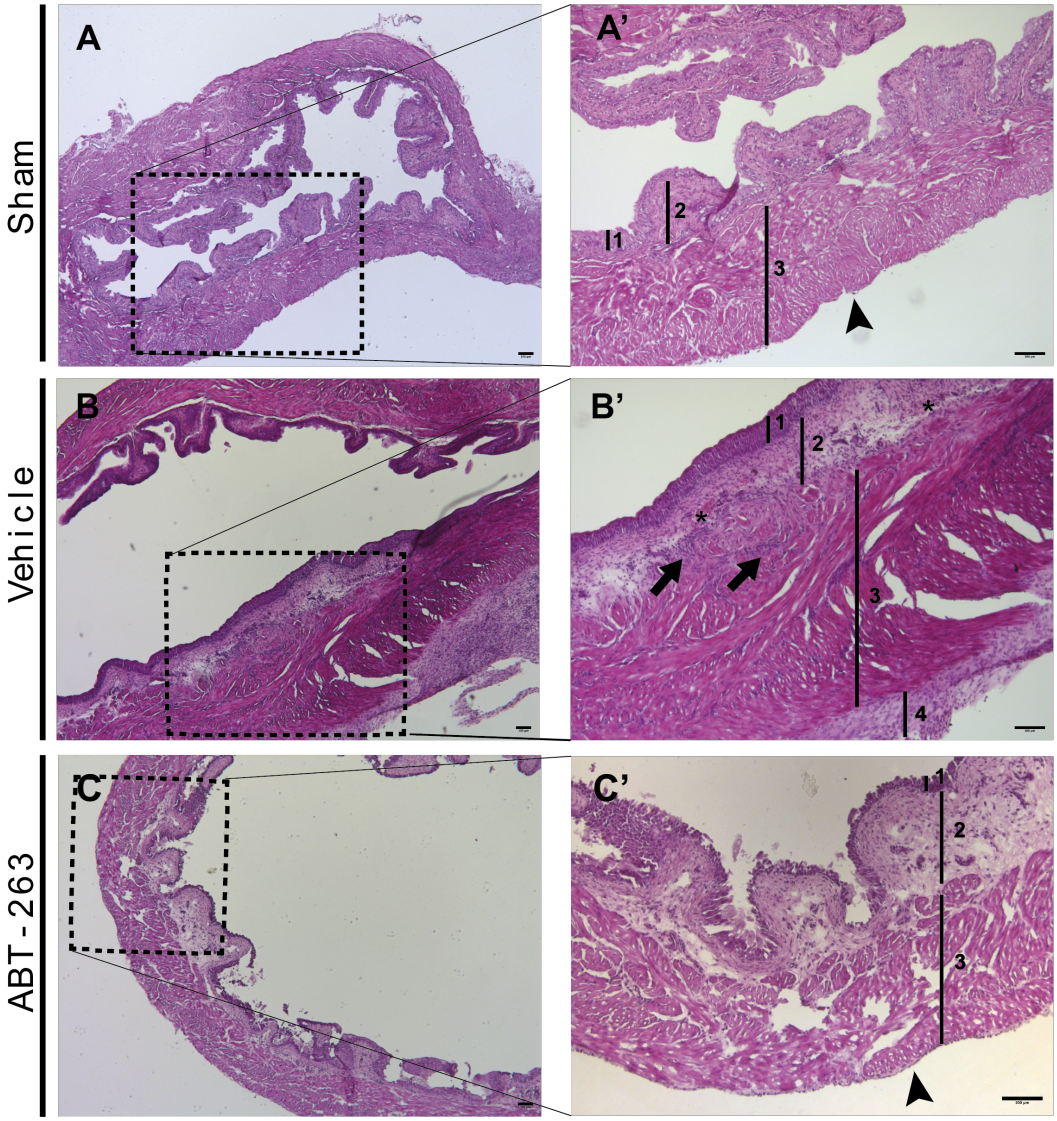

Figure 29 - Spinal cord injury induces bladder inflammation when compared to controls (Sham). ABT-263 appears to reduce the state of inflammation. (A) Sham injured animals presenting a normal voided bladder structure. (A') Close up of image A highlighting the different layers of the bladder. All layers are normal. (B) Vehicle treated SCI animals with an abnormally distended voided bladder. The dotted rectangle highlights an area that has lost the natural folding of an empty bladder and the abnormal tissue bellow the urothelium. (B') Magnification of image B. (1) Simple hyperplasia of the urothelium. (2) Increase in thickness of the submucosa with the presence of mixed inflammatory infiltrates (mononuclear and polymorphonuclear neutrophils) (arrows) and haemorrhage (asterisk). (3) Presence of mixed inflammatory infiltrates between the smooth muscle spindles (arrows). (C) ABT-263 treated SCI animals with an abnormally distended voided bladder. (C') Close up of image C. There is a reduction of the histological inflammatory characteristics compared to the Vehicle-treated animals. (n=3). (1) mucosa/urothelium (pseudostratified transition epithelium); (2) submucosa (3) detrusor muscle (3 layers); (4) adventitia; (Arrowhead) Serosa. H&E staining. 5μm. (A; B; C) 50x. (A'; B'; C') 100x. Scale bars = 100μm.

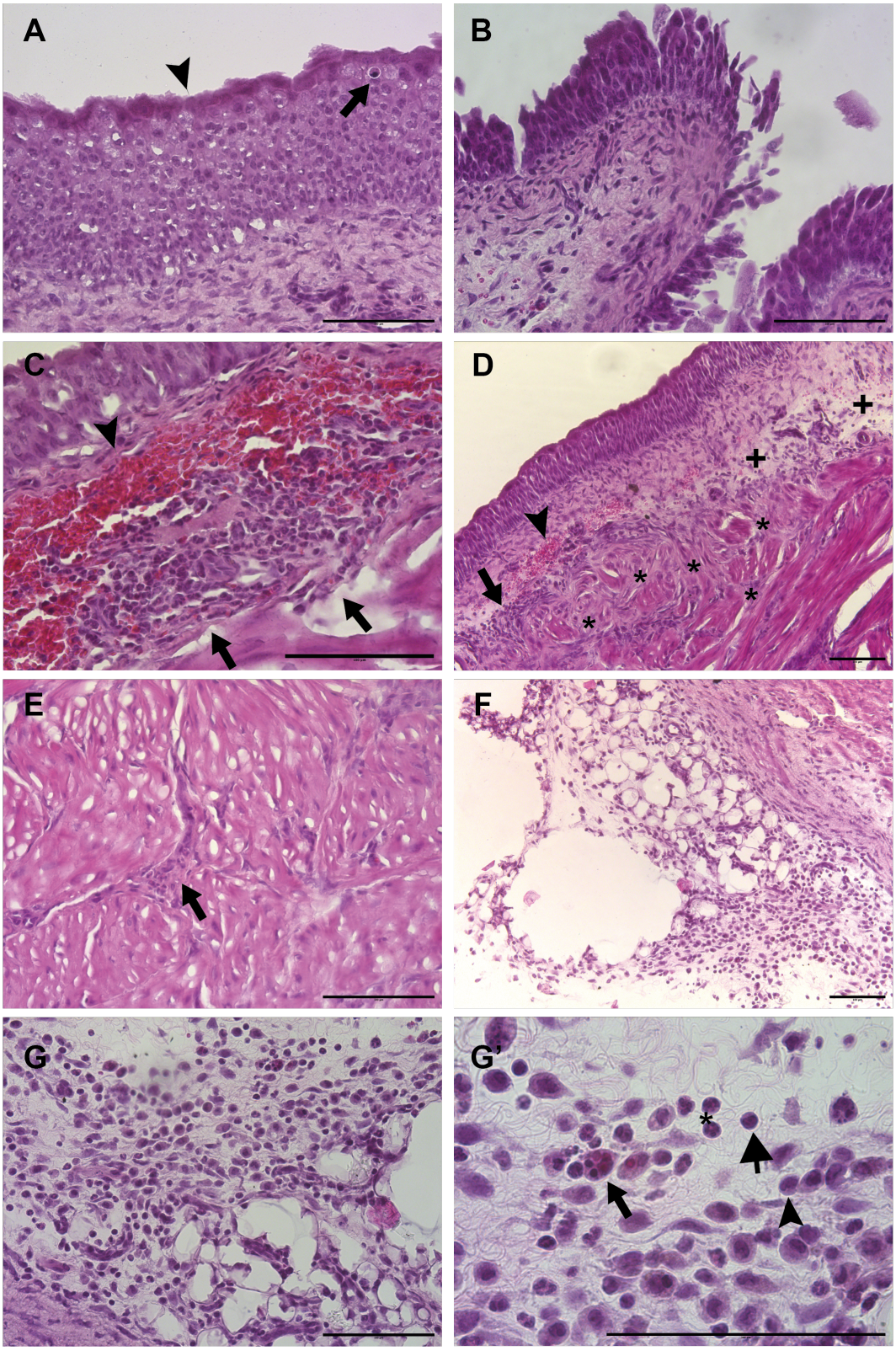

Figure 30 – Bladder representative images of spinal cord injury induced changes. (A) Urothelium Hyperplasia, simple, multifocal, mild. (arrowheads) Eosinophilic inclusions, umbrella cells, in the image noticeable by the stronger eosinophilic coloration of the umbrella cells. (arrow) Apoptotic body. (B) Urothelium erosion, multifocal, mild. (C) (arrowhead) Haemorrhage, multifocal, moderate. (arrows) Mixed inflammatory infiltrate (neutrophils and mononuclear cells such as macrophages, monocyte and plasma cells), multifocal, moderate. (D) (arrow) Mixed inflammatory infiltrate, multifocal, mild. Macrophages with haemosiderin pigment. (arrowhead) Haemorrhage, multifocal, mild. (plus signs) Oedema, multifocal, mild. (asterisks) Fibrosis, multifocal, mild. Extending from the submucosa to the muscularis propria, between the muscle bundles. (E) Mixed inflammatory infiltrates, mainly composed of mononuclear cells (lymphocytes, macrophages, monocytes) in the connective

tissue between muscle bundles, mild. (F) Mixed inflammatory infiltrates of the fat and connective tissue of the adventitia, diffuse, moderate. (G) Mixed inflammatory infiltrates of the fat and connective tissue of the adventitia, diffuse, moderate. (G') Detail. (long arrow) macrophage with phagocytized apoptotic bodies. (short arrow) lymphocyte. (arrowhead) monocyte. (asterisk) two neutrophils. (n=3). H&E. (A, B, C, E, G) 400x. (D, F) 200x. (G') 1000x. Scale bars = 100μm

4.3. Peripheral senescent cells after spinal cord injury

We used the SA-β-galactosidase enzyme activity, a marker of senescence, to measure senescence in the liver, spleen and bladder of sham, vehicle- and ABT-263-treated spinal cord injured animals using a SA-β-gal kit. Senescent cells appear in blue. Quantification was done using QuPath.

4.3.1. Liver

4.3.1.1. ABT-263-treated animals present a higher number of senescent cells in the liver at 15 days post-injury compared to controls and vehicle-treated animals

All experimental groups showed a diffuse distribution of senescent cells, which appeared to be predominantly located in zone 2 of the lobule (Fig. 31). These cells were small and mainly located in the sinusoids, consistent with cells such as HSCs, KCs and endothelial cells (Fig. 31). Moreover, the inflammatory cell foci in the liver's parenchyma also presented SA-β-gal positive cells (Fig. 31C'').

Both histopathological and quantification analysis revealed a significant increase in the number of senescent cells in ABT-263-treated animals compared to controls and vehicle-treated animals (Fig. 31C, 31C´and 32). In addition, SCI did not induce a statistically significant increase in senescent cells compared to controls (Fig. 32).

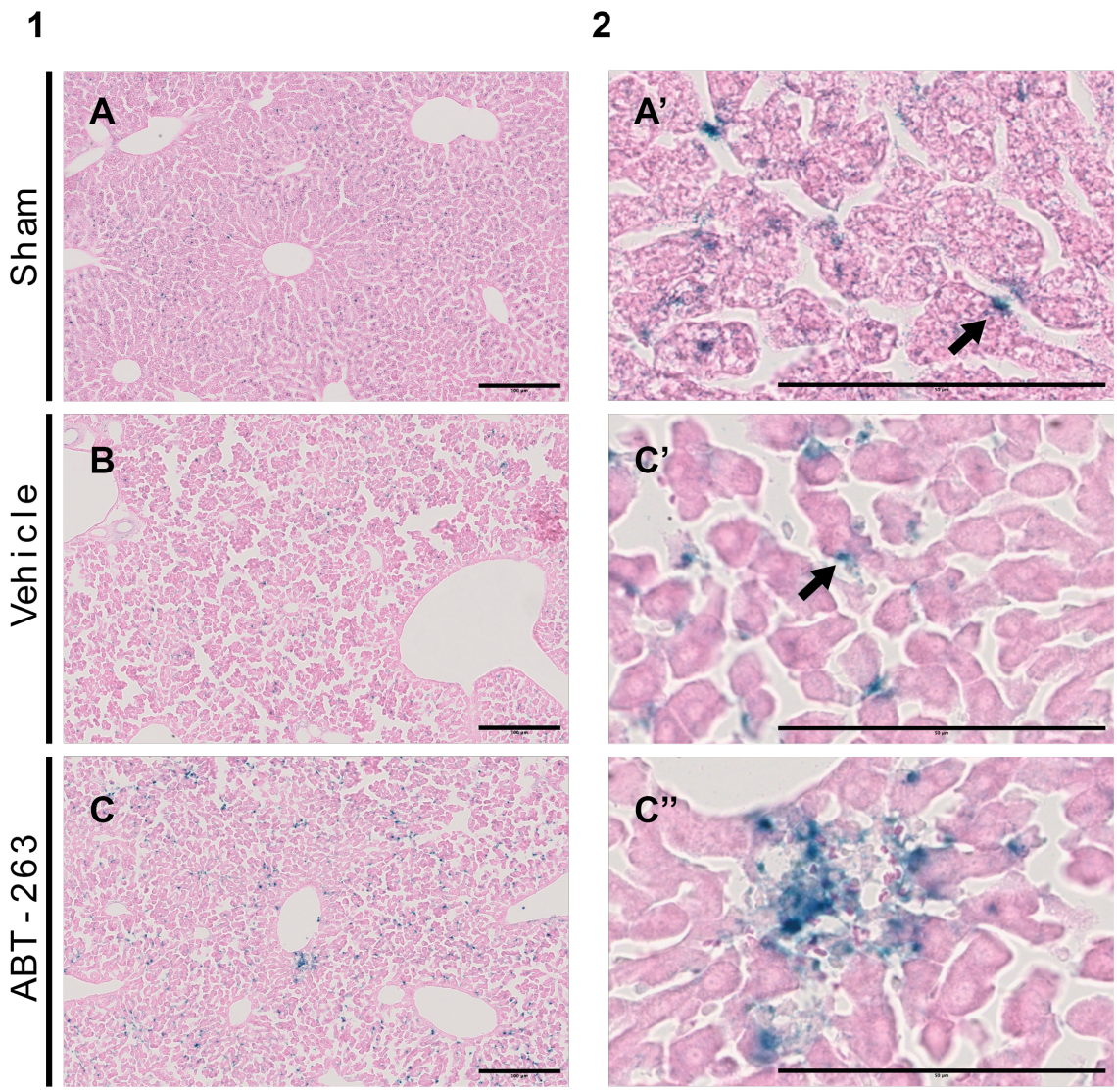

Figure 31 - ABT-263 animals appear to present a higher number of senescent cells at 15 days post-injury. 1- (A), (B) and (C) representative liver transversal sections showing a diffuse distribution of senescent cells (blue) in sham-, vehicle- and ABT-263-treated spinal cord injured animals. 100x. Scale bars = 100μm. 2- (A'), (C') and (C'') details showing that the main location of senescent cells, which is in the sinusoids (arrows) and in inflammatory cell infiltrates (C''). (n=3). 800x. Scale bars = 50μm. SA-β-gal staining.

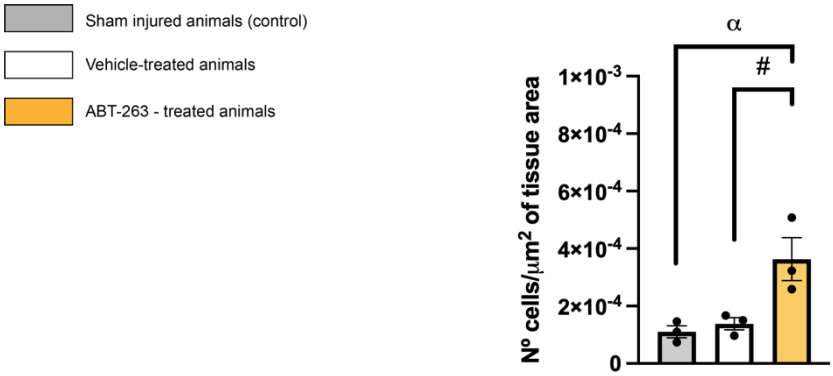

Figure 32 - ABT-263 treatment induces an increase in senescent cells in the liver. The number of senescent cells was automatically counted using QuPath and normalized for the area of tissue analysed. This calculation was performed in sham (grey), vehicle- (white) and ABT-263-treated animals (yellow). (n=3). Data is presented as the number of cells per μm^2 of tissue area and expressed as mean ± SEM. #p<0.05, vehicle versus ABT-263; αp<0.05, sham versus ABT-263.

4.3.2. Spleen

4.3.2.1. Spinal cord injury appears to induce an increase in spleen's senescence at 15 days post-injury

All experimental groups showed a multifocal distribution of senescent cells predominantly located in the red pulp of the spleen (Fig. 33). The detected SA-β-gal positive senescent cells are most probably erythrocytes/macrophages (Fig. 33C'). We also observed an apparent increase in the number of senescent cells in the vehicle- and ABT-263-treated spinal cord injured animals when compared to controls (Fig. 33). Upon quantification, these microscopic findings corresponded to a slight increase, although not statistically significant, in the number of senescent cells in the SCI cohorts (Fig. 34).

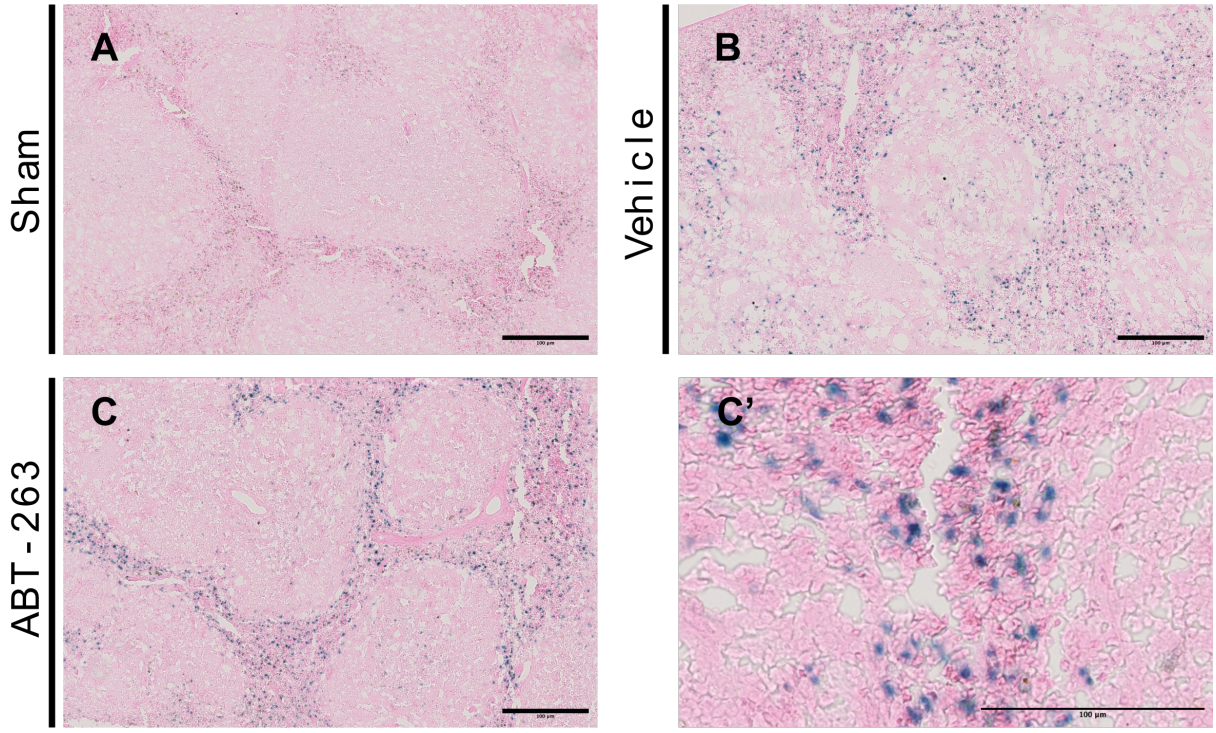

Figure 33 - Spinal cord injury appears to induce senescence in the spleen. (A), (B) and (C) representative spleen transversal sections showing a diffuse distribution of senescent cells (blue) in sham-, vehicle- and ABT-263-treated spinal cord injured animals, respectively. 100x. (C') detail showing the main location of senescent cells, which is in the red pulp of the spleen. (n=3). 400x. Scale bars = 100µm. SA-β-gal staining.

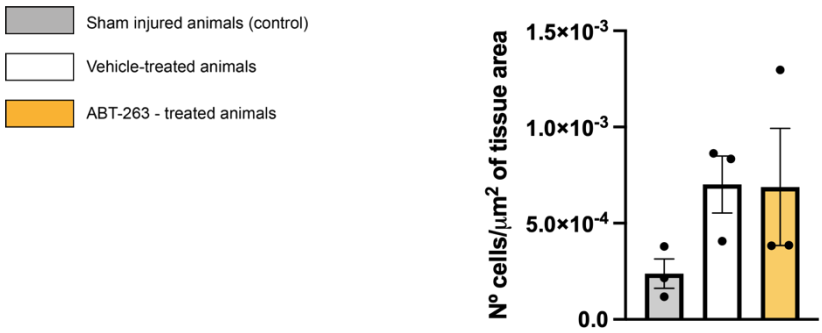

Figure 34 - Spinal cord injury appears to induce a slight increase in the number of senescent cells. The number of senescent cells was automatically counted using QuPath and normalized for the area of tissue analysed. This calculation was performed in sham (grey), vehicle- (white) and ABT-263-treated animals (yellow). (n=3). Data is presented as the number of cells per μm^2 of tissue area and expressed as mean ± SEM.

4.3.3. Bladder

4.3.3.1. Spinal cord injury does not induce an increase in senescence in the bladder at 15 days post-injury

All experimental groups showed a multifocal distribution of SA-β-gal positive cells, mostly in the outermost layer of the bladder's transitional epithelium, the umbrella cells (Fig. 35B'). Upon quantification with Qupath, we did not observe any statistical differences between groups (Fig. 36).

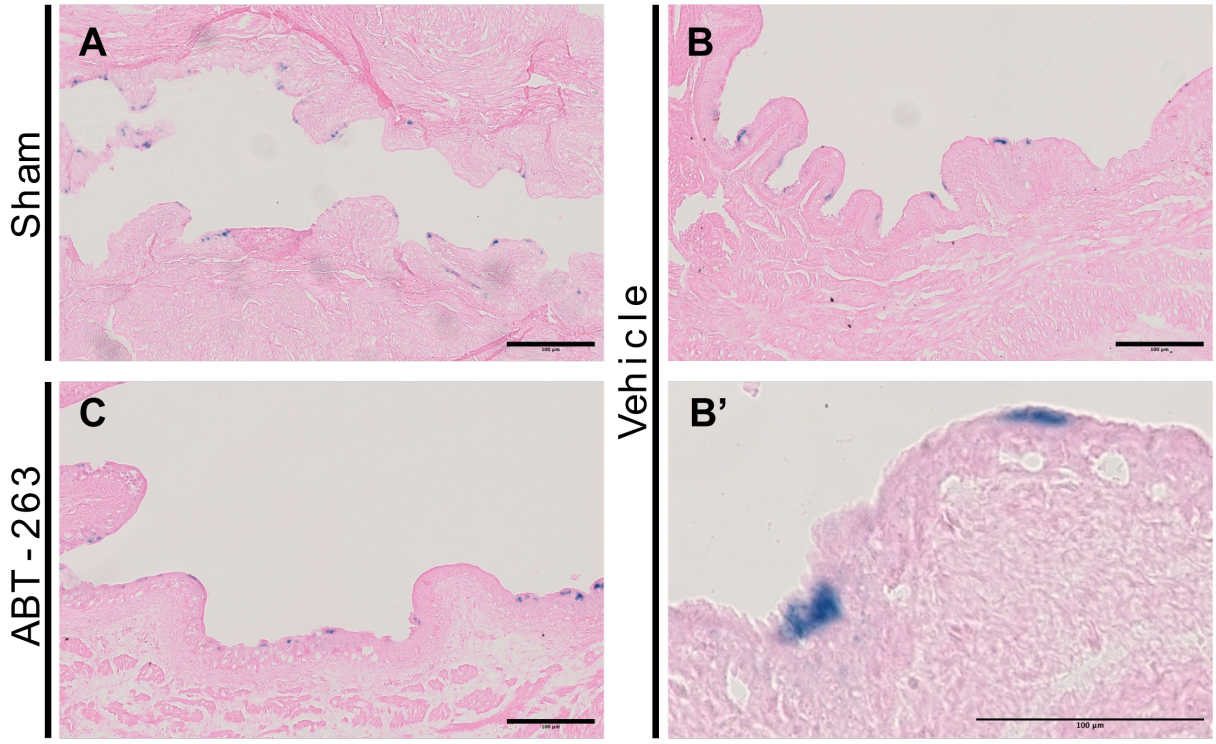

Figure 35 - Spinal cord injury does not induce senescence in the bladder. (A), (B) and (C) representative bladder longitudinal sections showing a diffuse distribution of senescent cells (blue) mainly located in the outer layer of transitional epithelium of the bladder (umbrella cells) of sham, vehicle- and ABT-263-treated spinal cord injured animals, respectively. 100x. (B') detail showing senescent umbrella cell. (n=3). 400x. Scale bars = 100μm. SA-β-gal staining.

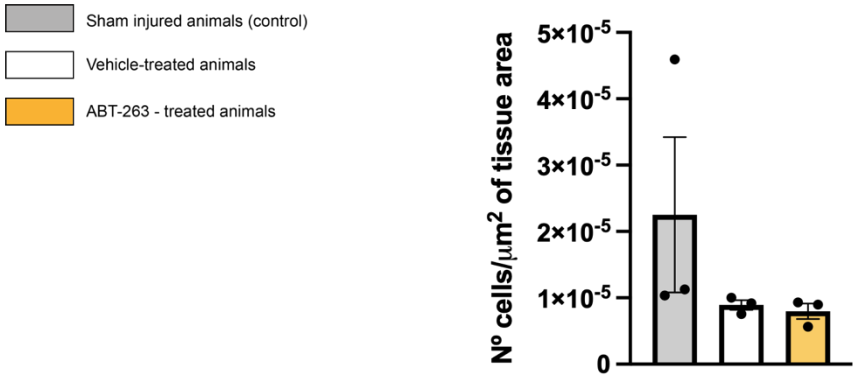

Figure 36 – Spinal cord injury does not alter the number of senescent cells in the bladder at 15 dpi. The number of senescent cells was automatically counted using QuPath and normalized for the area of tissue analysed. This calculation was performed in sham (grey), vehicle- (white) and ABT-263-treated animals (yellow). (n=3). Data is presented as the number of cells per μm^2 of tissue area and expressed as mean ± SEM.

5. Discussion

SCI causes devastating motor and sensory disability below the level of injury, but is also the main culprit of other less-discussed secondary conditions observed in these patients (Ahuja et al. 2017). The peripheric organ pathology seen after a SCI is most often associated with AD, respiratory, bowel and bladder dysfunction, osteoporosis, metabolic syndrome and immunodeficiency, among others (Bloom et al. 2020; Goodus and McTigue 2020). These conditions are a consequence of the severance of ANS tracts and its supraspinal control, and from the systemic and chronic inflammation (Teasell et al. 2000; Anthony and Couch 2014; Sun et al. 2016; Ahuja et al. 2017; Bloom et al. 2020).

Paramos-de-Carvalho, Martins, et al. (2021) have shown that senescent cells are induced in the spinal cord after an injury and create a pro-inflammatory and pro-fibrotic environment that can be reverted by the treatment with the senolytic drug ABT-263. As senescent cells produce SASP factors that can induce senescence in neighbouring tissues, we hypothesized that the pathology described in peripheral organs could be partially mediated by the induction of senescent cells in these organs, in the context of a SCI, and that it could also be ameliorated by the same senolytic treatment.

The organs were chosen in function of their importance. The liver due to its influence on the overall metabolism and main role in the systemic inflammatory response, thus contributing to the multiple organ dysfunction induced after SCI (Goodus and McTigue 2020). The spleen, as it is a lymphoid organ with important functions in immunity and blood filtration (Noble et al. 2018). And the bladder, control of which becomes extremely affected after a SCI (Herrera et al. 2010; Wu et al. 2022).

5.1. An inflammatory state in the spinal cord is observed at 30 days post-injury and is not efficiently modulated by ABT-263 administration during sub-acute phase

We started by evaluating the proteomic content of spinal cord homogenates at 30 dpi, and compared it with data obtained from 15 dpi (Paramos-de-Carvalho, Martins, et al. 2021) (Annex 1). At 30 dpi, we found a decrease in the number of factors being injury-induced, only 9, in contrast with the 35 factors detected at 15 dpi (Fig. 7). This result suggests the surge of a cytokine storm at early time-points after the injury (sub-acute phase), well documented in the literature (Hellenbrand et al. 2021). At 30 dpi, from the 9 factors upregulated only 3 were already present at 15 dpi, and were interestingly identified as potential SASP factors (Fig. 9). Thus reinforcing the previously described persistence over time of senescent cells in the spinal cord after injury (Paramos-de-Carvalho, Martins, et al. 2021).

Our analysis showed that there are 3 factors (**IL-28A/B, PEDF and Thrombopoietin**) (Fig. 8) specifically induced in the spinal cord at 30 dpi that are significantly modulated by ABT-263; 3 factors (**Angiopoietin-1, CCL12 and IL-7**) that are specifically induced in the spinal cord at 30 dpi but are not modulated by ABT-263; and, finally, 3 factors (**IL-33, CCL11 and I-TAC**) (Fig. 9) that were still elevated at 30 dpi but lost their regulation by ABT-263.

IL-28A/B, also known, respectively, as IFN-λ2 and IFN-λ3, belong to the third family of interferons (IFNs) (Roselli et al. 2018). Classically, IFNs have been associated with autocrine and paracrine factors secreted by many cells in response to viral infections. However, recently it was shown that they also possess other immunomodulatory functions (Roselli et al. 2018). IFNs were identified as potential therapeutic targets due to their pro-inflammatory role in the CNS (Manivasagam et al. 2022). They act through signalling of myeloid cells that, in turn, lead to Th1 cell maintenance of neuroinflammation, with continued inflammatory cytokine production (Manivasagam et al. 2022). Th1 cells secrete cytokines such as IFN-γ and TNF-α (Raphael et al. 2015). IFN-γ activates macrophages and dendritic cells, and is considered a SASP factor along with TNF-α (Raphael et al. 2015; Calcinotto et al. 2019; Paramos-de-Carvalho, Jacinto, et al. 2021). In addition to this, IL-28A/B also induces G1 cell cycle arrest via induction of the cell cycle inhibitor p21 (Witte et al. 2010), which is characteristic of a senescent state. Although this does not directly imply the development of a senescent phenotype, it makes IL-28A/B a SASP candidate. Considering our data, the increase in IL-28A/B observed is probably contributing for continuing inflammation in the spinal cord and senescence induction. The fact that ABT-263 treatment reduced the levels of IL-28A/B further strengthens its SASP potential.

PEDF, is a neurotrophic protein and a potent angiogenic inhibitor (He et al. 2015; Winokur et al. 2017), detected in a variety of tissues including the CNS (Yabe et al. 2010).

The induction of PEDF observed might be associated with the attempt at axonal regeneration and neuronal plasticity that happens during this phase. In fact, it has been shown that PEDF is an important mediator of axonal regeneration in adult mammalian regenerative injury paradigms. PEDF does this by promoting neurite outgrowth and neuronal survival of dorsal root ganglion neurons through the NF-kB pathway and Trk-dependent neurotrophic factors (Stevens et al. 2019). This has also been observed *in vitro* in spinal cord motor neurons in embryonic avian cultures (Houenou et al. 1999). Interestingly, in a non-regenerative paradigm, like our study, Stevens et al. (2019) identified 3 genes of the PEDF pathway that were upregulated (*ccl2*, *ccl5*, and *ccl6*) and are known to be associated with axonal regeneration (Kwon et al. 2015). In our study, the activation of PEDF occurred only at a chronic time-point where a mature glial scar has already been formed. As this scar is known to partially restrict axonal regrowth, we anticipate that although activated, PEDF will not be able to promote axonal repair (Ahuja et al. 2017; Bradbury and Burnside 2019). In addition, PEDF seems to inhibit angiogenesis in the spinal cord (Menezes et al. 2020). Furthermore, PEDF has been shown to induce pro-inflammatory cytokine secretion in microglia cells (Sanagi et al. 2005; Takanohashi et al. 2005), thus contributing to the inflammatory microenvironment of the spinal cord. As the ABT-263 treatment reduced the levels of PEDF, it is possible that it is produced by senescent cells or induced by an upstream factor secreted by senescent cells. Thus, this beneficial effect of ABT-263 might help ameliorate the inflammatory state in the spinal cord at 30 dpi.

Thpo is a cytokine produced by the kidney and liver, classically involved in the proliferation and late-stage maturation of megakaryocytes, thus promoting haemostasis (Kaushansky 2003). The need to control haemorrhage caused by the injury might justify the increase of Thpo levels in vehicle-treated injured animals. However, at 30 dpi this control becomes less needed because this stage corresponds to a late stage of the injury. More recently, Thpo and its receptor (Mpl) were detected in the CNS and it is believed that Thpo is produced in neural tissues, as its molecular weight does not allow it to cross the blood-brain barrier (Ivanova et al. 2010). A potential role of Thpo in a neural context has been demonstrated in a neonatal rat model of ischemia injury, with this factor playing a neuroprotective role. In addition to this, it is also hypothesized that Thpo may have similar mechanisms of neural protection as erythropoietin (Yang et al. 2016; Li et al. 2020). Interestingly, the chronic inflammation present in the spinal cord may be responsible for the induction of Thpo levels locally (Ivanova et al. 2010). Supporting this possibility is the induction of Thpo by IL-6 signalling in the liver (Kaushansky 2005), and the fact that patients with meningitis show elevated levels of Thpo (Ivanova et al. 2010). Even though Thpo role might be beneficial, or at least not detrimental to the spinal cord, the treatment with ABT-263 leads to the reduction of Thpo levels. This might be an indirect consequence of reducing

inflammation in the spinal cord that would then lead to lower levels of inflammation-induced Thpo.

IL-7 becomes upregulated only at 30 dpi. This cytokine is a SASP factor, has strong chemotactic properties for macrophages, promotes neuronal apoptosis and limits functional recovery (Bao et al. 2018; Yuan et al. 2019). **CCL12,** a member of the CCL2 family, is also specifically increased at 30 dpi. It is a pro-inflammatory factor and acts on the same receptor as CCL2. CCL2 is increased in the spinal cord at 15 dpi and is a known SASP factor, with important functions in the chemotaxis of macrophages, senescent cell clearance and paracrine senescence (Eggert et al. 2016; Gonzalez-Meljem et al. 2018; Paramos-de-Carvalho, Jacinto, et al. 2021). Finally, **Angiopoietin-1**, an angiogenic factor, is also upregulated at 30 dpi, possibly involved in vascular remodelling (Ritz et al. 2012; Yao et al. 2021). These factors are, therefore, contributing to the pro-inflammatory microenvironment of the spinal cord, characteristic of the chronic inflammatory state of this time-point. ABT-263 did not modulate these factors and for that reason we would suggest that these are not produced by senescent cells and are indeed markers of the perpetuation of inflammation that is sustained by the increased infiltration by several immune cells. Another possibility is that ABT-263 is no longer efficient in modulating these particular inflammatory pathways at this later time-point, since its administration was only performed during the sub-acute phase.

IL-33, **CCL11** and **I-TAC** (also known as CXCL11), are inflammatory cytokines that continue elevated at 30 dpi (Fig. 9). These three cytokines are also known SASP factors (Saito et al. 2020; Paramos-de-Carvalho, Jacinto, et al. 2021; Paramos-de-Carvalho, Martins, et al. 2021; Yamagishi et al. 2022). IL-33 has been shown to be upregulated in the nuclei of astrocytes in the spinal cord of mice with contusive SCI at least for 42 dpi (Pomeshchik et al. 2015). This type of expression is associated with the suppression of the transcription factor NF-kB and, thus, a reduction of the pro-inflammatory NF-kB-triggered genes (Ali et al. 2011; Liu et al. 2017). As suggested by Pomeshchik et al. (2015), this can be a compensatory mechanism to inhibit an excessive inflammatory response. Nonetheless, both pro- and anti-inflammatory functions have been attributed to this cytokine depending on the specific situation, often being considered an alarm mediator released from damaged cells (Lamkanfi and Dixit 2009; Milovanovic et al. 2012; Sattler et al. 2013). The induction of this factor at 15 and 30 dpi after SCI is thus explained. Its modulation by ABT-263 at 15 dpi probably translates the pro-inflammatory improvement observed. The loss of modulation at 30 dpi, on the other hand, is probably justified by a reduction in effectiveness of ABT-263 and the slow reappearance of senescent cells. Counteracting any possible anti-inflammatory effect of IL-33 are the cytokines CCL11 and I-TAC, also upregulated. These are a good example of a deleterious pro-inflammatory SASP, contributing to a chronic inflammatory environment in the spinal cord.

These cytokines are SASP factors that were maintained over time in the spinal cord from 15 dpi to 30 dpi. This correlates with the chronic accumulation of senescent cells observed by Paramos-de Carvalho, Martins, et al. (2021). Moreover, we should draw attention to IL-7, a SASP factor absent at 15 dpi and only induced at 30 dpi. This situation reveals the dynamic nature of the senescence/SASP profile, which might change over time. Moreover, the fact that ABT-263 regulates these SASP factors at 15 dpi but not at 30 dpi, strongly suggests the loss of ABT-263 activity and the induction of new senescent cells that over time start to increase again and may have changed their inflammatory profile. Contributing to this idea, is the lower proportion of upregulated factors that were downregulated by ABT-263 at 30 dpi, only 33%, compared with the 77% at 15 dpi. Thus, with the loss of ABT-263 effectiveness soon after the end of its administration, the regulation of IL-28 A/B, PEDF and Thpo by ABT-263 that we see at 30 dpi might be explained by the indirect induction of these factors (a possibility described above) and, consequently, an earlier modulation by ABT-263 of their inductors, which translates into the significant decrease seen at 30 dpi.

5.2. ABT-263 appears to induce hepatotoxicity in the liver and the histopathology induced by spinal-cord injury is mild at 15 days post-injury

At 15 dpi the cytokine arrays revealed a statistically significant increase in the levels of inflammatory factors (**Leptin**, **IL-6, Reg3G and Complement Factor D**), fibrosis factor (**Periostin**), growth factor (**VEGF**), **LIF** and **FGF acidic** in the liver (Fig.10) (Table 2). The 8 factors found upregulated in the liver after SCI were not successfully decreased by ABT-263 treatment. Even though 3 of these cytokines are known SASP factors, the fact that the senolytic had no effect at this time-point, probably indicates that these factors were not being produced by senescent hepatic cells. Furthermore, the upregulation of these factors does not match with the increase of senescent cells seen in ABT-263-treated injured animals (Fig. 32).

The increase in the number of senescent cells in the ABT-263-treated spinal cord injured animals at 15 dpi is most probably due to ABT-263 hepatotoxicity. Indeed, an increase in ALT levels (a marker of hepatocellular injury) has been identified after ABT-263 treatment in humans (Wilson et al. 2010; McGill 2016). These phenotypic alterations in the senescent profile at 15 dpi are most probably one of the reasons behind the increase in the number of factors (30) that are upregulated at 30 dpi in ABT-263-treated animals (Fig. 12). The majority of these factors are implicated in liver fibrosis and HSCs activation (**Angiopoietin-1; CCL2; CXCL9; I-TAC; Gas 6; IFN-γ; IL-5; IL-11; IL-27p28; IL-33; Lipocalin-2; MMP-2; Osteopontin; Pref-1; VEGF**); followed by factors associated with liver inflammation (**CCL2; CCL6; CCL-12; I-TAC; IFN-γ; IL-7; IL-11; IL-28A/B; IL-33;**

Osteopontin; Leptin; RAGE; TNF-α); and, even, factors associated with NAFLD and the progression of NASH (**RAGE; Retinol Binding Protein 4 (RBP4); Gas6; IL-11; Vascular Cell Adhesion Molecule 1 (VCAM-1); WISP-1**) (Table 2). Thus, these observations indicate chronic liver dysfunction at 30 dpi probably caused by ABT-263. Nonetheless, two factors, **Periostin** (pro-fibrogenic, pro-senescence) (Kumar et al., 2018) and **Pentraxin 3** (implicated in liver inflammation) (Feder et al., 2020) were upregulated in vehicle-treated injured animals and were successfully decreased with the ABT-263 treatment (Fig. 11). Even though ABT-263 probably no longer has any senolytic effect by 30 dpi, this modulation possibly happens due to events initiated at earlier time-points, either indirectly by induction and modulation of an upstream factor or directly by an earlier modulation of the factor, between the 15 and the 30 dpi. For example, Periostin, was also upregulated in vehicle-treated injured animals at 15 dpi, but is only decreased by ABT-263 at 30 dpi.

An increase in **Leptin** in the context of SCI has been associated with the disruption of sympathetic innervation of the white adipose tissue (the main source of Leptin), the increase over time of fat mass compared to lean mass, the larger cross-sectional area of fat tissue, as well as, systemic inflammation and hyperinsulinemia (Fried et al. 2000; Lu and Li 2000; Rayner and Trayhurn 2001; Jeon et al. 2003; Gorgey et al. 2014; Pérez-Pérez et al. 2020). Glucocorticoids and proinflammatory factors (TNF-α, IL-1 and IL-6) are known to increase the secretion of Leptin (Lee and Fried 2009; Tsubai et al. 2017; Pérez-Pérez et al. 2020). Systemic chronic inflammation, described after SCI, is also responsible for hypothalamic Leptin resistance, which further aggravates the problem by preventing the negative feedback loop of Leptin secretion (Pérez-Pérez et al. 2020). Leptin is increased in the spinal cord at 15 dpi (personal communication). As TNF-α and IL-1 are also elevated in the spinal cord at this time point (Paramos-de-Carvalho, Martins, et al. 2021), this contributes to the idea of a systemic effect of these cytokines (SASP) in the elevation of Leptin in the liver. IL-6, elevated in the liver, can also contribute to the increase of Leptin levels in SCI animals. Leptin can also be the main culprit for the elevation of the VEGF levels observed in the liver, by inducing its production in HSCs (Martínez-Uña et al. 2020).

When considering the histopathology and senescence profile of the liver at 15 dpi it is possible to find similarities with the proteomic profile discussed above.

The liver H&E staining revealed glycogen depletion in SCI samples (vehicle- and ABT-treated) compared to controls (Fig. 17). Glycogen is a polymer of glucose, usually stored in the liver and muscle. Under elevated energy expenditure, it is broken down and released as glucose (Kanungo et al. 2018; Petersen and Shulman 2018).

One of the reasons for this glycogen depletion might be associated with a lower intake of food by the paralyzed animals, associated with pain and discomfort from the oral gavages being performed or due to mobility difficulties. Furthermore, SCI is correlated with

metabolic syndrome, insulin resistance and diabetes type II (Goodus and McTigue, 2020). An increase in insulin resistance or deficient production of insulin would decrease glycogen storage in the liver. On one hand, the decrease in insulin levels in these acute time points can be explained by deficient vascularization of the β islets in the pancreas, with reduced production of insulin. This situation has already been described in T10 contusion SCI mouse model, from 7 to 14 dpi (Jing et al. 2018). On the other hand, the fast accumulation of fat in the liver and hyperglycaemia associated with IL-6 inflammation in the liver after the SCI are associated with whole-body insulin resistance (Schmidt-Arras and Rose-John 2016; Goodus and McTigue 2020).

Leptin, which is upregulated in the liver, has also been connected to both the promotion and the decrease of glycogen in liver hepatocytes (Kamohara et al. 1997; Denroche et al. 2012; D'souza et al. 2017; Martínez-Uña et al. 2020). These conflicting findings are probably correlated with factors such as nutritional status, fed vs. fasting, diet, adiposity, and physical exercise among others (D'souza et al. 2017). Considering this, we cannot exclude a possible effect of leptin on the glycogen depletion that we observed.

The fact that glycogen depletion is still present in ABT-263-treated injured animals is probably due to the lack of modulation of factors such as Leptin and IL-6 (Fig. 10) that continue to contribute to the liver pathology.

H&E also revealed an increase in the number of inflammatory foci (Fig. 19), often associated with necrosis in the SCI animals, suggesting the presence of an inflammatory stimulus. This type of inflammation might be driven by an increase in intestinal permeability and gut dysbiosis, with bacterial translocation to the blood arriving in the liver through the portal tracts (Goodus & McTigue, 2020). This has been proven in mice with the exact same injury as the one in our study (Kigerl et al. 2016). In fact, tight junction breakdown of epithelial cells persists for 4 weeks after SCI in mice (Goodus & McTigue, 2020; Kigerl et al., 2018). Leptin will probably contribute to this observation, because it can sensitize KCs causing a hyper-inflammation response to gut-derived low-dose bacterial endotoxins (Martínez-Una et al., 2020). Our cytokine arrays also revealed a significant elevation in the pro-inflammatory cytokines and SASP factors IL-6 and LIF; Reg3G and Complement Factor D (Fig. 11). All these factors are associated with inflammatory states in the liver and may be correlated with this increase in inflammatory infiltrates (Norris et al. 2014; Schmidt-Arras and Rose-John 2016; Chen et al. 2019; Barratt and Weitz 2021; Yuan et al. 2022). The lack of reduction of these inflammatory infiltrates in the ABT-263-treated animals, again, might be explained by the also absent modulation of these upregulated factors.

To further evaluate the inflammatory status of our livers at 15 dpi, KCs and T lymphocytes were quantified. The number of KCs kept constant across experimental groups

and were close to 15% (Fig. 21). This value is described as a standard percentage of KCs in the total liver cell population (Kolios et al. 2006). Previous reports showed statistically significant increases in liver KCs at 23 and 42 dpi in T8 SCI rats (Goodus et al. 2018; Goodus et al. 2021). The lack of an increase in our vehicle-treated injured animals might be due to being too early to see this change. Although Sauerbeck et al. (2015) reported robust liver inflammation right after thoracic SCI, demonstrated by an increase in cytokine and $CD68^+$ (macrophage) mRNA; and the $CD68^+$ area, it is important to notice this is not a KC-specific marker. Even though, in our case it is not possible to observe an increase in the area of $Clec4f^+$ Kupffer cells, this does not mean that there is not activation of these cells at the molecular level. For example, M2b-macrophages (induced by exposure to immune complexes and agonists of TLRs or IL-1R, like LPS, which we hypothesized that are being responsible for the increase in inflammatory infiltrates) express both pro- and anti-inflammatory cytokines, namely TNF-α, IL-1, IL-6, IL-10^{high}, and IL-12^{low}. As we know IL-6 is upregulated in our SCI livers. In addition, it is important to note that IL-6 is also produced by M1-macrophages. Hepatocyte necrosis seen in some of our inflammatory foci also activates KCs (Nguyen-Lefebvre and Horuzsko 2015). Thus, we can possibly infer that KC activation is present.

The number of T lymphocytes also kept constant across experimental groups (Fig. 22). The cells observed with immunohistochemistry had a normal distribution characteristic of the resident T lymphocyte population in the liver (Fig. 20) (Wang and Zhang 2019). The accumulation of these cells in the liver has been associated with obesity and metabolic syndrome (Breuer et al. 2019; Herck et al. 2019). In the liver, although it has been observed a slight increase in these cells 23 days after injury, this was only statistically significant with prior SCI liver inflammation (Goodus et al., 2021). Thus, the lack of change in the number of T lymphocytes is probably justified by the reason stated above and by the early time-point (15 dpi).

Steatosis is another histopathological characteristic strongly associated with SCI, having been identified in the liver of T8 SCI rats at 42 dpi (Sauerbeck et al. 2015; Goodus et al. 2018; Goodus et al. 2021). In our study, H&E did not reveal steatosis, only some small isolated cytoplasmatic vacuoles in a few hepatocytes; therefore, we performed an Oil Red O staining to better evaluate the lipidic content of the liver. At 15 dpi, SCI seemed to histologically induce a slight increase in the liver's lipidic content compared to controls (Fig. 23). However, there were no statistically significant differences between experimental groups (Fig. 24). Simultaneously, when comparing with Goodus et al. (2015) findings they also did not see a statistically significant increase in the liver at 14 dpi. In fact, it only significantly increased at 1 dpi and then at 21 dpi. After an acute response, this suggests a chronic evolution of steatosis and that our time point was too early to see this type of pathology. In

addition to this, at the proteomic level Leptin, LIF and FGF acidic, all anti-steatotic factors, were significantly elevated and ABT-263 was unsuccessful in reducing their levels (Xu et al. 2020; O'brien et al. 2022; Yuan et al. 2022). Thus, this might justify the non-development of steatosis at this time point. At chronic timepoints (30 dpi), the upregulation of these factors stopped, which might translate into the development of steatosis in more chronic stages of the injury.

Finally, at 15 dpi there was no SCI-induced increase in fibrosis or iron sequestration (Fig. 25 and 26). Nonetheless, in the case of fibrosis, the cytokine arrays revealed the upregulation of several pro-fibrotic cytokines, namely Leptin, Periostin and LIF (Hisaka et al. 2004; Kumar et al. 2018; Martínez-Uña et al. 2020; Petrescu et al. 2022). Similarly, Leptin and IL-6 are known to promote iron sequestration in the liver. Thus, there might exist a time lag between the signalling and these phenotypic changes. Therefore, the follow-up of more chronic time points is warranted.

Lastly, when considering the senescent profile, SA-β-gal$^+$ cells were small and appeared to be in the sinusoids (Fig. 31). Considering this, they can be KCs, HSCs, T lymphocytes, or even endothelial cells (Thoolen et al., 2010). They were also present in the inflammatory infiltrates, probably accounting for hepatocytes or immune cells such as neutrophils and mononuclear cells (macrophages, lymphocytes and monocytes).

Senescence of HSCs is often found in fibrotic livers as it plays an important homeostatic mechanism to limit fibrosis (Krizhanovsky et al. 2008; M. Zhang et al. 2021). Therefore, the localization of the SA-β-gal$^+$ cells and the microenvironment which suggests the presence of active HSCs (upregulated Periostin and LIF) (Hisaka et al. 2004; Sugiyama et al. 2016; Kumar et al. 2018), will probably imply the presence of senescent HSCs. Nevertheless, this would not explain the increase of senescent HSCs in ABT-263 treated animals, as this upregulation in pro-fibrotic factors is only present in vehicle-treated injured animals, unless ABT-263 is toxic to the liver and actually promotes activation of HSCs in a rate higher than the elimination of their senescent counterparts. Thus, more HSCs activation translates into more HSCs senescence.

There is little information about liver sinusoidal endothelial cell (LSEC) senescence. Nonetheless, LSEC senescence has been associated with pro-inflammatory SASPs (IL-6 included, which is upregulated in our study); liver fibrosis through the activation of HSCs and hypoxia; and the loss of liver regenerative capacity (Duan et al. 2022; Wan et al. 2022). Both a pro-inflammatory SASP and activation of HSCs are implied in our study, which might indicate LSEC senescence.

Senescent KCs/macrophages have been associated in other disease models with prolonged pro-inflammatory phenotypes, impaired phagocytosis, antigen-presenting failure, among others (Lee et al. 2021; Sadhu et al. 2021; Sharma et al. 2022). The SASP of

senescent hepatic cells attracts macrophages and influences their polarization (M1/M2). This is necessary for a successful removal of senescent cells, thus preventing their accumulation. However, age, other external stressors and cellular senescence in other cell types can induce macrophage senescence, leading to their dysfunction (Sharma et al., 2021). TNF-α and IL-6 have been identified in the SASP of senescent macrophages (Sadhu et al., 2021; Sharma et al., 2021). Nonetheless, when considering the possibility of induced senescent cells being KCs/macrophages we cannot overlook the fact that SA-β-galactosidase can be induced in non-senescent macrophages as part of a reversible response to physiological stimuli (IL-4 and IL-13) (Hall et al. 2017). In Hall et al. (2017) study, they believe that $p16^{ink4a}$/SA-β-gal^+ macrophages acquired this phenotype due to physiological reprogramming to a M2-like phenotype. Considering this, we can now have a possible justification for the significant increase in senescent cells in the ABT-263 treated animals compared to vehicle-treated and sham-injured animals. ABT-263 could be promoting a M2-macrophage phenotype by decreasing deleterious SASP factors, thus increasing the number of positive SA-β-gal^+ KCs/macrophages. Indeed, it is known that the SASP can reduce the phagocytic capacity of macrophages and inhibit M2-macrophage polarization (Campbell et al. 2021). Activated HSCs have also been implicated in the M1 to M2 transformation (Chen et al. 2022). At the same time M2-macrophages can promote HSC activation (Roszer 2015).

Thus, the type of senescent cells present in the liver at this time-point is probably a combination of these cells (HSCs, KCs and LSECs) because they constantly communicate with each other, and for the fact that activated HSCs, which are most probably present in our study, induce senescence in LSECs and are associated with M1 to M2 macrophage transformation.

All in all, the proteomic profile partially correlated with the histopathology observed, with possible incongruences being explained by time lags between the molecular expression and the microscopic phenotypic activations, namely the striking differences between the pro-fibrotic microenvironment and the lack of collagen deposition/fibrosis. Interestingly, SA-β-gal^+ cells were increased in ABT-263 treated animals, most probably pointing towards some kind of toxicity of the senolytic in the liver at 15 dpi, which later translates into the great upregulation of pro-fibrotic and pro-inflammatory factors. Indeed, if the senescent cells identified at 15 dpi are in fact HSCs, this would probably justify the great upregulation of pro-fibrotic factors, and even pro-inflammatory factors, as these cells are also known to participate in inflammation (Fujita and Narumiya 2016). With a greater number of activated HSCs, the number of senescent HSCs would also increase.

5.3. The spleen of T9 spinal cord injured mice does not reveal significant pathological alterations at 15 days post-injury

Spleen histopathology was difficult to evaluate due to artefactual changes of the frozen slides. Nevertheless, there were no statistically significant histopathological changes in the spleens or differences between experimental groups (Fig. 27). This lack of significant changes in the spleen may be explained by a lower level of injury (T9 - midthoracic) that does not affect the spleen's sympathetic supraspinal control (high thoracic) (Noble et al. 2018). Moreover, we could not detect any significant differences in the number of senescent cells in the spleen after a SCI and/or ABT-263 treatment (Fig. 34). We could, however, identify senescent cells particularly at the level of the red pulp. This is not unexpected as this organ is physiologically responsible for the elimination of senescent erythrocytes (Boes and Durham 2017; Willard-Mack et al. 2019).

5.4. There is a delayed effect of ABT-263 in the chronic pro-inflammatory microenvironment of the bladder

At 15 dpi, the proteomic profile of the bladder revealed an upregulation of 14 factors mainly associated with bladder inflammation and interstitial cystitis (**CRP**, **CCL3, CXCL9**, **G-CSF**, **IL-5, IL-11**, **IL-12p40**, **IL-33**, **Complement Component C5/C5a, Complement Factor D**) as well as, a few related to bladder cancer (**CRP, G-CSF, EGF**, **Cystatin C, IGFBP-2, PD-ECGF, CXCL9, IL-5, IL-11**) (Fig. 14) (Table 2). There was an overall lack of modulation by ABT-263, with the majority of the 14 factors remaining elevated, and only EGF being decreased (Fig. 13). Interestingly, **IL-10**, an anti-inflammatory factor (Karlsson et al. 2021; The Human Protein Atlas 2022d), was significantly upregulated by the administration of ABT-263 when compared with both the control and the vehicle-treated injured animals, suggesting a beneficial modulation by the senolytic. The lack of modulation by ABT-263 in reducing the levels of the remaining factors, suggests that they are not induced or produced by senescent cells. Indeed, there is no accompanying increase in the number of senescent cells as would be expected with the upregulation observed (Fig. 36). Both vehicle-treated and ABT-263-treated spinal cord injured animals do not show an increase in the number of these cells compared with the controls. The need to perform daily manual voiding of the bladders of the SCI animals in both experimental groups might be masking the effects of ABT-263 in this group. However, this procedure was done for the whole duration of the experiment. In addition to this, the fact that half (15) of the 31 factors upregulated at 30 dpi are modulated by ABT-263 contradicts the idea of manual voiding as a confounding factor.

At 30 dpi there is an upregulation of pro-inflammatory (**CRP, IL-5, IL-33, Complement Component C5/5a, IL-12p40, CCL17, IL-1α, IFN-γ, IL-28A/B, and Lipocalin-**

2), anti-inflammatory (**IL-10, IL-11, GDF-15, IL-13, IL-27p28**) growth (**IGFBP-1, -2, -3, PD-ECGF, FGF-21, HGF**), cell adhesion (**WISP-1** and **Periostin**) and vascular modulation factors (**Endoglin**, **Angiopoeitin-1**, **MMP-2** and **Proliferin**) (Table 2). At 30 dpi we expected a reduction of ABT-263 effectiveness, as it seemed to happen in the spinal cord and the liver. Interestingly, however, we observe a modulation of the factors in the ABT-263-treated groups. This suggests that between 15 dpi and 30 dpi ABT-263 was successful in modulating these deleterious factors. This earlier modulation would, then, be responsible for the decrease seen at 30 dpi, either directly by the elimination of senescent cells or indirectly by the initiation of cascades which led to the reduction of these factors. Supporting this intermediate modulation is the phenotypic improvement in bladder function in ABT-263 treated animals seen until 20 dpi in the Paramos-de-Carvalho, Martins, et al. (2021) study. In addition to this, a possible anti-inflammatory effect of ABT-263 during this intermediate phase might also be responsible by this level of reduction, as only one of the modulated factors is a SASP factor (Hernández-Silva et al. 2022).

From 15 dpi to 30 dpi other factors, such as vascular modulation factors (Endoglin, Angipoietin-1, MMP-2 and Proliferin) and tissue remodelling factor (MMP-3) (Karlsson et al. 2021; The Human Protein Atlas 2022d), become upregulated suggesting some kind of tissue remodelling in the bladder, probably an adaptation to the dysfunction caused by the SCI and even by our daily manipulation. Endoglin, for example, is primarily expressed in proliferating vascular endothelial and smooth muscle cells and is highly expressed in endothelial cells during tumour angiogenesis and inflammation (Fujita et al. 2009). Indeed, these factors are also often implicated in bladder cancer (Sakamoto et al. 2008).

Interestingly, some of the factors found upregulated in both time-points have also been known to be increased in the urine of patients with kidney dysfunction, namely **EGF**, **Complement Factor D**, **Cystatin C**, **FGF-21**, **RBP4** and **IGFBP-1** (Van Kleffens et al. 2001; Conti et al. 2006; Worthmann et al. 2010; Domingos et al. 2016; Cortvrindt et al. 2022). Therefore, we cannot disregard this situation as a possible cause for our observations. Indeed, kidney dysfunction has been described after SCI and the elevated urine pressures present in our animals can lead to kidney damage (Karin et al. 2008; Fischer et al. 2012; Vaidyanathan, Soni, et al. 2012; Vaidyanathan, Selmi, et al. 2012). Supporting this hypothesis, is the fact that our bladder homogenates were most certainly contaminated with urine, as no cleaning procedure was performed.

EGF was the only factor modulated by ABT-263 at 15 dpi (Fig. 13). Beyond its possible function as a biomarker for kidney disease, this factor is a potent mitogen and tumour promotor, and it is associated with bladder cancer (Izumi et al. 2012). In fact, it promotes cell proliferation, and reduces apoptosis and angiogenesis (Pache 2006). It is also a known SASP factor (Aravinthan and Alexander 2016). This may explain the modulation

ability of ABT-263. Thus, this might suggest that our ABT-263 treated animals have lower probability of bladder tumorigenesis after SCI, a common comorbidity. The risk of bladder cancer is 16 to 28 times higher in SCI patients than in the normal population, and it is possibly correlated with chronic inflammation (Kalisvaart et al. 2010). In addition to this, this factor has also been associated with uroepithelium hyperplasia (Cheng et al. 2002). This pathology was in fact identified in our samples, as discussed below, and, similarly, to the ABT-263 reduction of EGF, we also see a reduction in the degree of uroepithelium hyperplasia.

When comparing the 15 dpi proteomic profile with the histopathology (Fig. 29 and 30), it is possible to observe a tight correlation between the two, represented by the increase in pro-inflammatory and specific factors associated with interstitial cystitis, namely CCL4, CXCL9, IL-12p40, IL-33 (Gonzalez et al. 2014; Kochiashvili and Kochiashvili 2014; Guo et al. 2018; Jensen et al. 2018). The H&E staining of the vehicle- and ABT-263-treated SCI samples revealed chronic cystitis, with the typical histopathological characteristics of urothelium desquamation (erosion), infiltration of the submucosa with mononuclear inflammatory cells and a few neutrophils, a thickened connective tissue and hypertrophy of the muscularis layer (Breshears and Confer 2017). In addition to this, there was simple urothelium hyperplasia and the bladders were abnormally distended due to sustained increased urine volume. These characteristics appeared to improve in the ABT-263-treated injured group, except from the abnormal bladder distension. All in all, these changes can be justified by detrusor-sphincter dyssynergia, which leads to constant high intravesical pressure and promotes muscle hypertrophy, molecularly represented by the elevations in IGFBP-2 observed in our experimental groups, and abnormal distension (Perez et al. 2022). In addition to this, the release of neurotransmitters (norepinephrine) and other stress hormones, lead to urothelium tight junction disruption, which in turn causes loss of impermeability and inflammation. This inflammation further promotes the disruption of the urothelium and is potentially responsible for the chronic cystitis observed (Perez et al. 2022). The adventitia inflammation observed is probably due to the bladder's manual voiding performed in all SCI animals. This voiding, which was done twice daily, might also contribute to the cystitis observed and the haemorrhage seen in the bladder wall.

It was possible to identify SA-β-gal positive cells in the urothelium of the bladder (Fig. 35). Due to their location, in the superficial layer of the epithelium, and shape they most probably correspond to senescent umbrella cells. There is a lack of variation in the number of these cells as described previously, thus, what we observed was probably the physiologic shedding of senescent umbrella cells, which are quickly replaced by new umbrella cells coming from cells in the intermediate layer of the urothelium, in order to recover the barrier (Lavelle et al. 2002).

5.5. IL-28 A/B a possible systemic SASP factor inductor of peripheral pathology

IL-28A/B, already described in the spinal cord section, is an inflammatory factor, capable of causing G1 cell cycle arrest via induction of the cell cycle inhibitor p21 (Witte et al., 2010), which is characteristic of cellular senescence. Although this does not directly imply the development of a senescent phenotype, it makes IL-28A/B a SASP candidate. Considering that this factor is found in all the three organs at 30 dpi, possibly means it is produced in the spinal cord after injury or by another organ. After which, it becomes systemic and might contribute to the inflammatory profile observed not only in the spinal cord, but also in the liver and bladder. The fact that ABT-263 treatment reduced the levels of IL-28A/B in the spinal cord and bladder further strengthens its SASP potential, as this is translated in phenotypic improvements observed by Paramos-de-Carvalho, Martins, et al. (2021) in both organs.

5.6. Study Limitations

The main limitation of this study lies on the small number of animals used, which in some cases impaired the capacity to attain statistically significant conclusions.

The lack of senescent cell quantification and the absence of histopathological evaluation in peripheral organs at 30 dpi does not allow for a proper evaluation of the progression of senescence and its possible correlation with pathology over time. The characterization of the senescent profile also lacked the validation by a second or a third hallmark of senescence. Nonetheless, the characterization using SA-β-gal allowed a general characterization and enabled us to form an idea of the senescence profile in these peripheric organs after a SCI, with and without treatment with the senolytic ABT-263.

In addition to this, in the histopathological observations there were some limitations in the evaluation of the organs, as the sections had artefactual changes from being embedded in OCT and frozen. Furthermore, it would be very informative if we could have analysed the histology at later time points to allow the development of the pathology.

6. Final remarks

In the spinal cord, the factors that were decreased by ABT-263 at 15 dpi were no longer modulated at 30 dpi, suggesting a shift in the spinal cord senescence profile and/or a decrease in the effectiveness of ABT-263 for the specific 30 dpi proteomic spinal microenvironment, a time-point crucial in the perpetuation of chronic inflammation.

The liver microenvironment at 15 dpi revealed a chronic pro-inflammatory and pro-fibrotic microenvironment conducive of the liver pathology typically described after a SCI at later stages. The increased number of SA-β-gal at 15 dpi and the upregulation of pro-

inflammatory and pro-fibrotic factors at 30 dpi in ABT-263 treated animals suggest hepatotoxicity of this senolytic drug.

The bladder also revealed chronic inflammation and a pro-fibrotic/pro-tumoral microenvironment at 15 and 30 dpi. ABT-263 only reduced most of these factors at 30 dpi suggesting that senescent cells might be induced and modulated between 15 and 30 dpi.

The spleen appeared to not be affected by the SCI at 15 dpi.

At this stage, we do not have evidence for the existence of a systemic SASP originated in the spinal cord and responsible for the induction of senescent states at the periphery, underlying its pathology. Nevertheless, our study has identified a new potential factor, IL-28A/B, as a new possible systemic factor responsible for the multiorgan dysfunction observed after SCI, and have demonstrated ABT-263 efficacy in modulating its induction, both at central (spinal cord) and systemic (bladder) level.

7. References

Ahn H, Lee G, Kim J, Park J, Kang SG, Yoon SI, Lee E, Lee GS. 2021. Nlrp3 triggers attenuate lipocalin-2 expression independent with inflammasome activation. *Cells*. *10*(7). https://doi.org/10.3390/cells10071660

Ahuja CS, Wilson JR, Nori S, Kotter MR, Druschel C, Curt A, Fehlings MG. 2017. Traumatic spinal cord injury. *Nature Reviews Disease Primers*. 3. https://doi.org/10.1038/nrdp.2017.18

Ali S, Mohs A, Thomas M, Klare J, Ross R, Schmitz ML, Martin MU. 2011. The Dual Function Cytokine IL-33 Interacts with the Transcription Factor NF-κB To Dampen NF-κB–Stimulated Gene Transcription. *The Journal of Immunology*. *187*(4):1609–1616. https://doi.org/10.4049/jimmunol.1003080

Alizadeh A, Dyck SM, Karimi-Abdolrezaee S. 2019. Traumatic spinal cord injury: An overview of pathophysiology, models and acute injury mechanisms. *Frontiers in Neurology*. *10*. https://doi.org/10.3389/fneur.2019.00282

Allison DJ, Ditor DS. 2015. Immune dysfunction and chronic inflammation following spinal cord injury. *Spinal Cord*. 53(1):14–18. Nature Publishing Group. https://doi.org/10.1038/sc.2014.184

Andrew PS, Kaufman S. 2001. Splenic denervation worsens lipopolysaccharide-induced hypotension, hemoconcentration, and hypovolemia. *American Journal of Regulatory Integrative Comparative Physiology.* 280:1564-1572. http://www.ajpregu.org

Anthony DC, Couch Y. 2014. The systemic response to CNS injury. *Experimental Neurology*. 258:105–111). Academic Press Inc. https://doi.org/10.1016/j.expneurol.2014.03.013

Apodaca G, Kiss S, Ruiz W, Meyers S, Zeidel M, Birder L. 2003. Disruption of bladder epithelium barrier function after spinal cord injury. *American Journal of Physiology - Renal Physiology*, *284*:553-555. https://doi.org/10.1152/ajprenal.00359.2002

Aravinthan A, Alexander GJ. 2016. Senescence in chronic liver disease: Is the future in aging?. *Journal of Hepatology.* 65:825-834.

Aravinthan A, Challis B, Shannon N, Hoare M, Heaney J, Alexander GJ. 2015. Selective insulin resistance in hepatocyte senescence. *Experimental Cell Research*. *331*(1):38–45. https://doi.org/10.1016/j.yexcr.2014.09.025

Aravinthan A, Scarpani C, Tachtatzis P, Verma S, Penrhyn-Lowe S, Harvey R, Davies S, Allison M, Coleman N, Alexander G. 2013. Hepatocyte senescence predicts progression in non-alcohol-related fatty liver disease. *Journal of Hepatology*. *58*(3):407–408. https://doi.org/10.1016/j.jhep.2012.12.010

Asadipooya K, Lankarani KB, Raj R, Kalantarhormozi M. 2019. RAGE is a Potential Cause of Onset and Progression of Nonalcoholic Fatty Liver Disease. *International Journal of Endocrinology*. 2019. Hindawi Limited. https://doi.org/10.1155/2019/2151302

Badhiwala JH, Ahuja CS, Fehlings MG. 2019. Time is spine: A review of translational advances in spinal cord injury. *Journal of Neurosurgery: Spine.* 30(1):1–18. American Association of Neurological Surgeons. https://doi.org/10.3171/2018.9.SPINE18682

Balzan S, De Almeida Quadros C, De Cleva R, Zilberstein B, Cecconello I. 2007. Bacterial translocation: Overview of mechanisms and clinical impact. *Journal of Gastroenterology and Hepatology*. *22*(4):464–471. https://doi.org/https://doi.org/10.1111/j.1440-1746.2007.04933.x

Bankhead P, Loughrey MB, Fernández JA, Dombrowski Y, McArt DG, Dunne PD, McQuaid S, Gray RT, Murray LJ, Coleman HG, James JA, Salto-Tellez M, Hamilton PW. 2017. QuPath: Open source software for digital pathology image analysis. *Scientific Reports*. *7*(1). https://doi.org/10.1038/s41598-017-17204-5

Banks WA, Kastin AJ, Broadwell RD. 1995. Passage of Cytokines across the Blood-Brain Barrier. *Neuroimmunomodulation*. *2*(4):241–248. https://doi.org/10.1159/000097202

Bao C, Wang B, Yang F, Chen L. 2018. Blockade of Interleukin-7 Receptor Shapes Macrophage Alternative Activation and Promotes Functional Recovery After Spinal Cord Injury. *Neuroscience*. *371*:518–527. https://doi.org/10.1016/j.neuroscience.2017.10.022

Bárcena C, Stefanovic M, Tutusaus A, Joannas L, Menéndez A, García-Ruiz C, Sancho-Bru P, Marí M, Caballeria J, Rothlin CV, Fernández-Checa JC, García De Frutos P, Morales A. 2015. Gas6/Axl pathway is activated in chronic liver disease and its targeting reduces fibrosis via hepatic stellate cell inactivation. *Journal of Hepatology*. *63*:670–678.

Barratt J, Weitz I. 2021. Complement Factor D as a Strategic Target for Regulating the Alternative Complement Pathway. *Frontiers in Immunology*. 12. Frontiers Media S.A. https://doi.org/10.3389/fimmu.2021.712572

Basso DM, Fisher LC, Anderson AJ, Jakeman LB, McTigue DM, Popovich PG. 2006. Basso mouse scale for locomotion detects differences in recovery after spinal cord injury in five common mouse strains. *Journal of Neurotrauma*, *23*(5):635–659. https://doi.org/10.1089/neu.2006.23.635

Bigford GE, Garshick E. 2022. Systemic inflammation after spinal cord injury: A review of biological evidence, related health risks, and potential therapies. *Current Opinion in Pharmacology*. 67. Elsevier Ltd. https://doi.org/10.1016/j.coph.2022.102303

Blomster LV, Brennan FH, Lao HW, Harle DW, Harvey AR, Ruitenberg MJ. 2013. Mobilisation of the splenic monocyte reservoir and peripheral CX3CR1 deficiency adversely affects recovery from spinal cord injury. *Experimental Neurology*. *247*:226–240. https://doi.org/10.1016/j.expneurol.2013.05.002

Bloom O, Herman PE, Spungen AM. 2020. Systemic inflammation in traumatic spinal cord injury. *Experimental Neurology.* 325. Academic Press Inc. https://doi.org/10.1016/j.expneurol.2019.113143

Boes K, Durham A. 2017. Bone Marrow, Blood cells, and the Lymphoid/Lymphatic system. In: Zachary J, editor. *Pathologic Basis of Veterinary Disease*. 6th ed. Elsevier. p. 724–804.

Bradbury EJ, Burnside ER. 2019. Moving beyond the glial scar for spinal cord repair. *Nature Communications.* 10:1. Nature Publishing Group. https://doi.org/10.1038/s41467-019-11707-7

Breshears M, Confer A. 2017. The Urinary System. In: Zachary J, editor. *Pathologic Basis of Veterinary Disease*. 6th ed. Elsevier. p. 617–681.

Breuer DA, Pacheco MC, Washington MK, Montgomery SA, Hasty AH, Kennedy AJ. 2019. CD8 T cells regulate liver injury in obesity-related nonalcoholic fatty liver disease. *Am J Physiol Gastro-Intest Liver Physiol*. *318*. https://doi.org/10.1152/ajpgi.00040.2019.-Nonalcoholic

Brommer B, Engel O, Kopp MA, Watzlawick R, Müller S, Prüss H, Chen Y, DeVivo MJ, Finkenstaedt FW, Dirnagl U, Liebscher T, Meisel A, Schwab JM. 2016. Spinal cord injury-induced immune deficiency syndrome enhances infection susceptibility dependent on lesion level. *Brain*. *139*(3):692–707. https://doi.org/10.1093/brain/awv375

Budamagunta V, Foster T, Zhou D. 2021. Cellular senescence in lymphoid organs and immunosenescence. *Aging*. www.aging-us.com

Calcinotto A, Kohli J, Zagato E, Pellegrini L, Demaria M, Alimonti A. 2019. Cellular Senescence: Aging, Cancer, and Injury. *Physiol Rev*. *99*:1047–1078. https://doi.org/10.1152/physrev.00020.2018.-Cellular

Campbell RA, Docherty MH, Ferenbach DA, Mylonas KJ. 2021. The Role of Ageing and Parenchymal Senescence on Macrophage Function and Fibrosis. In *Frontiers in Immunology.* 12. Frontiers Media S.A. https://doi.org/10.3389/fimmu.2021.700790

Campbell SJ, Perry VH, Pitossi FJ, Butchart AG, Chertoff M, Waters S, Dempster R, Anthony DC. 2005. Central Nervous System Injury Triggers Hepatic CC and CXC Chemokine Expression that Is Associated with Leukocyte Mobilization and Recruitment to Both the Central Nervous System and the Liver. *American journal of Pathology.* 166(5):1487-1497.

Campbell SJ, Zahid I, Losey P, Law S, Jiang Y, Bilgen M, van Rooijen N, Morsali D, Davis A EM, Anthony DC. 2008. Liver Kupffer cells control the magnitude of the inflammatory response in the injured brain and spinal cord. *Neuropharmacology*. *55*(5):780–787. https://doi.org/10.1016/j.neuropharm.2008.06.074

Chakraborty R, Burns B. 2022. Systemic Inflammatory Response Syndrome. *Statpearls*. https://www.ncbi.nlm.nih.gov/books/NBK547669

Chang ZQ, Lee SY, Kim HJ, Kim JR, Kim SJ, Hong IK, Oh BC, Choi CS, Goldberg IJ, Park TS. 2011. Endotoxin activates de novo sphingolipid biosynthesis via nuclear factor kappa B-mediated upregulation of Sptlc2. *Prostaglandins & Other Lipid Mediators. 94*(1):44–52. https://doi.org/https://doi.org/10.1016/j.prostaglandins.2010.12.003

Chen J, Argemi J, Odena G, Xu MJ, Cai Y, Massey V, Parrish A, Vadigepalli R, Altamirano J, Cabezas J, Gines P, Caballeria J, Snider N, Sancho-Bru P, Akira S, Rusyn I, Gao B, Bataller R. 2020. Hepatic lipocalin 2 promotes liver fibrosis and portal hypertension. *Scientific Reports*. *10*(1). https://doi.org/10.1038/s41598-020-72172-7

Chen J, Huang X, Huang Z, Cao Y. 2022. Activated Hepatic Stellate Cells Promote the M1 to M2 Macrophage Transformation and Liver Fibrosis by Elevating the Histone Acetylation Level. *Disease Markers*. https://doi.org/10.1155/2022/9883831

Chen W, Zhang J, Fan HN, Zhu JS. 2018. Function and therapeutic advances of chemokine and its receptor in nonalcoholic fatty liver disease. *Therapeutic Advances in*

Gastroenterology. 11. SAGE Publications Ltd. https://doi.org/10.1177/1756284818815184

Chen Z, Downing S, Tzanakakis ES. 2019. Four Decades After the Discovery of Regenerating Islet-Derived (Reg) Proteins: Current Understanding and Challenges. *Frontiers in Cell and Developmental Biology.* 7. Frontiers Media S.A. https://doi.org/10.3389/fcell.2019.00235

Cheng J, Huang H, Zhang ZT, Shapiro E, Pellicer A, Sun TT, & Wu XR. 2002. Overexpression of Epidermal Growth Factor Receptor in Urothelium Elicits Urothelial Hyperplasia and Promotes Bladder Tumor Growth 1. *CANCER RESEARCH.* 62. http://aacrjournals.org/cancerres/article-pdf/62/14/4157/2495928/ch1402004157.pdf

Chuang YC, Tyagi V, Liu RT, Chancellor MB, Tyagi P. 2010. Urine and Serum C-Reactive Protein Levels as Potential Biomarkers of Lower Urinary Tract Symptoms. *Urol Sci.* 21(3).

Conti M, Moutereau S, Zater M, Lallali K, Durrbach A, Manivet P, Eschwège P, Loric S. 2006. Urinary cystatin C as a specific marker of tubular dysfunction. *Clinical Chemistry and Laboratory Medicine*. *44*(3).

Cooper AM, Khader SA. 2007. IL-12p40: an inherently agonistic cytokine. *Trends in Immunology.* 28(1):33–38. https://doi.org/10.1016/j.it.2006.11.002

Coppé JP, Desprez PY, Krtolica A, Campisi J. (2010). The senescence-associated secretory phenotype: The dark side of tumor suppression. *Annual Review of Pathology: Mechanisms of Disease.* 5:99–118. https://doi.org/10.1146/annurev-pathol-121808-102144

Cortvrindt C, Speeckaert R, Delanghe JR, Speeckaert MM. 2022. Urinary Epidermal Growth Factor: A Promising "Next Generation" Biomarker in Kidney Disease. *American Journal of Nephrology.* 53(5):372–387. S. Karger AG. https://doi.org/10.1159/000524586

Da Silva Alves E, De Aquino Lemos V, Ruiz Da Silva F, Lira FS, Dos Santos RVT, Rosa JPP, Caperuto E, Tufik S, De Mello MT. 2013. Low-grade inflammation and spinal cord injury: Exercise as therapy? *Mediators of Inflammation.* https://doi.org/10.1155/2013/971841

Darmadi D, Ruslie RH, Pakpahan C. 2022. Vascular Endothelial Growth Factor (VEGF) in Liver Disease In: Xu K, editor. *Tumor Angiogenesis and Modulators*. IntechOpen. https://doi.org/10.5772/intechopen.103113

David S, Kroner A. 2011. Repertoire of microglial and macrophage responses after spinal cord injury. *Nature Reviews Neuroscience*. *12*(7):388–399. https://doi.org/10.1038/nrn3053

De Alvaro C, Teruel T, Hernandez R, Lorenzo M. 2004. Tumor Necrosis Factor α Produces Insulin Resistance in Skeletal Muscle by Activation of Inhibitor κB Kinase in a p38 MAPK-dependent Manner. *Journal of Biological Chemistry*. *279*(17):17070–17078. https://doi.org/10.1074/jbc.M312021200

Degré D, Lemmers A, Gustot T, Ouziel R, Trépo E, Demetter P, Verset L, Quertinmont E, Vercruysse V, Le Moine O, Devière J, Moreno C. 2012. Hepatic expression of CCL2 in alcoholic liver disease is associated with disease severity and neutrophil infiltrates.

Clinical and Experimental Immunology. *169*(3):302–310. https://doi.org/10.1111/j.1365-2249.2012.04609.x

Delaney M, Kowalewska J, Treuting P. 2018. Urinary System. In: Treuting, Dintzis, Montine, editors. *Comparative Anatomy and Histology: A Mouse, Rat and Human Atlas.* 2nd ed. American Press. p. 275–301.

Denroche HC, Huynh FK, Kieffer TJ. 2012. The role of leptin in glucose homeostasis. *Journal of Diabetes Investigation*. *3*(2):115–129. https://doi.org/10.1111/j.2040-1124.2012.00203.x

Diapath. 2013. *Special Stains Handbook.* Diapath

Domingos MAM, Moreira SR, Gomez L, Goulart A, Lotufo PA, Benseñor I, Titan S. 2016. Urinary retinol-binding protein: Relationship to renal function and cardiovascular risk factors in chronic kidney disease. *PLoS ONE. 11*(9). https://doi.org/10.1371/journal.pone.0162782

Dong J, Viswanathan S, Adami E, Singh BK, Chothani SP, Ng B, Lim WW, Zhou J, Tripathi M, Ko NSJ, Shekeran SG, Tan J, Lim SY, Wang M, Lio PM, Yen PM, Schafer S, Cook SA, Widjaja AA. 2021. Hepatocyte-specific IL11 cis-signaling drives lipotoxicity and underlies the transition from NAFLD to NASH. *Nature Communications. 12*(1). https://doi.org/10.1038/s41467-020-20303-z

D'souza AM, Neumann UH, Glavas MM, Kieffer TJ. 2017. The glucoregulatory actions of leptin. *Molecular Metabolism.* *6*(9):1052–1065. https://doi.org/10.1016/j.molmet.2017.04.011

Duan J, Ruan B, Song P, Fang Z, Yue Z, Liu J, Dou G, Han H, Wang L. 2022. Shear stress–induced cellular senescence blunts liver regeneration through Notch–sirtuin 1–P21/P16 axis. *Hepatology*. *75*(3). https://journals.lww.com/hep/Fulltext/2022/03000/Shear_stress_induced_cellular_senescence_blunts.12.aspx

Eggert T, Wolter K, Ji J, Ma C, Yevsa T, Klotz S, Medina-Echeverz J, Longerich T, Forgues M, Reisinger F, Heikenwalder M, Wang XW, Zender L, Greten TF. 2016. Distinct Functions of Senescence-Associated Immune Responses in Liver Tumor Surveillance and Tumor Progression. *Cancer Cell*. *30*(4):533–547. https://doi.org/10.1016/j.ccell.2016.09.003

Ehling J, Bartneck M, Wei X, Gremse F, Fech V, Möckel D, Baeck C, Hittatiya K, Eulberg D, Luedde T, Kiessling F, Trautwein C, Lammers T, Tacke F. 2014. CCL2-dependent infiltrating macrophages promote angiogenesis in progressive liver fibrosis. *Gut*. *63*(12):1960–1971. https://doi.org/10.1136/gutjnl-2013-306294

Eldahan KC, Rabchevsky AG. 2018. Autonomic dysreflexia after spinal cord injury: Systemic pathophysiology and methods of management. In *Autonomic Neuroscience: Basic and Clinical.* 209:59–70. Elsevier B.V. https://doi.org/10.1016/j.autneu.2017.05.002

El-naseery NI, Mousa HSE, Noreldin AE, El-Far AH, Elewa YHA. 2020. Aging-associated immunosenescence via alterations in splenic immune cell populations in rat. *Life Sciences. 241*. https://doi.org/10.1016/j.lfs.2019.117168

Feder S, Haberl EM, Spirk M, Weiss TS, Wiest R, Buechler C. 2020. Pentraxin-3 is not related to disease severity in cirrhosis and hepatocellular carcinoma patients. *Clinical*

and Experimental Medicine. 20(2):289–297. https://doi.org/10.1007/s10238-020-00617-4

Ferreira-Gonzalez S, Lu WY, Raven A, Dwyer B, Man TY, O'Duibhir E, Lewis PJS, Campana L, Kendall TJ, Bird TG, Tarrats N, Acosta JC, Boulter L, Forbes SJ. 2018. Paracrine cellular senescence exacerbates biliary injury and impairs regeneration. *Nature Communications*. *9*(1). https://doi.org/10.1038/s41467-018-03299-5

Fischer MJ, Krishnamoorthi VR, Smith BM, Evans CT, St. Andre JR, Ganesh S, Huo Z, Stroupe KT. 2012. Prevalence of chronic kidney disease in patients with spinal cord injuries/disorders. *American Journal of Nephrology. 36*(6):542–548. https://doi.org/10.1159/000345460

Fleming JC, Bailey CS, Hundt H, Gurr KR, Bailey SI, Cepinskas G, Lawendy AR, Badhwar A. 2012. Remote inflammatory response in liver is dependent on the segmental level of spinal cord injury. Journal of Trauma and Acute Care Surgery. 72(5). https://journals.lww.com/jtrauma/Fulltext/2012/05000/Remote_inflammatory_response_in_liver_is_dependent.10.aspx

Fowler CJ, Griffiths D, de Groat WC. The neural control of micturition. Nat Rev Neurosci. 2008 Jun;9(6):453-66. doi: 10.1038/nrn2401.

Frazier KS, Seely JC, Hard GC, Betton G, Burnett R, Nakatsuji S, Nishikawa A, Durchfeld-Meyer B, Bube A. 2012. Proliferative and Nonproliferative Lesions of the Rat and Mouse Urinary System. *Toxicologic Pathology*. *40*(4):14S-86S. https://doi.org/10.1177/0192623312438736

Fried SK, Ricci MR, Russell CD, Laferrè B. 2000. Symposium: Adipocyte Function, Differentiation and Metabolism Regulation of Leptin Production in Humans 1,2. *J. Nutr*. 130. https://academic.oup.com/jn/article/130/12/3127S/4686231

Fujita K, Ewing CM, Chan DYS, Mangold LA, Partin AW, Isaacs WB, Pavlovich CP. 2009. Endoglin (CD105) as a urinary and serum marker of prostate cancer. *International Journal of Cancer. 124*(3):664–669. https://doi.org/10.1002/ijc.24007

Fujita T, Narumiya S. 2016. Roles of hepatic stellate cells in liver inflammation: A new perspective. *Inflammation and Regeneration. 36*(1). https://doi.org/10.1186/s41232-016-0005-6

Fung KY, Louis C, Metcalfe RD, Kosasih CC, Wicks IP, Griffin MDW, Putoczki TL. 2022. Emerging roles for IL-11 in inflammatory diseases. *Cytokine. 149*. https://doi.org/10.1016/j.cyto.2021.155750

Furuta K, Guo Q, Pavelko KD, Lee JH, Robertson KD, Nakao Y, Melek J, Shah VH, Hirsova P, Ibrahim SH (2021). Lipid-induced endothelial vascular cell adhesion molecule 1 promotes nonalcoholic steatohepatitis pathogenesis. *Journal of Clinical Investigation*. *131*(6). https://doi.org/10.1172/JCI143690

Gaudet AD, Fonken LK, Ayala MT, Dangelo HM, Smith EJ, Bateman EM, Schleicher WE, Maier SF, Watkins LR. 2018. Spinal Cord Injury in Rats Dysregulates Diurnal Rhythms of Fecal Output and Liver Metabolic Indicators. *Journal of Neurotrauma. 36*(12):1923–1934. https://doi.org/10.1089/neu.2018.6101

Gonzalez EJ, Arms L, Vizzard MA. 2014. The role(s) of cytokines/chemokines in urinary bladder inflammation and dysfunction. *BioMed Research International. 2014*. https://doi.org/10.1155/2014/120525

Gonzalez-Meljem JM, Apps JR, Fraser HC, Martinez-Barbera JP. 2018. Paracrine roles of cellular senescence in promoting tumourigenesis. *British Journal of Cancer. 118*(10):1283–1288. https://doi.org/10.1038/s41416-018-0066-1

Goodus MT, Carson KE, Sauerbeck A. Dey P, Alfredo AN, Popovich PG, Bruno RS, McTigue DM. 2021. Liver inflammation at the time of spinal cord injury enhances intraspinal pathology, liver injury, metabolic syndrome and locomotor deficits. *Experimental Neurology. 342*. https://doi.org/10.1016/j.expneurol.2021.113725

Goodus MT, McTigue DM. 2020. Hepatic dysfunction after spinal cord injury: A vicious cycle of central and peripheral pathology? *Experimental Neurology.* 325. Academic Press Inc. https://doi.org/10.1016/j.expneurol.2019.113160

Goodus MT, Sauerbeck A, Popovich PG, Bruno RS, McTigue DM. 2018. Dietary Green Tea Extract Prior to Spinal Cord Injury Prevents Hepatic Iron Overload but Does Not Improve Chronic Hepatic and Spinal Cord Pathology in Rats. *Journal of Neurotrauma. 35*(24):2872–2882. https://doi.org/10.1089/neu.2018.5771

Gorgey AS, Dolbow DR, Dolbow JD, Khalil RK, Castillo C, Gater DR. 2014. Effects of spinal cord injury on body composition and metabolic profile - Part I. In *Journal of Spinal Cord Medicine.* 37(6):693–702. Maney Publishing. https://doi.org/10.1179/2045772314Y.0000000245

Grumbles RM, Thomas CK. 2017. Motoneuron death after human spinal cord injury. *Journal of Neurotrauma*. *34*(3):581–590. https://doi.org/10.1089/neu.2015.4374

Guo M, Chang P, Hauke E, Girard BM, Tooke K, Ojala J, Malley SM, Hsiang H, Vizzard MA. 2018. Expression and function of chemokines CXCL9-11 in micturition pathways in cyclophosphamide (CYP)-induced cystitis and somatic sensitivity in mice. *Frontiers in Systems Neuroscience*. *12*. https://doi.org/10.3389/fnsys.2018.00009

Hall BM, Balan V, Gleiberman AS, Strom E, Krasnov P, Virtuoso LP, Rydkina E, Vujcic S, Balan K, Gitlin II, Leonova KI, Consiglio CR, Gollnick SO, Chernova OB, Gudkov A. 2017. p16(Ink4a) and senescence-associated B-galactosidase can be induced in macrophages as part of a reversible response to physiological stimuli. *Aging*. *9*(8):1867–1884.

Hamada Y, Hirano E. 2022. Regulation of Iron Metabolism in NAFLD/NASH. In: Kang JS, editors. *Non-alcoholic Fatty Liver Disease.* IntechOpen. https://doi.org/10.5772/intechopen.107221

He T, Liu W, Shen CAA. 2022. Anti-inflammatory properties of pigment epithelium-derived factor. *European Journal of Inflammation*. 20. SAGE Publications Inc. https://doi.org/10.1177/1721727X221138857

He X, Cheng R, Benyajati S, Ma JX. 2015. PEDF and its roles in physiological and pathological conditions: Implication in diabetic and hypoxia-induced angiogenic diseases. *Clinical Science*. 128(11):805–823. Portland Press Ltd. https://doi.org/10.1042/CS20130463

Helbig KJ, Ruszkiewicz A, Semendric L, Harley HAJ, McColl SR, Beard MR. 2004. Expression of the CXCR3 Ligand I-TAC by Hepatocytes in Chronic Hepatitis C and Its Correlation with Hepatic Inflammation. *Hepatology*. *39*(5):1220–1229. https://doi.org/10.1002/hep.20167

Hellenbrand DJ, Quinn CM, Piper ZJ, Morehouse CN, Fixel JA, Hanna AS. 2021. Inflammation after spinal cord injury: a review of the critical timeline of signaling cues and cellular infiltration. *Journal of Neuroinflammation.* 18(1). BioMed Central Ltd. https://doi.org/10.1186/s12974-021-02337-2

Henke AM, Billington ZJ, Gater DR. 2022. Autonomic Dysfunction and Management after Spinal Cord Injury: A Narrative Review. *Journal of Personalized Medicine*. *12*(7). https://doi.org/10.3390/jpm12071110

Herck MAV, Weyler J, Kwanten WJ, Dirinck EL, Winter BYD, Francque SM, Vonghia, L. 2019. The differential roles of T-cells in non-alcoholic fatty liver disease and obsity. *Frontiers in Immunology.* 10. Frontiers Media S.A. https://doi.org/10.3389/fimmu.2019.00082

Hernández-Silva D, Cantón-Sandoval J, Martínez-Navarro FJ, Pérez-Sánchez H, de Oliveira S, Mulero V, Alcaraz-Pérez F, Cayuela ML. 2022. Senescence-Independent Anti-Inflammatory Activity of the Senolytic Drugs Dasatinib, Navitoclax, and Venetoclax in Zebrafish Models of Chronic Inflammation. *International Journal of Molecular Sciences*. *23*(18). https://doi.org/10.3390/ijms231810468

Herrera JJ, Haywood-Watson IIRJ, Grill RJ. 2010. Acute and Chronic Deficits in the Urinary Bladder after Spinal Contusion Injury in the Adult Rat. *Journal of Neurotrauma.* 27:423-431

Hisaka T, Desmoulière A, Taupin JL, Daburon S, Neaud V, Senant N, Blanc JF, Moreau JF, Rosenbaum J. 2004. Expression of leukemia inhibitory factor (LIF) and its receptor gp190 in human liver and in cultured human liver myofibroblasts. Cloning of new isoforms of LIF mRNA. *Comparative Hepatology*. *3*. https://doi.org/10.1186/1476-5926-3-10

Holstege G, Collewijn H. 2009. Central Nervous System control of Micturition. In: Watson C, Paxinos G, Kayalioglu G, editors. *The Spinal Cord*. 1st ed.

Houenou LJ, D'Costa AP, Li L, Turgeon VL, Enyadike C, Alberdi E, Becerra SP. 1999. Pigment epithelium-derived factor promotes the survival and differentiation of developing spinal motor neurons. *Journal of Comparative Neurology*. *412*(3):506–514. https://doi.org/10.1002/(SICI)1096-9861(19990927)412:3<506::AID-CNE9>3.0.CO;2-E

Huang H, Xu C. 2022. Retinol-binding protein-4 and nonalcoholic fatty liver disease. *Chinese Medical Journal*. 135(10):1182–1189. Lippincott Williams and Wilkins. https://doi.org/10.1097/CM9.0000000000002135

Huby T, Gautier EL. 2022. Immune cell-mediated features of non-alcoholic steatohepatitis. *Nature Reviews Immunology.* 22(7):429–443. Nature Research. https://doi.org/10.1038/s41577-021-00639-3

Huda N, Liu G, Hong H, Yan S, Khambu B, Yin XM. 2019. Hepatic senescence, the good and the bad. *World Journal of Gastroenterology*. 25(34):5069–5081. Baishideng Publishing Group Co. https://doi.org/10.3748/wjg.v25.i34.5069

Hwang S, Yun H, Moon S, Cho YE, Gao B. 2021. Role of Neutrophils in the Pathogenesis of Nonalcoholic Steatohepatitis. *Frontiers in Endocrinology.* 12. Frontiers Media S.A. https://doi.org/10.3389/fendo.2021.751802

Ikura Y. 2014. Transitions of histopathologic criteria for diagnosis of nonalcoholic fatty liver disease during the last three decades. *World Journal of Hepatology*. *6*(12):894–900. https://doi.org/10.4254/wjh.v6.i12.894

Ivanova A, Wuerfel J, Zhang J, Hoffmann O, Ballmaier M, Dame C. 2010. Expression pattern of the thrombopoietin receptor (Mpl) in the murine central nervous system. *BMC Developmental Biology*. *10*. https://doi.org/10.1186/1471-213X-10-77

Iyer S, Cheng G. 2012. Role of Interleukin 10 Transcriptional Regulation in Inflammation and Autoimmune Disease. Crit Rev Immunol. 32(1):23-63.

Izumi K, Zheng Y, Li Y, Zaengle J, Miyamoto H. 2012. Epidermal growth factor induces bladder cancer cell proliferation through activation of the androgen receptor. *International Journal of Oncology*. *41*(5):1587–1592. https://doi.org/10.3892/ijo.2012.1593

Jeffries MA, Tom VJ. 2021. Peripheral immune dysfunction: A problem of central importance after spinal cord injury. *Biology.* 10(9). MDPI. https://doi.org/10.3390/biology10090928

Jelenik T, Kaul K, Séquaris G, Flögel U, Phielix E, Kotzka J, Knebel B, Fahlbusch P, Hörbelt T, Lehr S, Reinbeck AL, Müller-Wieland D, Esposito I, Shulman GI, Szendroedi J, Roden M. 2017. Mechanisms of insulin resistance in primary and secondary nonalcoholic fatty liver. *Diabetes*. *66*(8):2241–2253. https://doi.org/10.2337/db16-1147

Jensen M, Jia W, Schults AJ, Ye X, Prestwich GD, Oottamasathien S. 2018. IL-33 mast cell axis is central in LL-37 induced bladder inflammation and pain in a murine interstitial cystitis model. *Cytokine*. *110*:420–427. https://doi.org/10.1016/j.cyto.2018.05.012

Jeon JY, Steadward RD, Wheeler GD, Bell G, McCargar L, Harber V. 2003. Intact sympathetic nervous system is required for leptin effects on resting metabolic rate in people with spinal cord injury. *Journal of Clinical Endocrinology and Metabolism*. *88*(1):402–407. https://doi.org/10.1210/jc.2002-020939

Jing Y, Liu M, Bai F, Li D, Yang D. 2018. Pancreatic-islet microvascular vasomotion dysfunction in mice with spinal cord injury. *Neuroscience Letters*. *685*:68–74. https://doi.org/10.1016/j.neulet.2018.08.022

Jones TB. 2014. Lymphocytes and autoimmunity after spinal cord injury. *Experimental Neurology*. 258:78–90. Academic Press Inc. https://doi.org/10.1016/j.expneurol.2014.03.003

Kalin´ski P, Kalin´ski K, Vieira PL, Schuitemaker JHN, De Jong EC, Kapsenberg ML. 2001. Prostaglandin E 2 is a selective inducer of interleukin-12 p40 (IL-12p40) production and an inhibitor of bioactive IL-12p70 heterodimer. *Blood*. *97*(11):3466–3469. http://ashpublications.org/blood/article-pdf/97/11/3466/1674408/h8110103466.pdf

Kalisvaart JF, Katsumi HK, Ronningen LD, Hovey RM. 2010. Bladder cancer in spinal cord injury patients. *Spinal Cord*. *48*(3):257–261. https://doi.org/10.1038/sc.2009.118

Kamohara S, Burcelin R, Halaas J, Friedman J, Charron M. 1997. Acute stimulation of glucose metabolism in mice by leptin treatment. *Nature*. *389*:374–377.

Kanungo S, Wells K, Tribett T, El-Gharbawy A. 2018. Glycogen metabolism and glycogen storage disorders. *Annals of Translational Medicine*. *6*(24):474–474. https://doi.org/10.21037/atm.2018.10.59

Karin PH, Olof J, Berrum SI, Ann-Katrin K. 2008. Impaired Renal Function in Newly Spinal Cord Injured Patients Improves in the Chronic State—Effect of Clean Intermittent Catheterization?. *Journal of Urology*. *180*(1):187–191. https://doi.org/10.1016/j.juro.2008.03.051

Karlsson M, Zhang C, Méar L, Zhong W, Digre A, Katona B, Sjöstedt E, Butler L, Odeberg, J, Dusart P, Edfors F, Oksvold P, von Feilitzen K, Zwahlen M, Arif M, Altay O, Li X, Ozcan M, Mardinoglu A, et al. 2021. A single-cell type transcriptomics map of human tissues. *Sci. Adv*. 7. www.proteinatlas.org

Kaushansky K. 2003. Thrombopoietin: A tool for understanding thrombopoiesis. *Journal of Thrombosis and Haemostasis.* 1(7):1587–1592. https://doi.org/10.1046/j.1538-7836.2003.00273.x

Kaushansky K. 2005. The molecular mechanisms that control thrombopoiesis. *Journal of Clinical Investigation.* 115(12):3339–3347. https://doi.org/10.1172/JCI26674

Kazankov K, Jørgensen SMD, Thomsen KL, Møller HJ, Vilstrup H, George J, Schuppan D, Grønbæk H. 2019. The role of macrophages in nonalcoholic fatty liver disease and nonalcoholic steatohepatitis. *Nature Reviews Gastroenterology & Hepatology*. *16*(3):145–159. https://doi.org/10.1038/s41575-018-0082-x

Kigerl KA, Hall JCE, Wang L, Mo X, Yu Z, Popovich PG. 2016. Gut dysbiosis impairs recovery after spinal cord injury. *Journal of Experimental Medicine*. *213*(12):2603–2620. https://doi.org/10.1084/jem.20151345

Kigerl KA, Mostacada K, Popovich PG. 2018. Gut Microbiota Are Disease-Modifying Factors After Traumatic Spinal Cord Injury. *Neurotherapeutics.* 15(1):60–67. Springer New York LLC. https://doi.org/10.1007/s13311-017-0583-2

Klee NS, McCarthy CG, Lewis S, McKenzie JL, Vincent JE, Webb RC. 2018. Urothelial Senescence in the Pathophysiology of Diabetic Bladder Dysfunction—A Novel Hypothesis. *Frontiers in Surgery.* 5. Frontiers Media S.A. https://doi.org/10.3389/fsurg.2018.00072

Knight B, Lim R, Yeoh GC, Olynyk JK. 2007. Interferon-γ exacerbates liver damage, the hepatic progenitor cell response and fibrosis in a mouse model of chronic liver injury. *Journal of Hepatology*. *47*(6):826–833. https://doi.org/10.1016/j.jhep.2007.06.022

Kochiashvili G, Kochiashvili D. 2014. Urinary IL-33 and galectin-3 increase in patients with interstitial cystitis/bladder pain syndrome (review). *Georgian Medical News*. *12*(5): 232–233.

Kolios G, Valatas V, Kouroumalis E. 2006. *Role of Kupffer cells in the pathogenesis of liver disease*. http://www.wjgnet.com/1007-9327/12/7413.asp

Kourko O, Seaver K, Odoardi N, Basta S, Gee K. 2019. IL-27, IL-30, and IL-35: A Cytokine Triumvirate in Cancer. *Frontiers in Oncology*. 9. Frontiers Media S.A. https://doi.org/10.3389/fonc.2019.00969

Krizhanovsky V, Yon M, Dickins RA, Hearn S, Simon J, Miething C, Yee H, Zender L, Lowe SW. 2008. Senescence of Activated Stellate Cells Limits Liver Fibrosis. *Cell*. *134*(4):657–667. https://doi.org/10.1016/j.cell.2008.06.049

Kumar P, Smith T, Raeman R, Chopyk DM, Brink H, Liu Y, Sulchek T, Anania FA. 2018. Periostin promotes liver fibrogenesis by activating lysyl oxidase in hepatic stellate cells. *Journal of Biological Chemistry*. *293*(33):12781–12792. https://doi.org/10.1074/jbc.RA117.001601

Kuo HC. 2014. Potential urine and serum biomarkers for patients with bladder pain syndrome/interstitial cystitis. *International Journal of Urology*. 21(1):34–41. Blackwell Publishing. https://doi.org/10.1111/iju.12311

Kwon BK, Stammers AMT, Belanger LM, Bernardo A, Chan D, Bishop CM, Slobogean GP, Zhang H, Umedaly H, Giffin M, Street J, Boyd MC, Paquette SJ, Fisher CG, Dvorak MF. 2009. Cerebrospinal Fluid Inflammatory Cytokines and Biomarkers of Injury Severity in Acute Human Spinal Cord Injury. *Journal of Neurotrauma*. *27*(4):669–682. https://doi.org/10.1089/neu.2009.1080

Kwon MJ, Shin HY, Cui Y, Kim H, Le Thi AH, Choi JY, Kim EY, Hwang DH, Kim BG. 2015. CCL2 mediates neuron-macrophage interactions to drive proregenerative macrophage activation following preconditioning injury. *Journal of Neuroscience*. *35*(48):15934–15947. https://doi.org/10.1523/JNEUROSCI.1924-15.2015

Lamkanfi M, Dixit VM. 2009. IL-33 Raises Alarm. *Immunity*. *31*:5–7. https://doi.org/10.1073/pnas

Lavelle J, Meyers S, Ramage R, Bastacky S, Doty D, Apodaca G, Zeidel ML, Bastacky SD. 2002. Bladder permeability barrier: recovery from selective injury of surface epithelial cells. *American Journal of renal Physiology.* 283:242-253. https://doi.org/10.1152/ajprenal.00307.2001.-The

Lee EJ, Lee SJ, Kim S, Cho SC, Choi YH, Kim WJ, Moon SK. 2013. Interleukin-5 enhances the migration and invasion of bladder cancer cells via ERK1/2-mediated MMP-9/NF-κB/AP-1 pathway: Involvement of the p21WAF1 expression. *Cellular Signalling*. *25*(10):2025–2038. https://doi.org/10.1016/j.cellsig.2013.06.004

Lee K, Robbins PD, Camell CD. 2021. Intersection of immunometabolism and immunosenescence during aging. *Current Opinion in Pharmacology*. 57:107–116. Elsevier Ltd. https://doi.org/10.1016/j.coph.2021.01.003

Lee M, Fried SK. 2009. Integration of hormonal and nutrient signals that regulate leptin synthesis and secretion. *Am J Physiol Endocrinol Metab. 296*:1230–1238. https://doi.org/10.1152/ajpendo.90927.2008.-This

Li L, Xia Y, Ji X, Wang H, Zhang Z, Lu P, Ding Q, Wang D, Liu M. 2021. MIG/CXCL9 exacerbates the progression of metabolic-associated fatty liver disease by disrupting Treg/Th17 balance. *Experimental Cell Research*. *407*(2). https://doi.org/10.1016/j.yexcr.2021.112801

Li L, Yi C, Xia W, Huang B, Chen S, Zhong J, Fang X, Yang L, Xin H, Zheng S, Chong B, Fu Y, Chen C, Yang M. 2020. c-Mpl and TPO expression in the human cental nervous system neurons inhibits neuronal apoptosis. *Aging*.

Lin HY, Lu JH, Chuang SM, Chueh KS, Juan TJ, Liu YC, Juan YS. 2022. Urinary Biomarkers in Interstitial Cystitis/Bladder Pain Syndrome and Its Impact on Therapeutic Outcome. *Diagnostics.* 12(1). MDPI. https://doi.org/10.3390/diagnostics12010075

Liu J, An H, Jiang D, Huang W, Zou H, Meng C, Li H. 2004. Study of Bacterial Translocation From Gut After Paraplegia Caused by Spinal cord Injury in Rats. *Spine*. *29*(2). https://journals.lww.com/spinejournal/Fulltext/2004/01150/Study_of_Bacterial_Translocation_From_Gut_After.9.aspx

Liu T, Zhang L, Joo D, Sun SC. 2017. NF-κB signaling in inflammation. *Signal Transduction and Targeted Therapy*. 2. Springer Nature. https://doi.org/10.1038/sigtrans.2017.23

Lu H, Li C. 2000. Leptin: a multifunctional hormone. *Cell Research*. *10*:81–92.

Lucin KM, Sanders VM, Jones TB, Malarkey WB, Popovich PG. 2007. Impaired antibody synthesis after spinal cord injury is level dependent and is due to sympathetic nervous system dysregulation. *Experimental Neurology*. *207*(1):75–84. https://doi.org/10.1016/j.expneurol.2007.05.019

Lucin KM, Sanders VM, Popovich PG. 2009. Stress hormones collaborate to induce lymphocyte apoptosis after high level spinal cord injury. *Journal of Neurochemistry*. *110*(5):1409–1421. https://doi.org/10.1111/j.1471-4159.2009.06232.x

Luo XY, Takahara T, Kawai K, Fujino M, Sugiyama T, Tsuneyama K, Tsukada K, Nakae S, Zhong L, Li XK. 2013. IFN-deficiency attenuates hepatic inflammation and fibrosis in a steatohepatitis model induced by a methionine-and choline-deficient high-fat diet. *Am J Physiol Gastroin-Test Liver Physiol*. *305*:891–899. https://doi.org/10.1152/ajpgi.00193.2013.-Cytokines

Manivasagam S, Williams JL, Vollmer LL, Bollman B, Bartleson JM, Ai S, Wu GF, Klein RS. 2022. Targeting IFN-λ Signaling Promotes Recovery from Central Nervous System Autoimmunity. *The Journal of Immunology*. *208*(6):1341–1351. https://doi.org/10.4049/jimmunol.2101041

Martínez-Uña M, López-Mancheño Y, Diéguez C, Fernández-Rojo MA, Novelle MG. 2020. Unraveling the role of leptin in liver function and its relationship with liver diseases. *International Journal of Molecular Sciences*. *21*(24):1–33. https://doi.org/10.3390/ijms21249368

McGill MR. 2016. The past and present of serum aminotransferases and the future of liver injury biomarkers. *EXCLI Journal*. *15*:817–828. https://doi.org/10.17179/excli2016-800

Menezes K, Rosa BG, Freitas C, da Cruz AS, de Siqueira Santos R, Nascimento MA, Alves DVL, Bonamino M, Rossi MI, Borojevic R, Coelho-Sampaio T. 2020. Human mesenchymal stromal/stem cells recruit resident pericytes and induce blood vessels maturation to repair experimental spinal cord injury in rats. *Scientific Reports*. *10*(1). https://doi.org/10.1038/s41598-020-76290-0

Milovanovic M, Volarevic V, Radosavljevic G, Jovanovic I, Pejnovic N, Arsenijevic N, Lukic ML. 2012. IL-33/ST2 axis in inflammation and immunopathology. *Immunologic Research*. *52*(1–2):89–99. https://doi.org/10.1007/s12026-012-8283-9

Min B, Kim D, Feige MJ. 2021. IL-30† (IL-27A): a familiar stranger in immunity, inflammation, and cancer. *Experimental and Molecular Medicine*. 53(5):823–834. Springer Nature. https://doi.org/10.1038/s12276-021-00630-x

Mitra A, Satelli A, Yan J, Xueqing X, Gagea M, Hunter CA, Mishra L, Li S. 2014. IL-30 (IL27p28) Attenuates Liver Fibrosis Through Inducing NKG2D-Rae1 Interaction Between NKT and Activated Hepatic Stellate Cells in Mice. *Hepatology.* https://doi.org/10.1002/hep.27392/suppinfo

Moran CS, Campbell JH, Campbell GR. 1997. Human Leukemia Inhibitory Factor Upregulates LDL Receptors on Liver Cells and Decreases Serum Cholesterol in the Cholesterol-Fed Rabbit. *Arteriosclerosis, Thrombosis and Vascular Biology*. http://ahajournals.org

Moschen AR, Adolph TE, Gerner RR, Wieser V, Tilg H. 2017. Lipocalin-2: A Master Mediator of Intestinal and Metabolic Inflammation. *Trends in Endocrinology and Metabolism*. 28(5):388–397. Elsevier Inc. https://doi.org/10.1016/j.tem.2017.01.003

Mukhamedshina YO, Akhmetzyanova ER, Martynova EV, Khaiboullina SF, Galieva LR, Rizvanov AA. 2017. Systemic and local cytokine profile following spinal cord injury in rats: A multiplex analysis. *Frontiers in Neurology*. *8*. https://doi.org/10.3389/fneur.2017.00581

Muñoz-Espín D, Serrano M. 2014. Cellular senescence: From physiology to pathology. *Nature Reviews Molecular Cell Biology*. 15(7):482–496. Nature Publishing Group. https://doi.org/10.1038/nrm3823

Naim A, Pan Q, Baig MS. 2017. Matrix Metalloproteinases (MMPs) in Liver Diseases. *Journal of Clinical and Experimental Hepatology*. 7(4):367–372. Elsevier B.V. https://doi.org/10.1016/j.jceh.2017.09.004

Nazari A, Ahmadi Z, Hassanshahi G, Abbasifard M, Taghipour Z, Falahati-Pour SK, Khorramdelazad H. 2020. Effective treatments for bladder cancer affecting CXCL9/CXCL10/CXCL11/ CXCR3 axis: A review. *Oman Medical Journal*. 35(2). Oman Medical Specialty Board. https://doi.org/10.5001/omj.2020.21

Nguyen-Lefebvre AT, Horuzsko A. 2015. Kupffer Cell Metabolism and Function. *Journal Enzymology and Metabolism*. *1*(1).

Noble BT, Brennan FH, Popovich PG. 2018. The spleen as a neuroimmune interface after spinal cord injury. *Journal of Neuroimmunology*. 321:1–11. Elsevier B.V. https://doi.org/10.1016/j.jneuroim.2018.05.007

Norris CA, He M, Kang LI, Ding MQ, Radder JE, Haynes MM, Yang Y, Paranjpe S, Bowen WC, Orr A, Michalopoulos GK, Stolz DB, Mars WM. 2014. Synthesis of IL-6 by hepatocytes is a normal response to common hepatic stimuli. *PLoS ONE*. *9*(4). https://doi.org/10.1371/journal.pone.0096053

O'Brian D, Prunty M, Hill A, Shoag J. 2021. The Role of C-Reactive Protein in Kidney, Bladder, and Prostate Cancers. *Frontiers in Immunology*. 12. Frontiers Media S.A. https://doi.org/10.3389/fimmu.2021.721989

O'brien A, Zhou T, White T, Medford A, Chen L, Kyritsi K, Wu N, Childs J, Stiles D, Ceci L, Chakraborty S, Ekser B, Baiocchi L, Carpino G, Gaudio E, Wu C, Kennedy L, Francis H, Alpini G, Glaser S. 2022. FGF1 Signaling Modulates Biliary Injury and Liver Fibrosis in the Mdr2 −/− Mouse Model of Primary Sclerosing Cholangitis. *Hepatology CommuniCations*. *6*(7). https://doi.org/10.1002/hep4.1909/suppinfo

Ogrodnik M, Miwa S, Tchkonia T, Tiniakos D, Wilson CL, Lahat A, Day CP, Burt A, Palmer A, Anstee QM, Grellscheid SN, Hoeijmakers JHJ, Barnhoorn S, Mann DA, Bird TG, Vermeij WP, Kirkland JL, Passos JF, Von Zglinicki T, Jurk D. 2017. Cellular senescence drives age-dependent hepatic steatosis. *Nature Communications*. *8*. https://doi.org/10.1038/ncomms15691

Pache JC. 2006. EPIDERMAL GROWTH FACTORS. In: Laurent GJ, Shapiro SD, editors. *Encyclopedia of Respiratory Medicine.* Academic Press. p. 129–133. https://doi.org/https://doi.org/10.1016/B0-12-370879-6/00138-1

Pagadala M, Kasumov T, McCullough AJ, Zein NN, Kirwan JP. 2012. Role of ceramides in nonalcoholic fatty liver disease. *Trends in Endocrinology and Metabolism*. *23*(8):365–371. https://doi.org/10.1016/j.tem.2012.04.005

Pan W, Kastin AJ. 2008. Cytokine Transport Across the Injured Blood-Spinal Cord Barrier. *Curr Pharm Des.* 14(16):1620-1624.

Papatheodoridi AM, Chrysavgis L, Koutsilieris M, Chatzigeorgiou A. 2020. The Role of Senescence in the Development of Nonalcoholic Fatty Liver Disease and Progression to Nonalcoholic Steatohepatitis. *Hepatology*. 71(1):363–374. John Wiley and Sons Inc. https://doi.org/10.1002/hep.30834

Paramos-de-Carvalho D, Jacinto A, Saúde L. 2021. The right time for senescence. *ELife*. *10*. https://doi.org/10.7554/eLife

Paramos-de-Carvalho D, Martins I, Cristóvão AM, Dias AF, Neves-Silva D, Pereira T, Chapela D, Farinho A, Jacinto A, Saúde L. 2021. Targeting senescent cells improves functional recovery after spinal cord injury. *Cell Reports*. *36*(1). https://doi.org/10.1016/j.celrep.2021.109334

Peiseler M, Tacke F. 2021. Inflammatory mechanisms underlying nonalcoholic steatohepatitis and the transition to hepatocellular carcinoma. *Cancers*. 13(4):1–26. MDPI AG. https://doi.org/10.3390/cancers13040730

Perez NE, Godbole NP, Amin K, Syan R, Gater DR. 2022. Neurogenic Bladder Physiology, Pathogenesis, and Management after Spinal Cord Injury. *Journal of Personalized Medicine*. *12*(6). https://doi.org/10.3390/jpm12060968

Pérez-Pérez A, Sánchez-Jiménez F, Vilariño-García T, Sánchez-Margalet V. 2020. Role of leptin in inflammation and vice versa. *International Journal of Molecular Science.* 21(16):1–24. MDPI AG. https://doi.org/10.3390/ijms21165887

Petersen MC, Shulman GI. 2018. Mechanisms of Insulin Action and Insulin Resistance. *Physiological Reviews*. *98*(4):2133–2223. https://doi.org/10.1152/physrev.00063.2017

Petrescu AD, Grant S, Williams E, An SY, Seth N, Shell M, Amundsen T, Tan C, Nadeem Y, Tjahja M, Weld L, Chu CS, Venter J, Frampton G, McMillin M, DeMorrow S. 2022.

Leptin Enhances Hepatic Fibrosis and Inflammation in a Mouse Model of Cholestasis. *The American Journal of Pathology*, *192*(3):484–502. https://doi.org/10.1016/j.ajpath.2021.11.008

Pivovarova-Ramich O, Loske J, Hornemann S, Markova M, Seebeck N, Rosenthal A, Klauschen F, Castro JP, Buschow R, Grune T, Lange V, Rudovich N, Ouwens DM. 2021. Hepatic wnt1 inducible signaling pathway protein 1 (WISP-1/CCN4) associates with markers of liver fibrosis in severe obesity. *Cells*. *10*(5). https://doi.org/10.3390/cells10051048

Pomeshchik Y, Kidin I, Korhonen P, Savchenko E, Jaronen M, Lehtonen S, Wojciechowski S, Kanninen K, Koistinaho J, Malm T. 2015. Interleukin-33 treatment reduces secondary injury and improves functional recovery after contusion spinal cord injury. *Brain, Behavior, and Immunity*. *44*:68–81. https://doi.org/10.1016/j.bbi.2014.08.002

Popovich PG, Stuckman S, Gienapp IE, Whitacre CC. 2001. Alterations in Immune Cell Phenotype and Function after Experimental Spinal Cord Injury. *Journal of Neurotrauma*. *18*(9):957–966. https://doi.org/10.1089/089771501750451866

Poulsen KL, Ross CK, Chaney JK, Nagy LE. 2022. Role of the chemokine system in liver fibrosis: a narrative review. *Digestive Medicine Research*. *5*:30–30. https://doi.org/10.21037/dmr-21-87

Pusterla T, Nèmeth J, Stein I, Wiechert L, Knigin D, Marhenke S, Longerich T, Kumar V, Arnold B, Vogel A, Bierhaus A, Pikarsky E, Hess J, Angel P. 2013. Receptor for advanced glycation endproducts (RAGE) is a key regulator of oval cell activation and inflammation-associated liver carcinogenesis in mice. *Hepatology*. *58*(1):363–373. https://doi.org/10.1002/hep.26395

Raphael I, Nalawade S, Eagar TN, Forsthuber TG. 2015. T cell subsets and their signature cytokines in autoimmune and inflammatory diseases. *Cytokine*. 74(1):5–17. Academic Press. https://doi.org/10.1016/j.cyto.2014.09.011

Rayner DV, Trayhurn P. 2001. Regulation of leptin production: Sympathetic nervous system interactions. *Journal of Molecular Medicine*. 79(1):8–20. https://doi.org/10.1007/s001090100198

Reiman RM, Thompson RW, Feng CG, Hari D, Knight R, Cheever AW, Rosenberg HF, Wynn TA. 2006. Interleukin-5 (IL-5) augments the progression of liver fibrosis by regulating IL-13 activity. *Infection and Immunity*. *74*(3):1471–1479. https://doi.org/10.1128/IAI.74.3.1471-1479.2006

Rhinn M, Ritschka B, Keyes WM. 2019. Cellular senescence in development, regeneration and disease. *Development (Cambridge)*. *146*(20). https://doi.org/10.1242/dev.151837

Ritz MF, Graumann U, Gutierrez B, Hausmann O. 2012. Traumatic Spinal Cord Injury Alters Angiogenic Factors and TGF-Beta1 that may Affect Vascular Recovery. *Current Neurovascular Research*. *7*(4):301–310. https://doi.org/10.2174/156720210793180756

Roselli F, Chandrasekar A, Morganti-Kossmann MC. 2018. Interferons in traumatic brain and spinal cord injury: Current evidence for translational application. *Frontiers in Neurology*. 9. Frontiers Media S.A. https://doi.org/10.3389/fneur.2018.00458

Roszer T. 2015. Understanding the mysterious M2 macrophage through activation markers and effector mechanisms. *Mediators of Inflammation*. Hindawi Limited. https://doi.org/10.1155/2015/816460

Sadhu S, Decker C, Sansbury BE, Marinello M, Seyfried A, Howard J, Mori M, Hosseini Z, Arunachalam T, Finn AV, Lamar JM, Jourd'heuil D, Guo L, MacNamara KC, Spite M, Fredman G. 2021. Radiation-Induced Macrophage Senescence Impairs Resolution Programs and Drives Cardiovascular Inflammation. *The Journal of Immunology*. *207*(7):1812–1823. https://doi.org/10.4049/jimmunol.2100284

Sahin H, Borkham-Kamphorst E, Kuppe C, Zaldivar MM, Grouls C, Al-samman M, Nellen A, Schmitz P, Heinrichs D, Berres ML, Doleschel D, Scholten D, Weiskirchen R, Moeller MJ, Kiessling F, Trautwein C, Wasmuth HE. 2012. Chemokine Cxcl9 attenuates liver fibrosis-associated angiogenesis in mice. *Hepatology*. *55*(5):1610–1619. https://doi.org/10.1002/hep.25545

Saito Y, Chikenji TS, Matsumura T, Nakano M, Fujimiya M. 2020. Exercise enhances skeletal muscle regeneration by promoting senescence in fibro-adipogenic progenitors. *Nature Communications*. *11*(1). https://doi.org/10.1038/s41467-020-14734-x

Sakamoto S, Ryan AJ, Kyprianou N. 2008. Targeting vasculature in urologic tumors: Mechanistic and therapeutic significance. *Journal of Cellular Biochemistry*. 103(3):691–708. https://doi.org/10.1002/jcb.21442

Salgado JV, Goes MA, Salgado Filho N. 2021. FGF21 and Chronic Kidney Disease. *Metabolism: Clinical and Experimental*. 118. W.B. Saunders. https://doi.org/10.1016/j.metabol.2021.154738

Sanagi T, Yabe T, Yamada H. 2005. The regulation of pro-inflammatory gene expression induced by pigment epithelium-derived factor in rat cultured microglial cells. *Neuroscience Letters*. *380*(1–2):105–110. https://doi.org/10.1016/j.neulet.2005.01.035

Santin Y, Lluel P, Rischmann P, Gamé X, Mialet-Perez J, Parini A. 2020. Cellular Senescence in Renal and Urinary Tract Disorders. *Cells*. 9(11). NLM (Medline). https://doi.org/10.3390/cells9112420

Sarafi MN, Garcia-Zepeda EA, Maclean JA, Charo IF, Luster AD. 1997. Murine Monocyte Chemoattractant Protein (MCP)-5: A Novel CC Chemokine That Is a Structural and Functional Homologue of Human MCP-1. *J. Exp. Med*. 185(1). http://rupress.org/jem/article-pdf/185/1/99/1109306/5348.pdf

Sattler S, Smits HH, Xu D, Huang FP. 2013. The evolutionary role of the IL-33/ST2 system in host immune defence. *Archivum Immunologiae et Therapiae Experimentalis*. 61(2):107–117. https://doi.org/10.1007/s00005-012-0208-8

Sauerbeck A, Laws JL, Bandaru VVR, Popovich PG, Haughey NJ, McTigue DM. 2015. Spinal cord injury causes chronic liver pathology in rats. *Journal of Neurotrauma*. 32(3):159–169. Mary Ann Liebert Inc. https://doi.org/10.1089/neu.2014.3497

Sauerbeck A, Schonberg DL, Laws JL, McTigue DM. 2013. Systemic iron chelation results in limited functional and histological recovery after traumatic spinal cord injury in rats. *Experimental Neurology*. *248*:53–61. https://doi.org/10.1016/j.expneurol.2013.05.011

Sawase K, Nomata K, Kanetake H, Saito Y. 1998. The expression of platelet-derived endothelial cell growth factor in human bladder cancer. *Cancer Letters*. *130*:35–41.

Scheff SW, Rabchevsky AG, Fugaccia I, Main JA, Lumpp JE. 2003. Experimental Modeling of Spinal Cord Injury: Characterization of a Force-Defined Injury Device. *Journal of Neurotrauma*. *20*(2):179–193. https://doi.org/10.1089/08977150360547099

Schmidt-Arras D, Rose-John S. 2016. IL-6 pathway in the liver: From physiopathology to therapy. *Journal of Hepatology*. *64*:1403–1415.

Scott CL, Zheng F, De Baetselier P, Martens L, Saeys Y, De Prijck S, Lippens S, Abels C, Schoonooghe S, Raes G, Devoogdt N, Lambrecht BN, Beschin A, Guilliams M. 2016. Bone marrow-derived monocytes give rise to self-renewing and fully differentiated Kupffer cells. *Nature Communications*. *7*. https://doi.org/10.1038/ncomms10321

Sharma R, Diwan B, Sharma A, Witkowski JM. 2022. Emerging cellular senescence-centric understanding of immunological aging and its potential modulation through dietary bioactive components. *Biogerontology.* 23(6):699–729. Springer Science and Business Media B.V. https://doi.org/10.1007/s10522-022-09995-6

Shimabukuro T, Matsuyama H, Baba Y, Jojima K, Suyama KI, Aoki A, Suga A, Yamamoto N, Naito K. 2005. Expression of thymidine phosphorylase in human superficial bladder cancer. *International Journal of Urology*. *12*(1):29–34. https://doi.org/10.1111/j.1442-2042.2004.00992.x

Siegel A, Zalcman SS. 2009. The neuroimmunological basis of behavior and mental disorders. *The Neuroimmunological Basis of Behavior and Mental Disorders*. Springer US. https://doi.org/10.1007/978-0-387-84851-8

Smirne C, Rigamonti C, De Benedittis C, Sainaghi PP, Bellan M, Burlone ME, Castello LM, Avanzi GC. 2019. Gas6/TAM Signaling Components as Novel Biomarkers of Liver Fibrosis. *Disease Markers.* Hindawi Limited. https://doi.org/10.1155/2019/2304931

Sroga JM, Jones TB, Kigerl KA, McGaughy VM, Popovich PG. 2003. Rats and mice exhibit distinct inflammatory reactions after spinal cord injury. *Journal of Comparative Neurology*. *462*(2):223–240. https://doi.org/https://doi.org/10.1002/cne.10736

Stevens AR, Ahmed U, Vigneswara V, Ahmed Z. 2019. Pigment Epithelium-Derived Factor Promotes Axon Regeneration and Functional Recovery After Spinal Cord Injury. *Molecular Neurobiology*. *56*(11):7490–7507. https://doi.org/10.1007/s12035-019-1614-2

Sugiyama A, Kanno K, Nishimichi N, Ohta S, Ono J, Conway SJ, Izuhara K, Yokosaki Y, Tazuma S. 2016. Periostin promotes hepatic fibrosis in mice by modulating hepatic stellate cell activation via αv integrin interaction. *Journal of Gastroenterology*. *51*(12):1161–1174. https://doi.org/10.1007/s00535-016-1206-0

Sun X, Jones ZB, Chen X, Zhou L, So KF, Ren Y. 2016. Multiple organ dysfunction and systemic inflammation after spinal cord injury: A complex relationship. *Journal of Neuroinflammation*. 13(1). BioMed Central Ltd. https://doi.org/10.1186/s12974-016-0736-y

Tai C, Roppolo JR, De Groat WC. 2006. Spinal reflex control of micturition after spinal cord injury. *Restor Neurol Neurosci.* 24(2):69-78.

Takanohashi A, Yabe T, Schwartz JP. 2005. Pigment epithelium-derived factor induces the production of chemokines by rat microglia. *GLIA*. *51*(4):266–278. https://doi.org/10.1002/glia.20203

Tan Z, Liu Q, Jiang R, Shoto SS, Maillet I, Quesniaux V, Tang J, Zhang W, Sun B, Ryffel B. 2018. Interleukin-33 drives hepatic fibrosis through activation of hepatic stellate cells. *Cellular & Molecular Immunology*. *15*(4):388–398. https://doi.org/10.1038/cmi.2016.63

Tang Z, Gillatt D, Rowe E, Koupparis A, Holly JMP, Perks CM. 2019. IGFBP-2 acts as a tumour suppressor and plays a role in determining chemosensitivity in bladder cancer cells. *Oncotarge. 10*(66):7043–7057. www.oncotarget.com

Taura K, De Minicis S, Seki E, Hatano E, Iwaisako K, Osterreicher CH, Kodama Y, Miura K, Ikai I, Uemoto S, Brenner DA. 2008. Hepatic Stellate Cells Secrete Angiopoietin 1 That Induces Angiogenesis in Liver Fibrosis. *Gastroenterology*. *135*(5):1729–1738. https://doi.org/10.1053/j.gastro.2008.07.065

Teasell RW, Arnold JMO, Krassioukov A, Delaney GA. 2000. Cardiovascular consequences of loss of supraspinal control of the sympathetic nervous system after spinal cord injury. *Archives of Physical Medicine and Rehabilitation*. *81*(4):506–516. https://doi.org/10.1053/mr.2000.3848

The Human Protein Atlas [Internet]. 2022a. *Protein Summary: IL-6*. [accessed 2022 October 15]. https://www.proteinatlas.org/ENSG00000136244-IL6

The Human Protein Atlas [Internet]. 2022b. *Protein Summary: LIF*. [accessed 2022 October 15]. https://www.proteinatlas.org/ENSG00000128342-LIF

The Human Protein Atlas [Internet]. 2022c. *Protein Summary: VEGF*. [accessed 2022 October 15]. https://www.proteinatlas.org/ENSG00000112715-VEGFA

The Human Protein Atlas [Internet]. 2022d. *The Human Protein Atlas: Protein Summary*. [accessed 2022 October 15]. https://www.proteinatlas.org/

Thoolen B, Maronpot RR, Harada T, Nyska A, Rousseaux C, Nolte T, Malarkey DE, Kaufmann W, Küttler K, Deschl U, Nakae D, Gregson R, Vinlove MP, Brix AE, Singh B, Belpoggi F, Ward JM. 2010. Proliferative and nonproliferative lesions of the rat and mouse hepatobiliary system. *Toxicologic Pathology*. *38*(7). https://doi.org/10.1177/0192623310386499

Tiegs G, Horst AK. 2022. TNF in the liver: targeting a central player in inflammation. *Seminars in Immunopathology.* 44(4):445–459. Springer Science and Business Media Deutschland GmbH. https://doi.org/10.1007/s00281-022-00910-2

Tokarzewicz A, Guszcz T, Onopiuk A, Kozlowski R, Gorodkiewicz E. 2018. Utility of cystatin C as a potential bladder tumour biomarker confirmed by surface plasmon resonance technique. *Indian Journal of Medical Research*. *147*:46–50. https://doi.org/10.4103/ijmr.IJMR_124_16

Tse C, Shoemaker AR, Adickes J, Anderson MG, Chen J, Jin S, Johnson EF, Marsh KC, Mitten MJ, Nimmer P, Roberts L, Tahir SK, Xiao Y, Yang X, Zhang H, Fesik S, Rosenberg SH, Elmore SW. 2008. ABT-263: a potent and orally bioavailable Bcl-2

family inhibitor. *Cancer Res.* 68(9):3421-3428. https://doi.org/10.1158/0008-5472.CAN-07-5836

Tsubai T, Noda Y, Ito K, Nakao M, Seino Y, Oiso Y, Hamada Y. 2017. Insulin elevates leptin secretion and mRNA levels via cyclic AMP in 3T3-L1 adipocytes deprived of glucose. *Heliyon*. *3*(194). https://doi.org/10.1016/j.heliyon.2016

Tutusaus A, de Gregorio E, Cucarull B, Cristóbal H, Aresté C, Graupera I, Coll M, Colell A, Gausdal G, Lorens JB, García de Frutos P, Morales A, Marí M. 2020. A Functional Role of GAS6/TAM in Nonalcoholic Steatohepatitis Progression Implicates AXL as Therapeutic Target. *CMGH*. *9*(3):349–368. https://doi.org/10.1016/j.jcmgh.2019.10.010

Tyagi P, Barclay D, Zamora R, Yoshimura N, Peters K, Vodovotz Y, Chancellor M. 2010. Urine cytokines suggest an inflammatory response in the overactive bladder: A pilot study. *International Urology and Nephrology*. *42*(3):629–635. https://doi.org/10.1007/s11255-009-9647-5

Ueno M, Ueno-Nakamura Y, Niehaus J, Popovich PG, Yoshida Y. 2016. Silencing spinal interneurons inhibits immune suppressive autonomic reflexes caused by spinal cord injury. *Nature Neuroscience*. *19*(6):784–787. https://doi.org/10.1038/nn.4289

Vaidyanathan S, Selmi F, Abraham KA, Hughes P, Singh G, Soni B. 2012. Hydronephrosis and renal failure following inadequate management of neuropathic bladder in a patient with spinal cord injury: Case report of a preventable complication. *Journal of Patient Safety in Surgery*. 6(22). http://www.pssjournal.com/content/6/1/22

Vaidyanathan S, Soni B, Abraham Abraham K, Hughes P, Singh G. 2012. Fatal Renal Failure in a Spinal Cord Injury Patient with Vesicoureteric Reflux Who Underwent Repeated Ureteric Reimplantations Unsuccessfully: Treatment Should Focus on Abolition of High Intravesical Pressures rather than Surgical Correction of Reflux. *Case Reports in Urology*. *2012*:1–5. https://doi.org/10.1155/2012/603715

Van Kleffens M, Lindenbergh-Kortleve DJ, Koster JG, Van Neck JW, Flyvbjerg A, Rasch R, Drop SLS, Van Buul-Offers SC. 2001. The role of the IGF axis in IGFBP-1 and IGF-I induced renal enlargement in Snell dwarf mice. *Journal of Endocrinology*. *170*:333–346. http://www.endocrinology.org

Walter MJ, Kajiwara N, Karanja P, Castro M, Holtzman MJ. 2001. Interleukin 12 p40 Production by Barrier Epithelial Cells during Airway Inflammation. *J. Exp. Med.* 193(3). http://www.jem.org/cgi/content/full/193/3/339

Wan Y, Li X, Slevin E, Harrison K, Li T, Zhang Y, Klaunig JE, Wu C, Shetty AK, Dong XC, Meng F. 2022. Endothelial dysfunction in pathological processes of chronic liver disease during aging. *FASEB Journal*. 36(1). John Wiley and Sons Inc. https://doi.org/10.1096/fj.202101426R

Wang Y, Zhang C. 2019. The Roles of Liver-Resident Lymphocytes in Liver Diseases. *Frontiers in immunology*. 10:1582. NLM (Medline). https://doi.org/10.3389/fimmu.2019.01582

Wasmuth HE, Lammert F, Zaldivar MM, Weiskirchen R, Hellerbrand C, Scholten D, Berres ML, Zimmermann H, Streetz KL, Tacke F, Hillebrandt S, Schmitz P, Keppeler H, Berg T, Dahl E, Gassler N, Friedman SL, Trautwein C. 2009. Antifibrotic Effects of

CXCL9 and Its Receptor CXCR3 in Livers of Mice and Humans. *Gastroenterology*. *137*(1). https://doi.org/10.1053/j.gastro.2009.03.053

Weinhage T, Wirth T, Schütz P, Becker P, Lueken A, Skryabin BV, Wittkowski H, Foell D. 2020. The Receptor for Advanced Glycation Endproducts (RAGE) Contributes to Severe Inflammatory Liver Injury in Mice. *Frontiers in Immunology*. *11*. https://doi.org/10.3389/fimmu.2020.01157

Weiskirchen R, Tacke F. 2017. Interleukin-33 in the pathogenesis of liver fibrosis: Alarming ILC2 and hepatic stellate cells. *Cellular and Molecular Immunology*. *14*(2):143–145. https://doi.org/10.1038/cmi.2016.62

Wen Y, Jeong S, Xia Q, Kong X. 2016. Role of osteopontin in liver diseases. *International Journal of Biological Sciences*. 12(9):1121–1128. Ivyspring International Publisher. https://doi.org/10.7150/ijbs.16445

Widjaja AA, Dong J, Adami E, Viswanathan S, Singh BK, Wen Lim W, Zhou J, Pakkiri LS, Tan J, Yun Lim S, Wang M, Holgate R, Hearn A, Chothani SP, Felkin LE, Dear JW, Drum C., Cook, SA. 2019. Redefining Interleukin 11 as a regeneration-limiting hepatotoxin. https://doi.org/10.1101/830018

Widjaja AA, Singh BK, Adami E, Viswanathan S, Dong J, D'Agostino GA, Lim WW, Tan J, Paleja BS, Tripathi M, Lim SY, Shekeran SG, Chothani SP, Rabes A, Sombetzki M, Bruinstroop E, Min LP, Sinha RA, et al. 2019. Inhibiting Interleukin 11 Signaling Reduces Hepatocyte Death and Liver Fibrosis, Inflammation, and Steatosis in Mouse Models of Nonalcoholic Steatohepatitis. *Gastroenterology*. *157*(3):777-792.e14. https://doi.org/10.1053/j.gastro.2019.05.002

Willard-Mack CL, Elmore SA, Hall WC, Harleman J, Kuper CF, Losco P, Rehg JE, Rühl-Fehlert C, Ward JM, Weinstock D, Bradley A, Hosokawa S, Pearse G, Mahler BW, Herbert RA, Keenan CM. 2019. Nonproliferative and Proliferative Lesions of the Rat and Mouse Hematolymphoid System. *Toxicologic Pathology*. *47*(6):665–783. https://doi.org/10.1177/0192623319867053

Wilson WH, O'Connor OA, Czuczman MS, LaCasce AS, Gerecitano JF, Leonard JP, Tulpule A, Dunleavy K, Xiong H, Chiu YL, Cui Y, Busman T, Elmore SW, Rosenberg SH, Krivoshik AP, Enschede SH, Humerickhouse RA. 2010. Navitoclax, a targeted high-affinity inhibitor of BCL-2, in lymphoid malignancies: A phase 1 dose-escalation study of safety, pharmacokinetics, pharmacodynamics, and antitumour activity. *The Lancet Oncology*. *11*(12):1149–1159. https://doi.org/10.1016/S1470-2045(10)70261-8

Winokur P, Subramanian P, Bullock J, Arocas V, Becerra P. 2017. Comparison of two neutrophilic serpins reveals a small fragment with cell survival activity. *Molecular Vision*.

Wischhusen J, Melero I, Fridman WH. 2020. Growth/Differentiation Factor-15 (GDF-15): From Biomarker to Novel Targetable Immune Checkpoint. *Frontiers in Immunology*. 11. Frontiers Media S.A. https://doi.org/10.3389/fimmu.2020.00951

Witte K, Witte E, Sabat R, Wolk K. 2010. IL-28A, IL-28B, and IL-29: Promising cytokines with type I interferon-like properties. *Cytokine and Growth Factor Reviews*. 21(4):237–251. https://doi.org/10.1016/j.cytogfr.2010.04.002

World Health Organization, Bickenbach J, International Spinal Cord Society. 2013. International perspectives on spinal cord injury.

Worthmann K, Peters I, Kümpers P, Saleem M, Becker JU, Agustian PA, Achenbach J, Haller H, Schiffer M. 2010. Urinary excretion of IGFBP-1 and -3 correlates with disease activity and differentiates focal segmental glomerulosclerosis and minimal change disease. *Growth Factors*. *28*(2):129–138. https://doi.org/10.3109/08977190903512594

Wu D, Tao J, Ding J, Qu P, Lu Q, Zhang W. 2013. Interleukin-11, an interleukin-6-like cytokine, is a promising predictor for bladder cancer prognosis. *Molecular Medicine Reports*. *7*(2):684–688. https://doi.org/10.3892/mmr.2012.1199

Wu SY, Jhang JF, Liu HH, Chen JT, Li JR, Chiu B, Chen SL, Kuo HC. 2022. Long-Term Surveillance and Management of Urological Complications in Chronic Spinal Cord-Injured Patients. *Journal of Clinical Medicine*. 11(24). MDPI. https://doi.org/10.3390/jcm11247307

Xi S, Zheng X, Li X, Jiang Y, Wu Y, Gong J, Jie Y, Li Z, Cao J, Sha L, Zhang M, Chong Y. 2021. Activated Hepatic Stellate Cells Induce Infiltration and Formation of CD163+ Macrophages via CCL2/CCR2 Pathway. *Frontiers in Medicine*. *8*. https://doi.org/10.3389/fmed.2021.627927

Xu Z, Wu Y, Wang F, Li X, Wang P, Li Y, Wu J, Li Y, Jiang T, Pan X, Zhang X, Xie L, Xiao, J, Liu Y. 2020. Fibroblast Growth Factor 1 Ameliorates Diabetes-Induced Liver Injury by Reducing Cellular Stress and Restoring Autophagy. *Frontiers in Pharmacology*. *11*. https://doi.org/10.3389/fphar.2020.00052

Yabe T, Sanagi T, Yamada H. 2010. The Neuroprotective Role of PEDF: Implication for the Therapy of Neurological Disorders. *Current Molecular Medicine*. 10.

Yamagishi R, Kamachi F, Nakamura M, Yamazaki S, Kamiya T, Takasugi M, Cheng Y, Nonaka Y, Yukawa-Muto Y, Thuy LTT, Harada Y, Arai T, Loo TM, Yoshimoto S, Ando T, Nakajima M, Taguchi H, Ishikawa T, Akiba H, Ohtani N, et al. 2022. Gasdermin D–mediated release of IL-33 from senescent hepatic stellate cells promotes obesity-associated hepatocellular carcinoma. *Science Immunology*. *7*(72). https://doi.org/10.1126/sciimmunol.abl7209

Yang M, Liu L, Liang E, Chong BH, Li C. 2016. Thrombopoietin Has Neural Protective Effect in a Neonatal Rat Model of Hypoxic-Ischemic Brain Damage. *Blood*. *128*(22):5059–5059. https://doi.org/10.1182/blood.v128.22.5059.5059

Yao C, Cao X, Yu B. 2021. Revascularization After Traumatic Spinal Cord Injury. *Frontiers in Physiology*. 12. Frontiers Media S.A. https://doi.org/10.3389/fphys.2021.631500

Yazdani HO, Chen HW, Tohme S, Tai S, van der Windt DJ, Loughran P, Rosborough, BR, Sud V, Beer-Stolz D, Turnquist, HR, Tsung A, Huang H. 2018. IL-33 exacerbates liver sterile inflammation by amplifying neutrophil extracellular trap formation. *Journal of Hepatology*. *68*(1):130–139. https://doi.org/10.1016/j.jhep.2017.09.010

Yuan X, Wu Q, Wang P, Jing Y, Yao H, Tang Y, Han R, He W, Li Z, Zhang H, Xiu R. 2019. Intraspinal administration of interleukin-7 promotes neuronal apoptosis and limits functional recovery through JAK/STAT5 pathway following spinal cord injury. *Biochemical and Biophysical Research Communications*. *514*(3):1023–1029. https://doi.org/10.1016/j.bbrc.2019.04.159

Yuan Y, Li K, Teng F, Wang W, Zhou B, Zhou X, Lin J, Ye X, Deng Y, Liu W, Luo S, Zhang P, Liu D, Zheng M, Li J, Lu Y, Zhang H. 2022. Leukemia inhibitory factor protects against liver steatosis in nonalcoholic fatty liver disease patients and obese mice. *Journal of Biological Chemistry*. *298*(6). https://doi.org/10.1016/j.jbc.2022.101946

Zhang L, Bansal MB. 2020. Role of Kupffer Cells in Driving Hepatic Inflammation and Fibrosis in HIV Infection. *Frontiers in Immunology*. *11*. https://doi.org/10.3389/fimmu.2020.01086

Zhang M, Serna-Salas S, Damba T, Borghesan M, Demaria M, Moshage H. 2021. Hepatic stellate cell senescence in liver fibrosis: Characteristics, mechanisms and perspectives. *Mechanisms of Ageing and Development*. 199. Elsevier Ireland Ltd. https://doi.org/10.1016/j.mad.2021.111572

Zhang Y, Guan Z, Reader B, Shawler T, Mandrekar-Colucci S, Huang K, Wei Z, Bratasz A, Wells J, Powell ND, Sheridan JF, Whitacre CC, Rabchevsky AG, Nash MS, Popovich PG. 2013. Autonomic dysreflexia causes chronic immune suppression after spinal cord injury. *Journal of Neuroscience*. *33*(32):12970–12981. https://doi.org/10.1523/JNEUROSCI.1974-13.2013

Zhang Y, Mamun AAl, Yuan Y, Lu Q, Xiong J, Yang S, Wu C, Wu Y, Wang J. 2021. Acute spinal cord injury: Pathophysiology and pharmacological intervention (Review). *Molecular Medicine Reports*. 23(6). Spandidos Publications. https://doi.org/10.3892/mmr.2021.12056

Zhu NL, Asahina K, Wang J, Ueno A, Lazaro R, Miyaoka Y, Miyajima A, Tsukamoto H. 2012. Hepatic stellate cell-derived delta-like homolog 1 (DLK1) protein in liver regeneration. *Journal of Biological Chemistry*. *287*(13):10355–10367. https://doi.org/10.1074/jbc.M111.312751

Zhu Y, Tchkonia T, Fuhrmann-Stroissnigg H, Dai HM, Ling YY, Stout MB, Pirtskhalava T, Giorgadje N, Johnson KO, Giles CB, Wren JD, Niedernhofer LJ, Robbins PD, Kirkland JL. 2016. Identification of a novel senolytic agent, navitoclax, targeting the Bcl-2 family of anti-apoptotic factors. *Aging cell.* 15:428-435. https://doi.org/10.1111/acel.12445

Annex 1

Supplementary Table 1 - Spinal Cord Proteomic Profile. Legend: ↑ - upregulated in Vehicle or ABT-263 vs. Sham; ↑* - upregulated in ABT-263 vs. vehicle; ↓ - downregulated in ABT-263 vs. Vehicle; = - no regulation; ✓ - SASP factors.

	SPINAL CORD				
	15 dpi		**30 dpi**		**SASP Factors**
	Vehicle-treated SCI	**ABT-263-treated SCI**	**Vehicle-treated SCI**	**ABT-263-treated SCI**	
	SA-β-gal$^+$ ↑	SA-β-gal$^+$ ↓	SA-β-gal$^+$ ↑	SA-β-gal$^+$ =	
Factors					
Amphiregulin	↑	↓			✓
IGFBP-3	↑	↓			✓
IGFBP-5	↑	↓			
IL-11	↑	↓			
PDGF-BB	↑	↓			✓
Serpin E1	↑	↓			✓
CCL-6/C10	↑	↓			
Chemerin	↑	↓			
Endoglin/CD105	↑	↓			
Flt-3 Ligand	↑	↓			
IL-15	↑	↓			✓
LIX	↑	↓			
Lipocalin-2/NGAL	↑	↓			
M-CSF	↑	↓			✓
Pentraxin 2	↑	↓			
Pentraxin 3	↑	↓			
TNF-α	↑	↓			✓
CCL11/Eotaxin	↑	↓	↑	=	✓
CXCL11/I-TAC	↑	↓	↑	=	✓
IL-33	↑	↓	↑	=	✓
CCL20	↑	↓			✓
ICAM-1	↑	↓			✓
P-selectin	↑	↓			
VCAM-1	↑	↓			
Osteopontin	↑	↓	=	↑	
IL-10	↑	↓			
Leptin	↑	↓			
IGFBP-6	↑	↑			
MMP-3	↑	↑			
IL-12p40	↑	=			
Myeloperoxidase	↑	=			
Chitinase-3-like 1	↑	=			
FGF acidic	↑	=			
FGF-21	↑	=			
Endostatin	↑	=			
Proprotein Convertase 9	=	↓			
CCL2	=	↓			✓
IL-13	=	↓			
IL-27p28	=	↓			
RAGE	=	↓	=	↑	
Serpin F1/PEDF			↑	↓	
IL-28A/B			↑	↓	
Thrombopoietin			↑	↓	
Angiopoietin-1			↑	=	
CCL12/MCP-5			↑	=	
IL-7			↑	=	✓
IL-2			=	↓	
IL-3			=	↑	
CD40/TNFRSF5			=	↑	
CCL5/RANTES			=	↑↑*	
Total	Upregulated factors	ABT-263 modulated factors **(downregulated)**	Upregulated factors	ABT-263 modulated factors **(downregulated)**	
	35	32	9	4	

Supplementary Table 2 – Liver Proteomic Profile. Legend: ↑ - upregulated in Vehicle or ABT-263 vs. Sham; ↑* - upregulated in ABT-263 vs. vehicle; ↓ - downregulated in ABT-263 vs. Vehicle; = - no regulation; ✓ - SASP factor.

	LIVER				
	15 dpi		**30 dpi**		**SASP Factors**
	Vehicle-treated SCI	**ABT-263-treated SCI**	**Vehicle-treated SCI**	**ABT-263-treated SCI**	
	SA-β-gal⁺ =	SA-β-gal⁺ ↑↑*	SA-β-gal⁺ ND	SA-β-gal⁺ ND	
Factors					
IL-6	↑	=			✓
LIF	↑	=			✓
Reg3G	↑	=			
FGF acidic	↑	=			
Complement Factor D	↑	=			
VEGF	↑	=	↓	↑*	✓
Periostin	↑	=	↑	↓	
Leptin	↑	=	=	↑*	
Pentraxin 3			↑	↓	
M-CSF			=	↑*	✓
RAGE			=	↑↑*	
TNF-α			=	↑*	✓
CXCL11/I-TAC			=	↑*	✓
CCL-6/C10			=	↑*	
CCL12/MCP-5			=	↑↑*	
IFN-γ			=	↑*	✓
IL-7			=	↑*	✓
IL-11			=	↑*	
IL-23			=	↑↑*	
IL-28A/B			=	↑↑*	
CCL-2/MCP-1			=	↑*	✓
Lipocalin-2/NGAL			=	↑↑*	
MMP-2			=	↑↑*	
Osteopontin (OPN)			=	↑*	
Pref-1			=	↑*	
Angiopoietin-1			=	↑	
Gas 6			=	↑*	
IL-5			=	↑↑*	
IL-27p28			=	↑*	
IL-33			=	↑*	
IGFBP-1			=	↑↑*	
IGFBP-3			=	↑↑*	✓
CXCL9/MIG			=	↑↑*	
PEDF			↓	↑↑*	
RBP4			=	↑*	
WISP-1/CCN4			↓	↑*	
VCAM-1			↓	↑*	
Total	Upregulated factors	ABT-263 modulated factors **(downregulated)**	Upregulated factors	ABT-263 modulated factors **(upregulated)**	
	8	0	2	30	

Supplementary Table 3 – Bladder Proteomic Profile. Legend: ↑ - upregulated in Vehicle or ABT-263 vs. Sham; ↑* - upregulated in ABT-263 vs. vehicle; ↓ - downregulated in ABT-263 vs. Vehicle; = - no regulation; ✓ - SASP factor.

	BLADDER				
	15 dpi		**30 dpi**		**SASP Factors**
	Vehicle-treated SCI SA-β-gal⁺ =	**ABT-263-treated SCI** SA-β-gal⁺ =	**Vehicle-treated SCI** SA-β-gal⁺ ND	**ABT-263-treated SCI** SA-β-gal⁺ ND	
Factors					
EGF	↑	↓			✓
Complement Factor D	↑	=			
Cystatin C	↑	↑			
C-Reactive Protein	↑	=	↑	=	
PD-ECGF	↑	=	↑	↓	
IL-5	↑	=	↑	↓	
CXCL9/MIG	↑	↑			
G-CSF	↑	↑			
CCL3/CCL-4	↑	↑			✓
IL-33	↑	↑	↑	=	✓
C5/C5a	↑	↑	↑	=	
IL-12p40	↑	↑↑	↑	↓	
IGFBP-2	↑	↑	↑	↑	✓
IL-11	↑	↑	↑	↓	
Adiponectin/Acrp30	=	↑			
CCL11/Eotaxin	=	↑↑*			✓
CCL19/MIP-3β	=	↑			
Leptin	=	↑			
CCL17/TARC	=	↑	↑	=	
IL-1α	=	↑	↑	=	✓
IL-10	=	↑↑*	↑	=	
FGF-21	=	↑	↑	=	✓
RBP4	=	↑	↑	↓	
IL-1ra	=	↑	=	↑	
VEGF	↓	=			✓
Flt-3 Ligand	↓	=	↓	↓	
CCL21/6Ckine	↓	=			
IGFBP-6	↓	=			✓
FGF acidic	↓	=			
HGF			↑	=	
GM-CSF			↑	=	✓
IFN-γ			↑	=	
IGFBP-3			↑	=	✓
WISP-1/CCN4			↑	↑	
Periostin			↑	=	
Endoglin/CD105			↑	=	
Angiopoietin-1			↑	=	
MMP-2			↑	=	
Endostatin			↓	↓	
Proliferin			↑	↓	
IGFBP-1			↑	↓	
GDF-15			↑	↓	
IL-13			↑	↓	✓
IL-27p28			↑	↓	
IL-28A/B			↑	↓	
Lipocalin-2/NGAL			↑	↓	
Pref-1			↑	↓	
MMP-3			↑	↑	✓
Total	**Upregulated factors**	**ABT-263 modulated factors (downregulated)**	**Upregulated factors**	**ABT-263 modulated factors (downregulated)**	
	14	1	31	15	